C.P. No. 706

C.P. No. 706

MINISTRY OF AVIATION

AERONAUTICAL RESEARCH COUNCIL

CURRENT PAPERS

Free-Flight Measurements of Pressure and Heat Transfer in Regions of Separated and Reattached Flow at Mach Numbers up to 4

by

J. Picken, B.Sc.

LONDON: HER MAJESTY'S STATIONERY OFFICE

1965

PRICE 13s 0d NET

U.D.C. No. 533.696.4 : 533.6.011.6 : 532.526.5

C.P. No. 706

September, 1960

FREE-FLIGHT MEASUREMENTS OF PRESSURE AND HEAT TRANSFER IN REGIONS OF SEPARATED AND REATTACHED FLOW AT MACH NUMBERS UP TO 4

by

J. Picken, B.Sc.

SUMMARY

Local heat transfer and surface pressure have been measured over regions of separated flow associated with a turbulent boundary layer. The separated flow was appropriate to aft facing steps of various heights behind a sting mounted cone of 15° semi-angle. The maximum Mach number achieved was about 4 and the maximum Reynolds number about 50×10^6 based on cone length.

Two different forms of wake were detected: one associated with reattachment on the sting, i.e. a relatively great convergence of the wake boundary, and one associated with reattachment on a conical surface aft of the sting, i.e. a small wake convergence. Differing patterns of heat transfer and pressure distributions were obtained depending on which type of flow occurred.

Some collapse of the separated flow heat transfer data with respect to Mach number was obtained by comparing them with estimated values appropriate to local conditions outside the wake. Close to the step the heat flow in the separated region was about 25% of the estimated value for attached flow to a solid surface replacing the wake boundary. Towards and beyond reattachment the ratio of the two values rose to near unity. The measurements suggest that the amount of heat transfer rise at and beyond reattachment is dependent upon the wake convergence, becoming smaller as the convergence increases. This is qualitatively consistent with the known effect that increasing convergence implies increasing boundary layer thickness at reattachment.

There was no evidence of a marked maximum in the heat flux in the reattachment region.

Replaces R.A.E. Report No. Aero 2643 - A.R.C. 22618.

LIST OF CONTENTS

LIST OF TABLES

LIST OF ILLUSTRATIONS

1 INTRODUCTION

Flow separation is likely to become unavoidable and extensive with increasing Mach number and recent work has shown that the separation of the boundary layer can have a large effect on aerodynamic heating. A theoretical study by Chapman[1] predicts that a reduction, independent of Mach number, of 44% in overall heat input is achieved by detaching a laminar boundary layer. The reduction is relative to the heat input to a solid surface corresponding to the flow dividing boundary between the free stream and the separated air. This prediction is supported at least qualitatively by various wind tunnel experiments (e.g. Ref.2-4).

On the other hand the same paper predicts a marked Mach number effect for the turbulent flow case and indicates a large increase in overall heat input in a separated region at subsonic and low supersonic speeds. This prediction has not been substantiated by experiment. For example, Larson[2] measured a reduction of about 40% over a Mach number range of 0.3 to 4, which was apparently independent of Mach number.

A theoretical examination of heating distribution in a separated region has not yet been satisfactorily made for either laminar or turbulent flow regimes. Experiments have produced some apparently conflicting data notably relative to the existence of a peak heating rate near the reattachment region (cf. Refs. 3, 5, 6).

Most of the experimental work so far attempted has been at relatively low Reynolds numbers - about 18,000 to 1.6 million - and subject to the usual limitations of wind tunnel tests. A useful extension of the experimental data seemed possible by means of the free flight techniques, using rocket propelled models. This has the advantage of freedom from constraints, and the measurement of local heat fluxes is in some ways less subject to uncertainty because conduction effects are relatively unimportant on account of the suitability of time and space scales. There are of course obvious disadvantages such as lack of flow visualisation.

This note describes an exploratory series of experiments with a vehicle propelled by a single stage rocket motor and capable of achieving Mach numbers between 4 and 5 in free flight at low altitudes. Pressure and heat transfer data were obtained in regions of detached turbulent flow aft of sting supported heads with rearward facing steps.

2 DESCRIPTION OF TEST VEHICLE AND HEADS

The complete test vehicle is illustrated in Fig.1. A photograph of the heads flown is given in Fig.2.

2.1 Details of test heads

The heads belonged to a systematic family. They each consisted of a forward facing cone with a step down to an axial cylinder representing a sting then a divergence aft in the form of a truncated cone to the rocket motor diameter. These components will be subsequently referred to as the forward cone, the step, the sting and the aft cone respectively.

The forward cone had a base diameter of 11" and a semi-angle of 15°. The aft cone base diameter and semi-angle were 10.14" and 20° respectively. The base of the aft cone was at a constant distance of 21.1" from the base of the forward cone. Heads with three values of step heights, s, of 1", 2.56" and 4.13" were flown. The corresponding ratios of sting diameter to forward cone base diameter were 0.82, 0.54 and 0.25.

The tips of the forward cones were machined from solid mild steel to British Standard Specification S15. The remaining head components were fabricated from mild steel plate. The mean external wall thickness was 0.053" for the skirt of the forward cone and 0.030" for the other head components. The centre line averages of the surface finishes were assessed by Talysurf[7] and were of the order of 10 to 50 micro inches. A typical surface profile is illustrated in Fig.3.

A total of six vehicles was flown - two with each head configuration. One of each configuration was flown primarily to establish surface pressure distributions and thus obtain some assessment of the nature of the separated flow regions behind the steps. Heat transfer data were obtained from the other set. The selection of stations for temperature measurement was based on the information regarding reattachment obtained from the pressure-measuring flights. Details of the vehicle are summarised in tables 1 to 3.

2.2 Instrument installation

Free stream velocity, atmospheric pressure and ambient temperature were measured by instruments external to the vehicles in accordance with the usual procedures at the Aberporth range[8].

Static pressure was measured at 21 stations on each of the pressure-measuring heads as indicated in table 2 and Fig.4, by means of 465 Mc/s telemetry[9] and variable inductance transducers type GW2A[10]. Lateral and normal accelerometers were also included to confirm that flights were effectively at zero incidence.

Temperature measurements were taken approximately 80 times per second at each of 11 stations on the heads of the heat transfer vehicles by means of chromel-alumel thermocouples and a specially modified 465 Mc/s telemetry system[11]. A sub-commutation switch was included in the telemetry equipment to provide calibration voltages during flight at 12 levels appropriate to the temperature measurements. These were each sampled about 6 times per second. This allows account to be taken of any minor telemetry vagaries provided they do not occur too rapidly. The locations of the stations are indicated in Fig.4 and these together with local wall thicknesses are detailed in table 3. Inner panels of durestos were placed over each station to form insulating air gaps 0.1" thick in order to reduce free convective heat transfer from the measuring wall to the interior.

3 DESCRIPTION OF TESTS

The vehicles were ground launched at an elevation angle of 25° and were accelerated by the rocket motor to maximum Mach numbers between 3.8 and 4.0 in 3.3 to 3.6 seconds. The maximum heights attained were 9,000 ft to 11,000 ft in 19 seconds to 21 seconds. A summary of the flights is given in table 1. Typical trajectory data appropriate to head H2 are presented in Fig.5 and the variation of free stream Reynolds number per foot with Mach number in Fig.6.

The flights of all vehicles were satisfactory with the exception of that of H3 which suffered a telemetry failure soon after maximum velocity, apparently because of unduly high lateral accelerations occurring at this time.

4 DATA REDUCTION

Height and velocity were deduced from kiné-theodolite and radar measurements. Ambient temperatures and pressures were obtained from radiosonde measurements made about the time of flight. The order of the uncertainty of the basic data is given in table 4.

4.1 Pressure measurements

Pressure data were reduced by the usual procedures[12] to the ratio of the local static pressure to the free stream static pressure, p/p_o.

4.2 Temperature measurements

The thermocouple signals were read every cycle of the commutator switch, that is about every 1/80th second for each station and were smoothed and differentiated by means of cubic least square polynomials using the moving-arc technique over suitable stretches of data[13].

For a 'thermally-thin' skin the nett local heat flux is then given by

$$q_{nett} = c \sigma \tau_w \frac{dT_w}{dt} \qquad (1)$$

where q_{nett} = the nett local heat flux

T_w is the temperature
c is the specific heat
σ is the density
τ_w is the thickness

} of the measuring wall

This relationship assumes that temperature gradients normal to the surface of the wall are negligible. This was found to be a good approximation for most of the data, except those appropriate to the forward cone stations where the wall thickness was greater than elsewhere. Adjustments were made where necessary for such temperature gradients on the basis of the one-dimensional heat flow corrections presented in Ref.14.

We can write the heat balance equation as

$$q_{nett} \doteq q_{aero} + q_{lateral} - q_{radiation} - q_{conduction} - q_{free\ convection} \qquad \ldots (2)$$

where q_{aero} is the local aerodynamic heat flux and is the quantity we wish to evaluate,

$q_{lateral}$ is the change in local heat flux arising from temperature gradients in the plane of the wall,

$q_{radiation}$ is the nett local heat flux arising from radiation from both surfaces of the measuring wall,

$q_{conduction}$ is the local heat flux across the air gap between the measuring wall and the durestos inner wall, arising from the conductivity of air,

$q_{free\ convection}$ is the additional local heat flux across the air gap arising from free convection of the air in the gap.

Compared with q_{aero} the heat fluxes on the R.H.S. of equation (3) should have been for the most part relatively small and the data were mostly reduced on the assumption that

$$q_{nett} = q_{aero} \cdot \tag{3}$$

This assumption was not satisfactory for head H1 where temperature gradients induced significant modifications to the local heat fluxes to the sting. Adjustments were applied in this case from the relation

$$q_{lateral} = \tau_w \frac{\partial}{\partial x} \left(k_w \frac{\partial T_w}{\partial x} \right) \tag{4}$$

where k_w is the conductivity of the wall

x is the length measured parallel to the axis of the head from the step-sting junction.

No adjustments were made for the other heat flux components. An assessment of their likely magnitudes is made in Appendix 1 and estimates of the largest components - radiation and conduction to the interior from the measuring wall - is given in Fig.7. None of the corrections were significant for data appropriate to accelerating flight.

Heat transfer coefficients were evaluated from the relationship

$$h_m = \frac{q_{aero}}{(i_r - i_w)} \tag{5}$$

where i is the specific enthalpy of air

suffix r refers quantities to conditions for $q_{aero} = 0$.

The zero aerodynamic heat transfer specific enthalpy, i_r, was calculated from the relationship

$$i_r = i_o (1 + 0.2 R_o M_o^2) \tag{6}$$

where R is the recovery factor

suffix o refers to free stream conditions.

Where $q_{aero} = 0$, experimental values of R_o may be determined since then $i_w = i_r$. However, in this experiment, lack of information regarding the emissivity of the surface of the measuring wall and the temperature of the durestos inner wall were such that recovery factors derived in this way were not sufficiently reliable for use in the analysis, and a constant value of $R_o = 0.91$ was applied. This mean value is reasonably consistent with the present data when account is taken of the possible uncertainties (see section 5.2.2 below). It is also consistent with the wind tunnel turbulent flow results summarised in Ref.15 relative to enthalpy recovery on the forward cone.

The values of heat transfer coefficient so obtained in the separated flow regions and further aft were compared with the theory of van Driest appropriate to a turbulent attached boundary layer[16]. The comparison was made in terms of two theoretical heat transfer quantities:

(a) h_{fp}, the flat plate value of the heat transfer coefficient, evaluated appropriate to free stream conditions, local wall temperature and a length equal to half the wetted length of the forward cone plus the distance from the step-sting junction.

(b) h_A, evaluated in the same way as h_{fp}, except that instead of free stream conditions, local conditions appropriate to the local surface pressure and isentropic flow from the shoulder of the forward cone were taken.

Heat transfer coefficients based on Eckert's intermediate enthalpy theory[17] were also evaluated for stations on the forward cone

5 RESULTS AND DISCUSSION

Schematic diagrams of the salient features of the flow field over the separated flow regions based on the description given in Ref.18 are presented in Fig.8. The boundary layer on the forward cone separates from the solid surface at the shoulder and entrains a bubble of air behind the step. In the present experiment the measurements indicated that the boundary layer re-attached to the solid surface on either the sting or on the aft cone. Quite different levels of surface pressure and heat transfer were associated with these two modes of reattachment.

5.1 Surface pressures

Variations of surface pressure with Mach number at typical stations are illustrated in Fig.9. Theoretical surface pressures from Ref.19 appropriate to 15° and 20° semi-angle cones and appropriate to a 20° wedge[20] at zero incidence, are also given, for comparison with the experimental values.

5.1.1 Forward cone

On the forward cones the measured pressures deviated from the estimated values by amounts dependent on test vehicle and Mach number. On all test vehicles the deviations were greater than would be expected from random experimental uncertainty. Such a discrepancy could arise because the heads were, in fact, not at zero incidence. Now the stations on the forward cones were located at meridian intervals of 120° and thus the mean values of the surface pressure, $\bar{p}$, for three such stations, on the basis of first order theory, should be independent of small angles of incidence. A comparison of these mean values with theory[19] is made in Fig.10 and it can be seen that agreement is good.

5.1.2 Incidence effects

Angles of incidence and the orientation evaluated by means of Ref.21 and the mean surface pressures are presented for all three forward cones in Fig.11. The angles of incidence varied between about 1° and 3° and the rotational change in the windward meridian did not exceed about 180°. Also presented in this figure are similar data for the angle of incidence of the vehicle derived from accelerometer measurements and normal force coefficients, estimated on the assumption that all components were at the same angle of incidence. It can be seen that the angles of incidence of the vehicles as a whole are substantially less than those for the forward cones, being for

the most part less than 1°. Further, the windward meridians were in general different. The variations of both sets of angles were not oscillatory in character. There is no apparent influence of step height.

Such behaviour is suggestive of aeroelastic effects. Measurements of the stiffness of a similar vehicle indicate that it may not be inconsistent with the aerodynamic and structural properties of the vehicles.

5.1.3 Region of separated flow

The pressure distributions on the step and along the sting are plotted in Fig.12. For the most part the differences between the data appropriate to accelerating and decelerating flight were small on the step and sting suggesting that the influence of the incidence of the forward cone is not so significant there as on the forward cone itself (Figs.9a and 9c). Further confirmation that this is so is given by the good agreement between corresponding pressure measurements at the 0° and 180° meridian positions. The large differences between accelerating and decelerating pressure distributions which are apparent on head P2 (Fig.12b) are not incidence effects: they arise from the presence of differing modes of reattachment whose character is discussed in detail below.

In Fig.12a, appropriate to head P1, we see that the pressure distributions are qualitatively the same at all Mach numbers. The characteristic features are a region of low, almost constant static pressure extending from the base to about 1.5 step heights along the sting followed by a rapid rise in pressure extending to about 3 to 4 step heights from the base. The surface pressure then rises more gradually towards the free stream value until the aft cone, when there is a sharp rise to near the theoretical value for a cone in a free air stream (Fig.9a). The variation of the surface pressure along the sting is characteristic of flow behind a rearward facing step in a supersonic air stream and conforms in essentials to the qualitative description, appropriate to a step on a flat plate, given in Ref 18.

One would not expect the boundary layer reattachment point to be well defined by the pressure measurements. It probably occurs towards the end of the rapid rise in pressure, i.e. on the sting, from 3 to 4 step heights from the base. The gradual rise of pressure aft of this region is probably a feature arising from the axisymmetric flow field associated with the forward cone and is not a characteristic of 2-dimensional flow.

The static pressure variations for head P2 shown in Fig.12b are seen to be somewhat similar at the higher Mach numbers to those for head P1 except that the pressure tends to recover to a value greater than the free stream value. This latter feature is consistent with the axisymmetric flow expanding towards and reattaching on the smaller sting[22]. At the lower Mach numbers we obtain a somewhat different picture. The low pressure region is seen to be more extensive but the reduction in pressure not so great as for the other condition and the rise is more gradual, extending smoothly over the aft cone sting junction. Such a distribution of pressure suggests reattachment of the boundary layer on the aft cone and not on the sting. The static pressure variations for head P3 are similar at all Mach numbers and suggest that reattachment occurred on the rear cone over the whole speed range investigated.

In Fig.13 a direct comparison of the static pressure variations for the three heads is given in a plot of p/p_o against base calibres from the step for free stream Mach numbers of 2 and 3. The figure summarises the variation of surface pressure distribution as the step height increases.

The variation of the static pressure at the step-sting junction with Mach number gives a good indication of when the flow regime changes. This

variation is illustrated for the three heads in Fig.14. It is seen that at Mach numbers above 2.5 during accelerating flight and above 1.8 during decelerating flight the static pressure at the step-sting junction on head P2 is comparable with that on head P1 and thus indicates that reattachment is then on the sting. Below these Mach numbers this static pressure is comparable to that on head P3 thus indicating a similar flow regime and presumably reattachment to the aft cone. The hysteresis effect is discussed in section 5.1.4 below.

This interpretation is given a more quantitative basis in Fig.15. This shows the variation with Mach number of the angle between the initial direction of the expanded flow at the step to the free stream direction, θ, based on the static pressure at the step-sting junction given in Fig.14 for head P2, and the Prandtl-Meyer data of Ref. 10. That small negative values of θ occur at the lower Mach numbers is attributed to the influence of back pressures from the aft cone. Johannesen[23] noted a similar effect on a flat nosed cylinder with an annular gap of rectangular section in which a similar flow regime was obtained. The distance from the step-sting junction assuming θ is independent of x is also indicated in Fig.15. This assumption should give a fair approximation to the actual flow since the tendency for the angle to increase as the flow converges to the axis of the head will be compensated to some extent by the increase of static pressure due to rejection of air from the mixing layer. Schlieren photographs presented in Ref.3 of a sting mounted hemisphere-cylinder qualitatively support the assumption. Fig.15 confirms that at the higher Mach numbers reattachment on head P2 is on the sting some 3 to 4 step heights from the step-sting junction, while at the lower end of the Mach number range reattachment is on the aft cone.

The significance of these modes with respect to the measurement of base pressure has been examined by Kavanau[24] on a sting mounted cone cylinder model. He referred to the relevant wakes as undisturbed and disturbed respectively, since the former was unaffected by the location of the sting support.

5.1.4 Hysteresis effect on head P2

Some further discussion of the mechanism of the hysteresis effect apparent for the data on head P2 (e.g. Fig.14) is perhaps apposite. In the initial stages of accelerating flight the reattachment point is on the aft cone and this component exerts a dominating influence on the separation bubble. As the Mach number increases beyond about 1.8 the reattachment point moves forward along the aft cone towards the sting. The angle through which the flow turns just aft of reattachment also increases until the reattachment point reaches the vicinity of the aft cone/sting junction when the angle begins to diminish as the influence of the sting is felt. This gives rise to a reduction in recompression pressure and thus in bubble pressure. Hence there is an increase in the expansion angle at the step. This results in an unstable condition and a rapid movement of the reattachment point towards the base of the forward cone away from the influence of the aft cone corresponding to a Mach number of about 2.5.

During decelerating flight the separation bubble is initially not influenced by the aft cone but as the Mach number diminishes the reattachment point moves slowly aft along the sting towards the aft cone until about $M = 1.8$ when the influence of the aft cone results in an increase of recompression pressure and thus an increase of bubble pressure and a reduction of the expansion angle at the step. An unstable condition ensues and the reattachment point moves rapidly aft on the aft cone.

Thus we see that the hysteresis loop arises through the action of back pressures from the aft cone on bubble pressure during accelerating flight.

This action is absent during the decelerating part of the loop. The minor discrepancies outside the loop could arise from the different Reynolds number and wall temperature conditions appropriate to the flight history.

5.2 Heat transfer

Wall temperature histories for typical stations are presented in Fig.16 and wall temperature distributions along the heads at various Mach numbers are shown in Fig.17. The maximum temperature recorded was 710°K at station 1 on the forward cone of head H1. The history of the heat flux to the sting at 2" from the step on head H1 is given in Fig.18 to illustrate the correction required for temperature gradients along the surface of the sting. The correction was for the most part smaller at the other stations on this head and was negligible for stations on heads H2 and H3.

The convection for temperature gradients could not be determined accurately on head H1 for the station at 0.6" from the step because there was no other station between this point and the step. The temperature distributions, however, indicated that the convection was significant relative to the local heat flux in this region.

5.2.1 Heat flux to forward cone

A comparison of the heat fluxes to the forward cones of heads H1 (two stations) and H2 (one station) with the theoretical values of van Driest[16] and Eckert[17] is given in Fig.19. This figure illustrates the reliability of the experimental technique and gives a measure of confidence for heat transfer data from areas where theoretical comparisons are more uncertain or not available.

During heating, the heat flux lies for the most part between the two predictions. The histories for the two stations on head H1 are in fair agreement except near maximum velocity where the values differ by an amount greater than would be expected from the accuracy of the measurements. A discrepancy of this order could arise through the forward cone flying at an angle of incidence of up to about 2° in the plane of the thermocouples. Such an angle of incidence is comparable to the values derived from the pressure measurements on the forward cone of head P1 (Fig.11a). During cooling, the discrepancy between the theoretical value of van Driest[16] and nett heat flux is consistent with radiation from the wall surfaces of emissivity near unity and conduction to a cold durestos inner wall through the air gap (Fig.18c). This suggests that the original polished surface finish on the forward cone has by this stage been modified such that the surface is covered by a more highly emissive oxide coat. The extent of the development of such a coat is likely to be a strong function of the temperature history. Finishes of the more gently heated and less exposed areas of the separated flow region should not have been significantly modified.

5.2.2 Recovery factor

On the forward cone the recovery factors were in good agreement with the wind tunnel data summarised in Ref.15 for two out of the three stations at which it was possible to determine values. Ref.15 indicated that a value of about 0.88 is appropriate to zero heat transfer and local conditions for the present experiment. The relevant values at stations 1 on heads H1 and H2 were 0.88 and 0.89 respectively assuming that radiative and conductive heat losses were negligible. If an emissivity of unity had been obtained, these values would be increased by about 0.04. Thus the data from these two stations suggests that an emissive oxide coat was not established on the forward cones until after the times of zero heat transfer.

At the other forward cone station at which a recovery factor was determinable, namely station 2 on head H1, the value was 0.80. It is difficult to account for the discrepancy between this and the values at the other two stations. The discrepancy is equivalent to an error in heat flux of about 2.7 CHU/ft^2 sec or in wall temperature of about 35°K. The uncertainties of temperature and heat flux at the time of zero heat flux are estimated to be of the order of 16°K and 0.6 CHU/ft^2 sec respectively and are too small to explain the discrepancy. The maximum heat losses through radiation and conduction should not have exceeded 1.5 CHU/ft^2 sec and would of course be expected to be similar for all stations on the forward cones. Contact between the metal wall and the durestos cover at the station might be possible and could perhaps be the source of the discrepancy.

Fig.20 illustrates the variation of experimental recovery factor aft of the step with station position. On first examination it appears that the recovery factor tends to be greater close to the step. This trend is the reverse of that found by other investigators (e.g. Ref.6). However the uncertainty in the experimental determination of recovery factor on the sting in the present experiment is such that little weight can be attached to the variations suggested in Fig.20. The constant value of 0.91 relative to free stream conditions for the recovery factor used in the computation of the experimental heat transfer coefficients is reasonably compatible with the experimental values.

5.2.3 Reference heat transfer coefficients

It is convenient to refer the experimental heat transfer coefficients to the theoretical values, h_A and h_{fp}, described in section 4, the basis for which is illustrated diagrammatically in Fig.21.

h_A is approximately the value appropriate to attached flow aft of the step if the wake boundary were replaced by a solid surface. h_A enables some account to be taken of the substantial variations in local conditions that occur over the separated and reattached flow regions*. It also gives a basis of comparison with Chapman's theory[1] and with the results of some other investigators (e.g. Refs.2 and 3).

h_{fp} is the value of the heat transfer coefficient appropriate to a flat plate at zero incidence in the free air stream and takes no account of variations in local conditions. It is thus a less likely medium for collapsing the data than h_A. However, comparison of the data with h_{fp} allows an appreciation of relative magnitudes. This comparison might be regarded as analogous to the use of the surface pressure ratio, p/p_o, to correlate the pressure data. The variation of h_A/h_{fp} with p/p_o is illustrated in Fig.22 for M_o = 2 and 3.5 and accelerating flight conditions appropriate to head H1. The data for the higher values of p/p_o refer to isentropic recompression such as may be appropriate to the reattachment region.

5.2.4 Heat transfer aft of step

Detailed plots of h_m/h_{fp}, where h_m is the measured heat transfer coefficient, are given in Fig.23. From these the broad pattern of heat transfer variation behind the forward cone is clear. On, and immediately aft of, the step the heat transfer falls to a low value and then rises as

*A similar basis for estimating the heat transfer appropriate to attached flow to such bodies as hemisphere cylinders, where substantial variations in local conditions occur, has given fair agreement with measurements.

the region of reattachment is approached. As with the pressure distribution, the pattern of heat transfer variation changes as the reattachment point moves on to the aft cone.

Perhaps a clearer picture of the heat transfer measurements can be obtained from the h_m/h_A plots (Fig.24). For heads H1 and H3 the variation of h_m/h_A with distance along the sting is apparently unaffected by Mach number. All heads have closely similar values of h_m/h_A behind the step - about 0.25 - but thereafter the patterns differ: head H1 showing the effect of reattachment on the sting and head H3 reattachment on the aft cone. Head H2 shows clearly the effect of transition from one type of flow to the other over about the same Mach number ranges as for head P2. The relationships for heads H2 and H3 are similar at a Mach number of 2 but thereafter they begin to differ in form until at a Mach number of 3 the relationship for head H2 is similar to that for head H1.

Where reattachment is on the sting the most rapid rise is complete by about 2 step-heights aft of the step which on the basis of the pressure data of Figs.12 and 15 is interpreted as about 2/3 of the distance to reattachment. The subsequent level and slope of the rise seem to be influenced to some extent by the step height. The level is less for head H2 (step height 2.56") than it is for head H1 (step height 1") and the maximum less apparent and relatively further from the step in units of step height. The trend in level would seem to support qualitatively the remarks in Ref.2 regarding the thickening effect of convergence on the separated boundary layer in such an axially-symmetric configuration, giving rise to reduced heating at and subsequent to reattachment.

On head H3 where reattachment is on the aft cone the values of h_m/h_A rise to about unity near the base of the aft cone. There are no data aft of this point to establish whether this represents a maximum value. A level of unity is in conformity with the convergence effects because in this case there should be little convergence and boundary layer thickening relative to reattachment on the sting and hence at reattachment relatively greater heating. A plot indicating the effect for the three heads at $M_o = 3$ is given in Fig.25.

The discussion above is based on results for accelerating flight and on results for decelerating flight down to a Mach number of 3.0. At Mach numbers below 3 in decelerating flight the wall temperatures are similar to the recovery temperatures and trends in the heat transfer data become obscured by increased scatter.

5.2.5 Comparison with theory

Chapman expressed the results of his theory[1] in terms of the ratio Q_m/Q_A, where Q_m is the heat flux integrated over the model wall bounding the separated region, Q_A is the heat flux integrated over the wake boundary, assuming the latter to be a solid surface with the flow attached to it.

Values of the ratio appropriate to the Mach number range in the present experiment are given in table 5.

Some of the assumptions that Chapman made were manifestly invalid for the configuration tested. For example, the length of the reattachment zone was not small compared with the length of the separated boundary layer. Nor was the Mach number constant along the separated layer: in this respect reattachment on the aft cone conforms more closely to the theoretical model than reattachment to the sting. The walls of the models were not isothermal

though in the early stages of accelerating flight variations in wall temperature were small (Fig.17).

Some experimental values of Q_m/Q_A have been calculated for both modes of reattachment and are presented in table 5 for comparison with Chapman's theoretical values.

The experimental values were adjusted to isothermal wall conditions by assuming that the local heat transfer coefficients were independent of wall temperature. When reattachment occurred on the sting the reattachment point was assumed to be three step heights from the step and the wake boundary to be in the form of a truncated cone: when reattachment occurred on the aft cone the wake boundary was assumed to be a cylinder of the same diameter as the base of the forward cone. It is seen that the experimental values are in considerable disagreement with the magnitudes predicted by theory. Also from Fig.24 there does not seem to be any marked trend with Mach number over the range of the present investigation.

5.2.6 Comparison with other experiments

This conclusion is also corroborated by Larson's data in Ref.2. The test configuration in his investigation was a cone cylinder with an aft facing step followed by a sting and divergence aft to the cylinder diameter again - it was very similar to the test configuration of the present investigation. The overall scope of his measurements included Mach numbers from 0.3 to 4 and Reynolds numbers based on local stream conditions and wetted distance from the cone apex to reattachment of 10^5 to 4×10^6. For an evaluation of Q_A, the solid wall of the cylinder was actually replaced aft of the step and the heat transfer to it measured. It was implied that this measurement corresponded to the heat transfer appropriate to the wake replaced by a solid surface. - This implication would have been far from valid in the present investigation as can be seen from the comparison of the pressure distributions in Fig.13. - Larson found that over the Mach number range of his investigation Q_m/Q_A was about 0.6 and apparently independent of Mach number. He attributed the discrepancy between theory and experiment to an error in the basic assumption of the theory. Chapman assumed that the total temperature of air drawn into the boundary layer from the reverse flow region is the same as the wall temperature whereas Larson found from a probe survey that it was much closer to the total temperature of the flow outside the boundary layer.

Although Larson found no marked Mach number effect on Q_m/Q_A, he did find that the ratio varied as the Reynolds number to the power - 1/5. Values of the ratio based on his data are presented for comparison with the present experimental data in table 5. The two sets of values do not seem to correlate. The values for the present investigation are generally greater than his trend predicts. It may be that the trend with Reynolds number is sensitive to details of the geometry of the reattachment region.

Larson also varied the step height on his configuration but, because the heat flux over undefined areas of his variants was not taken into account, the effect of this variation could not be satisfactorily assessed. The data from the variants did however corroborate the trend with Reynolds number.

Powers et al[3] in a shock-tube investigation obtained a mean value of about 1/3 for h_m/h_A for turbulent flow in the wake of a step behind a hemisphere-cylinder. The ratios of sting to base diameter (0.3 and 0.6) were similar to those used in the present experiment (0.25, 0.54 and 0.82).

The basis of their h_A was a theoretical one which took dissociation into account. Reattachment in their experiment was on a cylindrical sting and appropriate to an expansion angle of about 20^o. The local Mach number prior to detachment was estimated to vary between about 1.8 and 2.1 corresponding to a local value just outside the wake boundary of about 2.8 to 3.0. The relevant local Reynolds number based on wetted distance from the stagnation point to reattachment for this flow regime varied from about 0.5×10^6 to 1.6×10^6. Within this range h_m/h_A was apparently independent of Reynolds number and observed variations within the separated region were less than the experimental scatter of about ± 20%. The mean value of 1/3 quoted is in fair agreement with the levels near the step-sting junction for the present data.

6 CONCLUSIONS

(a) Local heat transfer and surface pressure have been measured over regions of separated flow associated with a turbulent boundary layer. The separated flow was appropriate to aft facing steps of various heights behind a sting mounted cone of 15^o semi-angle. The maximum Mach number achieved was about 4 and the Reynolds number about 50×10^6 based on cone length.

(b) Two different forms of wake were detected: one associated with reattachment on the sting, i.e. a relatively great convergence of the wake boundary, and one associated with reattachment on a conical surface aft of the sting, i.e. a small wake convergence. Differing patterns of heat transfer and pressure distributions were obtained depending on which type of flow occurred, but for a given type of flow the trends in the heat transfer and pressure variations were similar (Fig.26).

(c) Some collapse of the separated flow heat transfer data with respect to Mach number was obtained by comparing them with estimated values appropriate to local conditions outside the wake. Close to the step the heat flow in the separated region was about 25% of the estimated value for attached flow over a solid surface replacing the wake boundary. Towards and beyond reattachment the ratio of the two values rose to near unity. The measurements suggest that the amount of rise at and beyond reattachment is dependent upon the wake convergence, becoming smaller as the convergence increases. This is qualitatively consistent with the known effect that increasing convergence implies increasing boundary layer thickness at reattachment.

(d) There was no evidence of a marked maximum in the heat flux in the reattachment region.

LIST OF SYMBOLS

Symbol		Units
B	Boltzmann's constant = 2.78×10^{-12} CHU/ft^2 sec $(^oK)^4$	
c	specific heat of wall	CHU/lb ^oK
d	base diameter of forward cone	ins
E	$= [1/\varepsilon_i + 1/\varepsilon_d - 1]^{-1}$	-

LIST OF SYMBOLS (CONTD)

Symbol		Units
h_A	theoretical heat transfer coefficient appropriate to local conditions and unseparated flow - see section 4.2	CHU/ft^2 sec ^oK
h_{fp}	theoretical heat transfer coefficient referring to free stream conditions	
h_m	experimental local heat transfer coefficient	
i	specific enthalpy of air	CHU/lb
k	thermal conductivity	CHU/ft ^oC sec
p	static pressure	lb/ft^2
q_{aero}	aerodynamic heat flux	CHU/ft^2 sec
$q_{conduction}$	heat flux conducted across internal air gap	
$q_{free\ convection}$	additional heat flux across air gap arising from free convection	
$q_{lateral}$	change in local heat flux arising from temperature gradients along the measuring wall	
q_{nett}	nett local heat flux	
$q_{radiation}$	nett local heat flux arising from the radiation from both surfaces of the measuring wall	
q_{re}	nett local radiative heat flux from the external surface of the measuring wall	
q_{ri}	nett local radiative heat flux from the internal surface of the measuring wall	
Q_A	aerodynamic heat flux, adjusted to isothermal wall conditions, integrated over the wake boundary assuming the latter to be a solid surface with the flow attached to it	CHU/sec
Q_m	aerodynamic heat flux, adjusted to isothermal wall conditions, integrated over the model wall bounding the separated region	CHU/sec
R	recovery factor	-
r_A	distance of reattachment point from axis of head	in.
r_b	radius of base of forward cone	
s	step height	

LIST OF SYMBOLS (CONTD)

Symbol		Units
T	temperature	^{o}K
T_t	temperature appropriate to incoming radiation	^{o}K
t	time	sec
x	wetted distance from step-sting junction	in.
y	wetted distance from apex of forward cone	in.
α	angle of incidence	degrees
ε	emissivity of surface appropriate to radiative heat flux	-
θ	angle between directions of local flow and free stream	degrees
ξ	$= x/s$	-
σ	density of measuring wall	lb/ft^3
τ	thickness	in.
ϕ	angular coordinate defining meridian	degrees

Suffixes

a	refers to internal air gap
d	refers to external surface of durestos wall
e	refers to external surface of measuring wall
i	refers to internal surface of measuring wall
o	refers to free stream conditions
r	refers to conditions where $q_{aero} = 0$
w	refers to measuring wall or measuring wall temperature conditions

LIST OF REFERENCES

No.	Author	Title, etc.
1	Chapman, D.R.	A theoretical analysis of heat transfers in regions of separated flow. NACA T.N.3792. October 1956.
2	Larson, H.K.	Heat transfer in separated flows. J.Aero/Space Sciences. November 1959.
3	Powers, W.E. Stetson, K.F. Adams, M.C.	A shock tube investigation of heat transfer in the wake of a hemisphere cylinder with application to hypersonic flight. I.A.S. Report No.59-35. January 1959.
4	Nielson, H.V.	Heat transfer on an afterbody immersed in the separated wake of a hemisphere. NACA R.M. A57K07a. January 1958.
5	Naysmith, A.	Heat transfer and boundary layer measurements in a region of supersonic flow separation and reattachment. A.R.C. 20,601. May 1958.
6	Gadd, G.E. Cope, W.F. Attridge, J.L.	Heat transfer and skin friction measurements at a Mach number of 2.44 for a turbulent boundary layer on a flat surface and in regions of separated flow. A.R.C. R & M 3148. October 1958.
7	Edited by Wright Baker, H.	Modern workshop technology. Vol.2, Chap.14, Cleaver-Hume Press, London. 1950.
8	Kerr, C.E.	An introduction to the apparatus at present in use in G.W., free flight research. Unpublished M.O.A. Report.
9	Walters, W. Irvine, F.	Laboratory anf field trials of single channel version of the R.A.E. G.W.465 megacycles sub-miniature telemetry system. Unpublished M.O.A. Report.
10	Collins, S.J.	Application of built-in constant thickness diaphragms to pressure and other transducers. Bristol Aeroplane Co. Tech. Note No.57. 1953.
11	Walters, W. Walker, D.	Further experiments in temperature measuring technique involving mixture of low level signal with variable inductance transducer output. Unpublished M.O.A. Report.
12	Lawrence, T. Walters, W.L.	Note on measurement of the pressure distribution down the tail cone of a bomb at transonic speeds using the rocket-boosted model technique. A.R.C.1 15497. July 1952.

LIST OF REFERENCES (CONTD)

No.	Author	Title, etc.
13	Picken, J.	Notes on a reduction procedure for temperature data from free flight telemetry. A.R.C. 21389. April 1959.
14	Picken, J.	Estimation of transient one-dimensional heat flux to a thick wall from the variation of temperature at an insulated surface. Unpublished M.O.A. Report.
15	Monaghan, R.J.	Formulae and approximations for aerodynamic heating rates in high speed flight. A.R.C. C.P. 360. October 1955.
16	Lee, D.B. Faget, M.A.	Charts adapted from van Driest's turbulent flat plate theory for determining values of turbulent aerodynamic friction and heat transfer coefficients. NACA T.N.3811. October 1956.
17	Eckert, E.R.G.	Survey on heat transfer at high speeds. Transactions of the American Society of Mechanical Engineers. Vol.78, pp.1273-1284. August 1956.
18	Fuller, L. Reid, J.	Experiments on two-dimensional base flow at M = 2.4. A.R.C. R & M 3064. February 1956.
19	Kopal, Z.	Tables of supersonic flow around cones. M.I.T. Technical Report No.1, Cambridge, Massachussets. P.18356. 1947.
20	Ames Research Staff	Equations, tables and charts for compressible flow. NACA Report 1135. 1953.
21	Kopal, Z.	Tables of supersonic flow around yawing cones. M.I.T. Technical Report No.3, Cambridge, Massachussets, 1947.
22	Hastings, R.C.	A note on the interpretation of base pressure measurements in supersonic flows. A.R.C. C.P. 409, June 1958.
23	Johannesan, W.H.	Experiments on supersonic flow past bodies of revolution with annular gaps of rectangular section. Philosophical Magazine SER 7, Vol.46, No.372. January 1955.
24	Kavanau, L.L.	Results of some base pressure experiments at intermediate Reynolds numbers with M = 2.84. Journ. Aero. Soc. Vol.21, pp.257-274. 1954.

LIST OF REFERENCES (CONTD)

No.	Author	Title, etc.
25	Johnson, H.A. Rubesin, M.W.	Design manual for determining the thermal characteristics of high speed aircraft. USAF T.R.5632. (P35235) September 1947.
26	Jakob, M.	Heat transfer. Vol.1. John Wiley and Son, New York. 1949.

APPENDIX 1

COMMENTS ON NON-AERODYNAMIC HEAT FLUXES TO MEASURING HEADS

On all heads the heat flux arising from radiation and conduction to the interior were significant towards the ends of the flights and in particular with respect to the definition of conditions for zero aerodynamic heat flux and thus the evaluation of experimental recovery factors.

The heat flux arising from radiation is composed of two components namely the radiation heat flux from the external surface of the measuring wall, q_{re}, and that from the internal surface, q_{ri}.

$$q_{re} = B \varepsilon_e (T_w^4 - T_t^4)$$

where B is Boltzmann's constant = 2.78×10^{-12} CHU/ft^2 sec $(^oK)^4$

ε is the emissivity of the surface

T_t is the temperature appropriate to the incoming radiation* to the external surface

suffix e refers to the external surface of the measuring wall.

$$q_{ri} = B E (T_w^4 - T_d^4) \qquad (7)$$

where $$E = \left[\frac{1}{\varepsilon_i} + \frac{1}{\varepsilon_d} - 1 \right]^{-1}$$

suffix i refers to the internal surface of the measuring wall

d refers to the external surface of the durestos wall.

At launch both surfaces of the measuring head were relatively free from oxidation. The emissivity of steel in this condition is of the order of 0.1 over the temperature range of the experiment[25]. However it is likely that the outside surface will oxidise during flight particularly if the wall becomes hot. In this condition the relevant surface emissivity becomes about 0.8[25]. The emissivity of the inside surface may also be increased by the decomposition of carboniferous emanations from the durestos inner wall as it is heated. The variation with temperature of the quotient of $q_{radiation}$ and surface emissivity is indicated in Fig.7. In view of the uncertainty of the surface condition no satisfactory estimate could be made for $q_{radiation}$ in this experiment.

*For example solar radiation which can give rise to a heat flux of 0.068 CHU/ft^2 sec.

The heat conducted across the air gap between the two walls may be obtained from

$$q_{conduction} \doteqdot \frac{k_a(T_w - T_d)}{\tau_a} \qquad (8)$$

where k_a is the mean thermal conductivity of air in the temperature range T_d to T_w

T_d is the temperature of the external durestos surface

τ_a is the thickness of the air gap.

The variation of $q_{conduction}$ with T_w for an assumed value of T_d is shown in Fig.7. Over the temperature range of the experiment $q_{conduction}$ is comparable in magnitude to $q_{radiation}$. It is also subject to uncertainty since it is dependent on the temperature of the insulated wall which might be subject to appreciable variations.

Free convection is not likely to make a significant contribution to the heat flux across the air gap compared with conduction, since under the conditions of the experiment the relevant Grashof number has a maximum value of the order of 6,500 for which free convection has been shown to have only a small effect on heat flux[26].

The diffusivity of the air gap was comparable to that of the measuring wall and thus effects on the heat flux across it arising from its heat capacity would be negligible.

TABLE 1

Summary of Flights

Reference No.	P1	P2	P3	H1	H2	H3
Date	30.4.58	16.7.58	2.10.58	21.7.58	2.10.58	4.2.59
All-up weight before firing lb	784	790	788	782	789	757
Telemetered measurements	Static pressure at 21 stations. Normal and lateral acceleration.			Temperature at 11 stations.		
Step height inches	1	2.56	4.13	1	2.56	4.13
Sting diameter/ base diameter	0.818	0.535	0.250	0.818	0.535	0.250
Length of sting, inches	19.6	15.3	11.0	19.6	15.3	11.0
Wetted length of aft cone	1.6	6.2	10.7	1.6	6.2	10.7
Mean wall thickness inches — Forward cone	-	-	-	0.0520	0.0545	0.0527
Mean wall thickness inches — Other head components	-	-	-	0.0310	0.0296	0.0298
Maximum velocity f/s	4334	4136	4261	4385	4187	4404
Maximum Mach No.	3.90	3.75	3.86	3.95	3.81	4.03
Time to maximum velocity, sec	3.34	3.40	3.46	3.38	3.36	3.60
Time to 2,000 f/s	9.44	8.00	9.20	9.80	8.30	9.10
Maximum altitude ft	9810	10,310	10,660	9220	9670	9120
Time to maximum altitude, sec	20.54	20.65	20.45	19.28	19.74	19.35

TABLE 2

Location of Pressure Orifices

Head Reference No.	P1					P2					P3				
Step height	1"					2.56"					4.13"				
Location	Station No.	Coordinates* y inches	x inches	ξ	φ degrees	Station No.	Coordinates* y inches	x inches	ξ	φ degrees	Station No.	Coordinates* y inches	x inches	ξ	φ degrees
Forward Cone	1	20.50	-	-	0	1	20.50	-	-	0	1	20.49	-	-	0
	2	20.50	-	-	120	2	20.51	-	-	120	2	20.48	-	-	120
	3	20.50	-	-	240	3	20.51	-	-	240	3	20.50	-	-	240
Step	4	-	0.25	0.25	180	4	-	0.7	0.27	180	4	-	1.00	0.24	180
	5	-	0.75	0.75	0	5	-	1.95	0.76	0	5	-	3.01	0.73	0
Sting	6	-	0.1	0.1	0	6	-	0.14	0.06	0	6	-	0.10	0.03	0
	7	-	0.8	0.8	0	7	-	1.87	0.72	0	7	-	1.79	0.43	0
	8	-	1.2	1.2	180	8	-	2.72	1.06	180	8	-	2.69	0.65	180
	9	-	1.6	1.6	0	9	-	3.64	1.42	0	9	-	3.59	0.87	0
	10	-	2.4	2.4	0	10	-	5.43	2.12	0	10	-	5.37	1.30	0
	11	-	2.8	2.8	180	11	-	6.32	2.47	180	11	-	6.28	1.52	180
	12	-	3.2	3.2	0	12	-	7.23	2.82	0	12	-	7.18	1.74	0
	13	-	4.0	4.0	0	13	-	9.42	3.52	0	13	-	8.99	2.18	0
	14	-	4.8	4.8	180	14	-	9.92	3.88	180	14	-	9.88	2.39	180
	15	-	5.6	5.6	0	15	-	10.81	4.22	0	15	-	10.78	2.61	0
	16	-	7.2	7.2	0	16	-	12.62	4.93	0					
	17	-	10.6	10.6	0	17	-	13.82	5.40	180					
	18	-	14.0	14.0	0	18	-	15.03	5.87	0					
	19	-	15.7	15.7	180										
	20	-	19.0	19.0	0										
Aft Cone	21	-	20.4	20.4	0	19	-	17.08	6.67	0	16	-	11.83	2.86	0
						20	-	18.59	7.26	180	17	-	12.86	3.11	180
						21	-	20.99	8.20	0	18	-	14.04	3.40	0
											19	-	15.26	3.70	180
											20	-	16.48	3.99	0
											21	-	18.80	4.55	0

* Coordinates are defined in Fig.1

y = wetted distance from apex of forward cone

x = wetted distance from step-sting junction

$\xi = \frac{x}{\text{step height}}$

ϕ = angular coordinate defining angular position normal to axis of symmetry

TABLE 3

Location of Thermocouples

Head Ref. No.	Step height inches	Station Ref. No.	Location of station					Local wall thickness inches	Surface C.L.A. micro-inches
			Component	Coordinates*					
				y inches	x inches	ξ	ϕ degrees		
H1	1	1	Forward Cone	19.22	-	-	0	0.0537	12-14
		2	"	19.22	-	-	180	0.0502	-
		3	Step	-	0.75	0.75	0	0.0335	-
		4	"	-	0.25	0.25		0.0335	-
		5	Sting	-	0.6	0.6		0.0300	30-35
		6		-	1.2	1.2		0.0301	-
		7		-	1.6	1.6		0.0301	-
		8		-	1.8	1.8		0.0301	40-45
		9		-	2.0	2.0		0.0301	-
		10		-	3.2	3.2		0.0304	40-45
		11	↓	-	7.2	7.2		0.0310	-
H2	2.56	1	Forward Cone	19.22	-	-		0.0545	18-20
		2	Sting	-	1.54	0.60		0.0295	20-25
		3		-	2.30	0.90		0.0294	-
		4		-	3.07	1.20		0.0295	15-17
		5		-	4.10	1.60		0.0297	-
		6		-	4.61	1.80		0.0296	18-20
		7		-	5.12	2.00		0.0295	-
		8		-	6.66	2.60		0.0296	-
		9		-	8.19	3.20		0.0297	-
		10		-	11.26	4.40		0.0296	-
		11	↓	-	13.00	5.08		0.0300	-
H3	4.13	1	Forward Cone	19.20	-	-		0.0527	13-15
		2	Step	-	2.06	0.50		0.0315	35-40
		3	Sting	-	2.06	0.50		0.0280	25
		4		-	5.50	1.33		0.0290	30-35
		5		-	9.50	2.30		0.0295	15-20
		6		-	13.96	3.38		0.0310	28
		7		-	15.16	3.67		0.0307	-
		8		-	15.76	3.82		0.0304	28
		9		-	16.56	4.01		0.0300	-
		10		-	18.16	4.40		0.0294	25
		11	↓	-	20.16	4.88	↓	0.0280	-

* Coordinates are defined in Fig.1

y - wetted distance from apex of forward cone

x - wetted distance from step-sting junction

$\xi = \frac{x}{\text{step height}}$

ϕ - angular coordinate defining angular position normal to axis of symmetry

TABLE 4

Uncertainty in Basic Measurements

Basic measurement	Uncertainty
Velocity	± 2 f/s
Height	± 5 ft
Ambient pressure	± 0.07 lb/in.^{2}
Ambient temperature	± 1°C
Surface pressure (Forward cone)	± 1.5 lb/in.^{2}
(Aft cone)	
Sting	± 0.5 lb/in.^{2}
Wall temperature (individual measurements)	random component ± 8°C
	systematic component ± 15°C

TABLE 5

Comparison of $\frac{Q_m}{Q_A}$ with Theory

Mach No.	Free stream	2		3			3.5
	Local*	3.0	2.2	4.5	4.4	3.4	5.2
Reynolds No. $\times 10^{-6}$	Free stream/ft	13.3	14.8	20.1	20.1	21.4	23.3
	Local*	14.0	45.5	14.9	20.1	56.1	19.7
Head Ref. No.		H1	H3	H1	H2	H3	H2
Mode of Reattachment**		s	a	s	s	a	s
$\frac{Q_m}{Q_A}$	Experiment	0.81	0.39	0.71	0.49	0.45	0.43
	Larson[2]/	0.38	0.30	0.38	0.35	0.29	0.35
	Chapman[1]	1.6		1.0			0.9

* Local values of Mach number and Reynolds number are appropriate to conditions just aft of detachment. The length for the latter is from the apex of the cone to reattachment.

** s denotes reattachment on the sting which is assumed to occur at 3 step heights from the step-sting junction

a denotes reattachment on the aft cone and for the purpose of evaluating Q_m/Q_A, reattachment is assumed to occur at x = 21.7".

/ Larson's value is obtained from $Q_m/Q_A = 10.2\ R_e^{-1/5}$.

The data for the present experiment are relevant to accelerating flight.

Printed in England for Her Majesty's Stationery Office by the Royal Aircraft Establishment, Farnborough. W.T.60.K4.

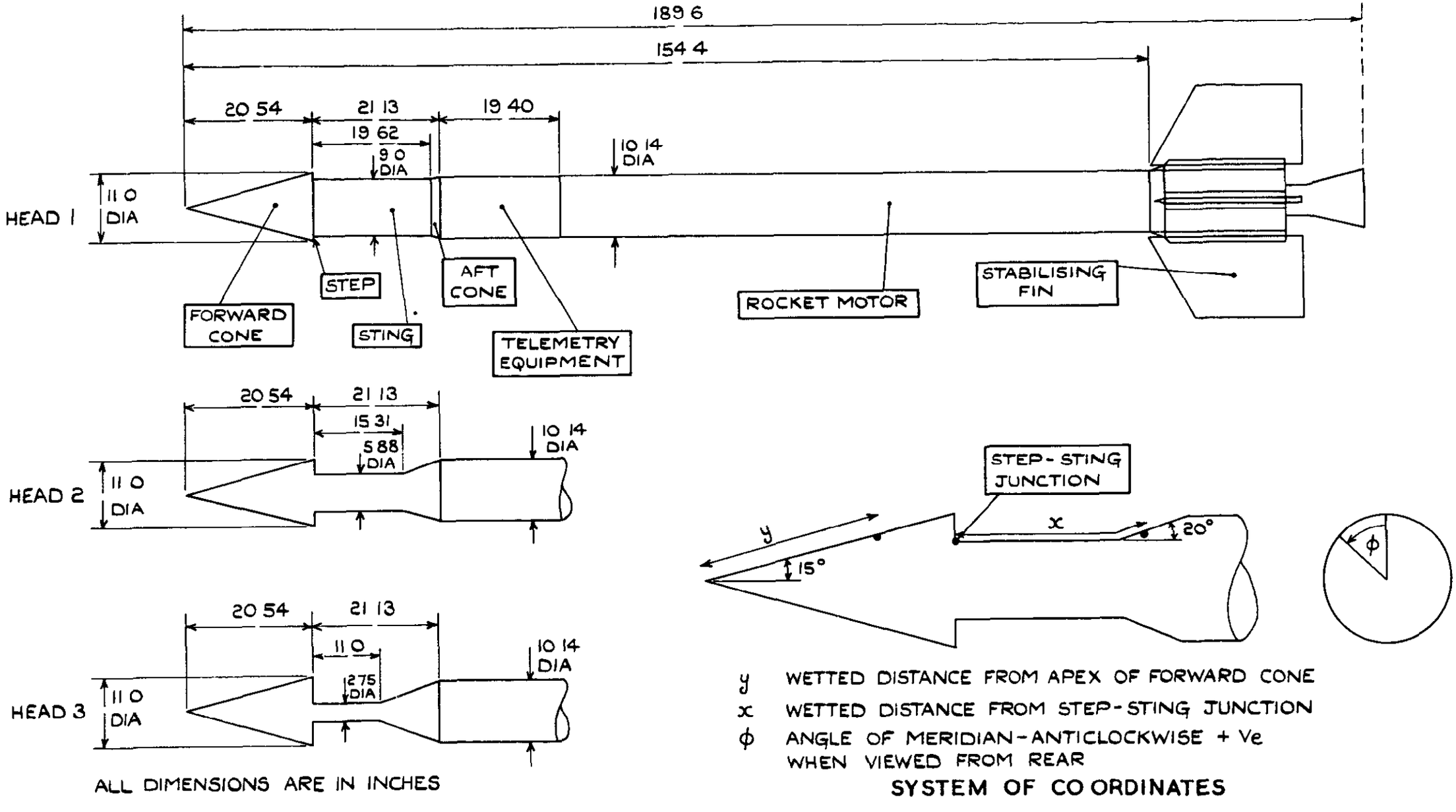

FIG.1. TEST VEHICLE AND HEADS.

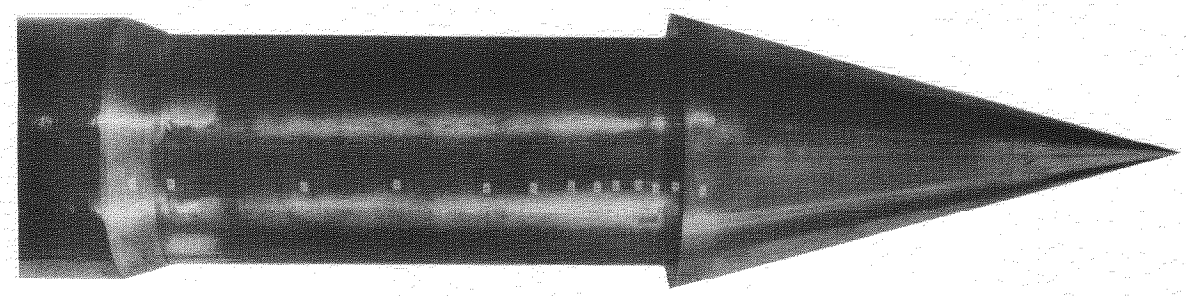

HEAD P1

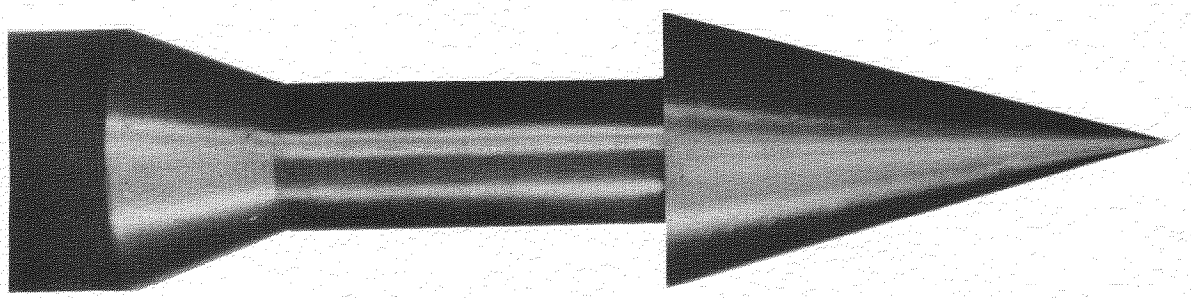

HEAD P2

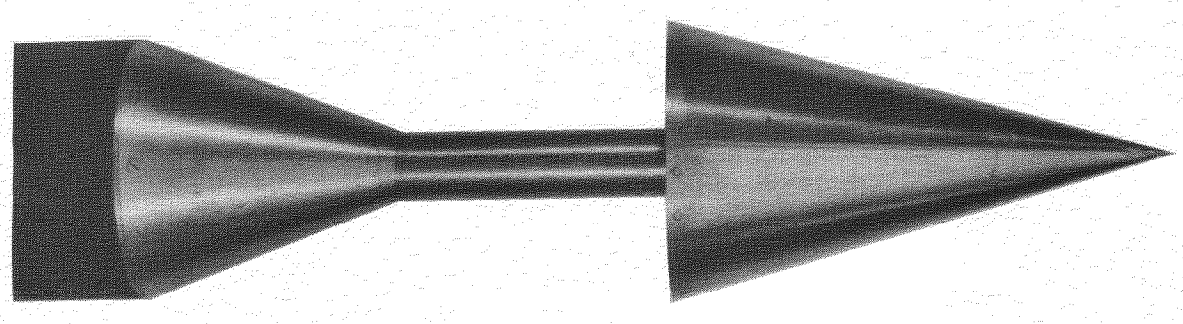

HEAD P3

FIG. 2. PHOTOGRAPHS OF HEADS

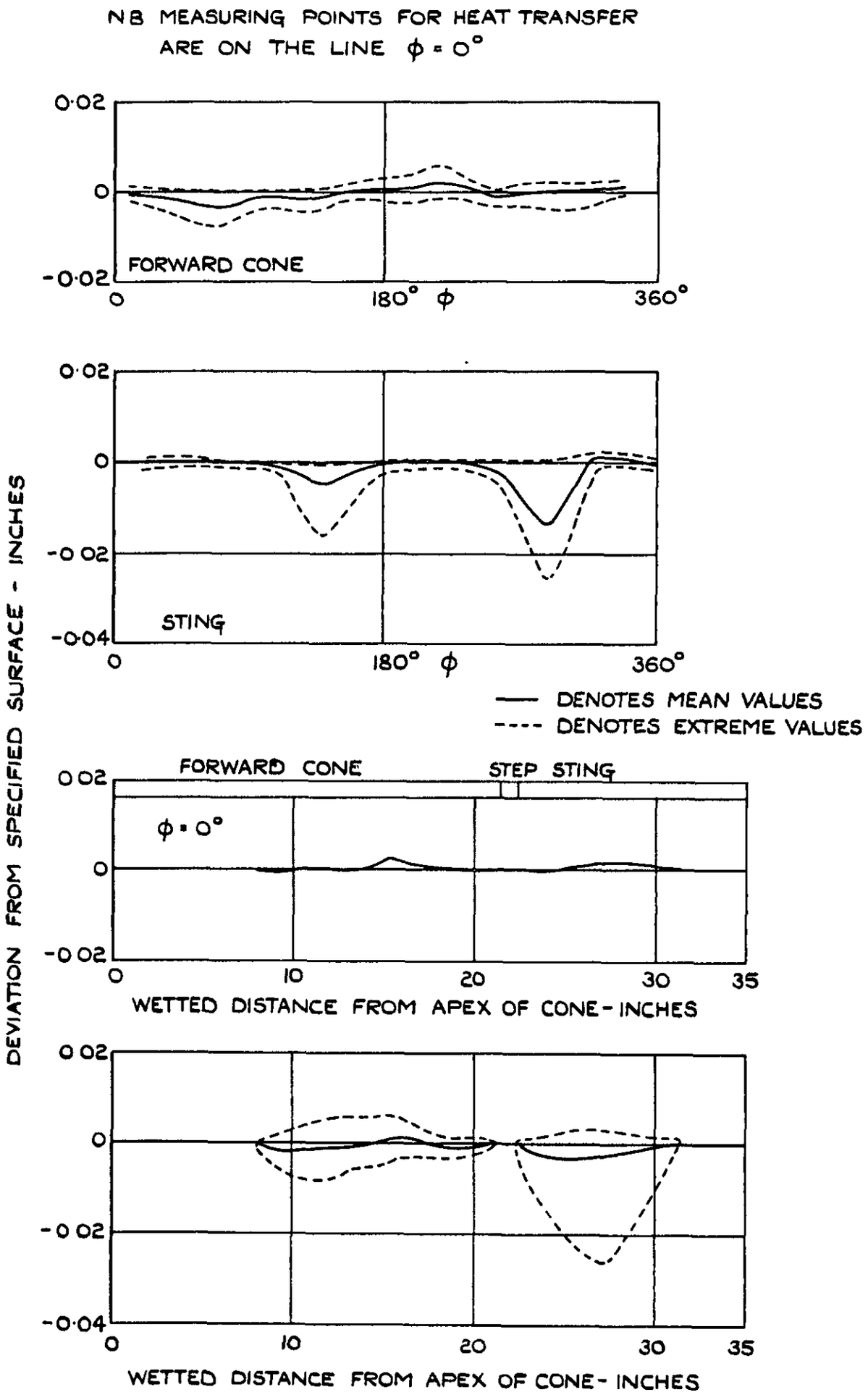

FIG. 3. TYPICAL SURFACE PROFILE (HEAD H1)

LOCATIONS OF MEASURING STATIONS ARE DENOTED THUS ●. ADJACENT NUMBERS ARE STATION REFERENCE NUMBERS LISTED IN TABLES 2 AND 3.

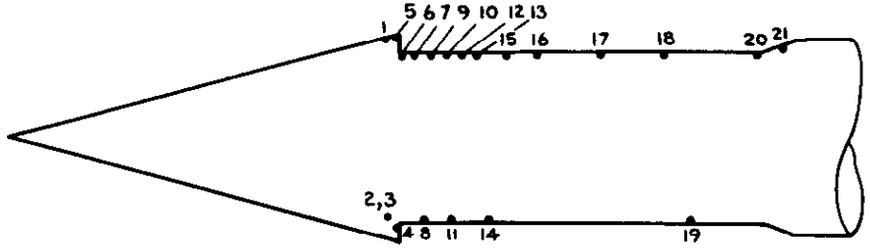

HEAD P1

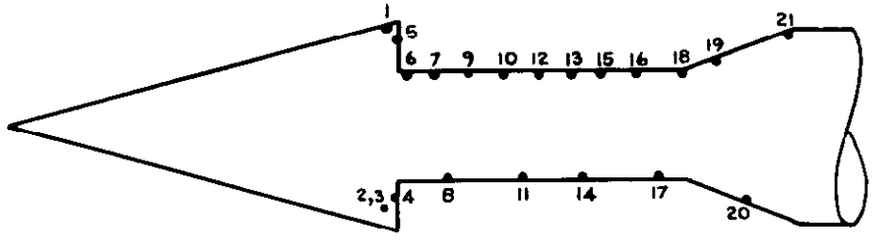

HEAD P2

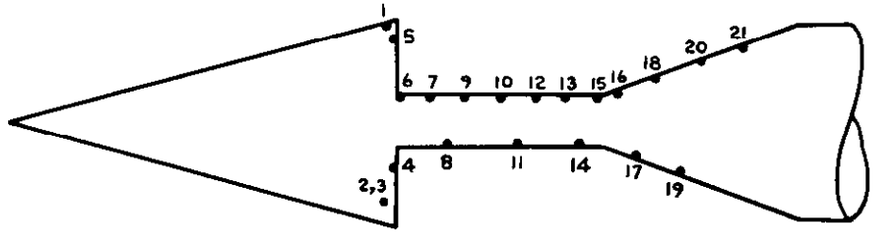

HEAD P3

PRESSURE - ORIFICE LOCATIONS

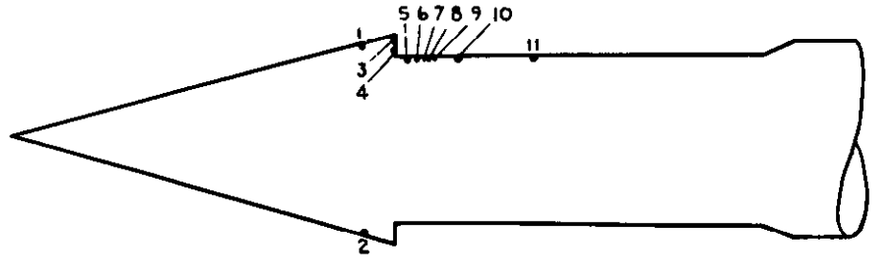

HEAD H1

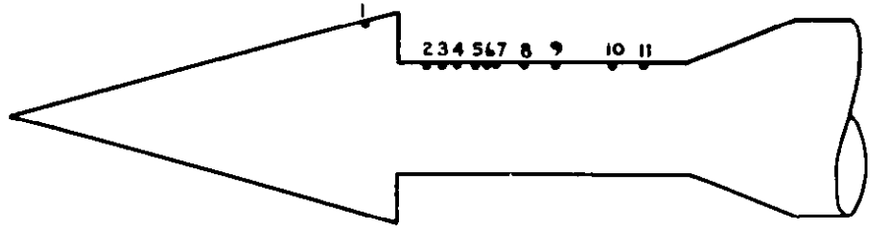

HEAD H2

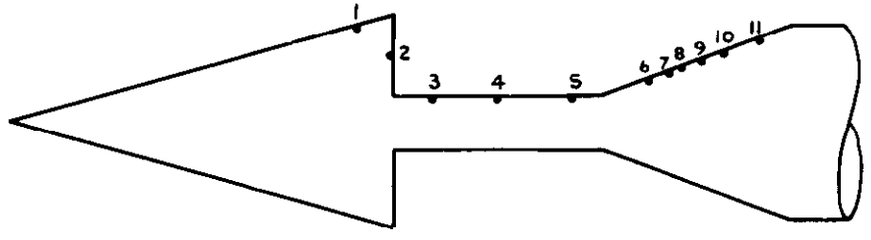

HEAD H3

THERMOCOUPLE LOCATIONS

FIG. 4. LOCATION OF MEASURING POINTS.

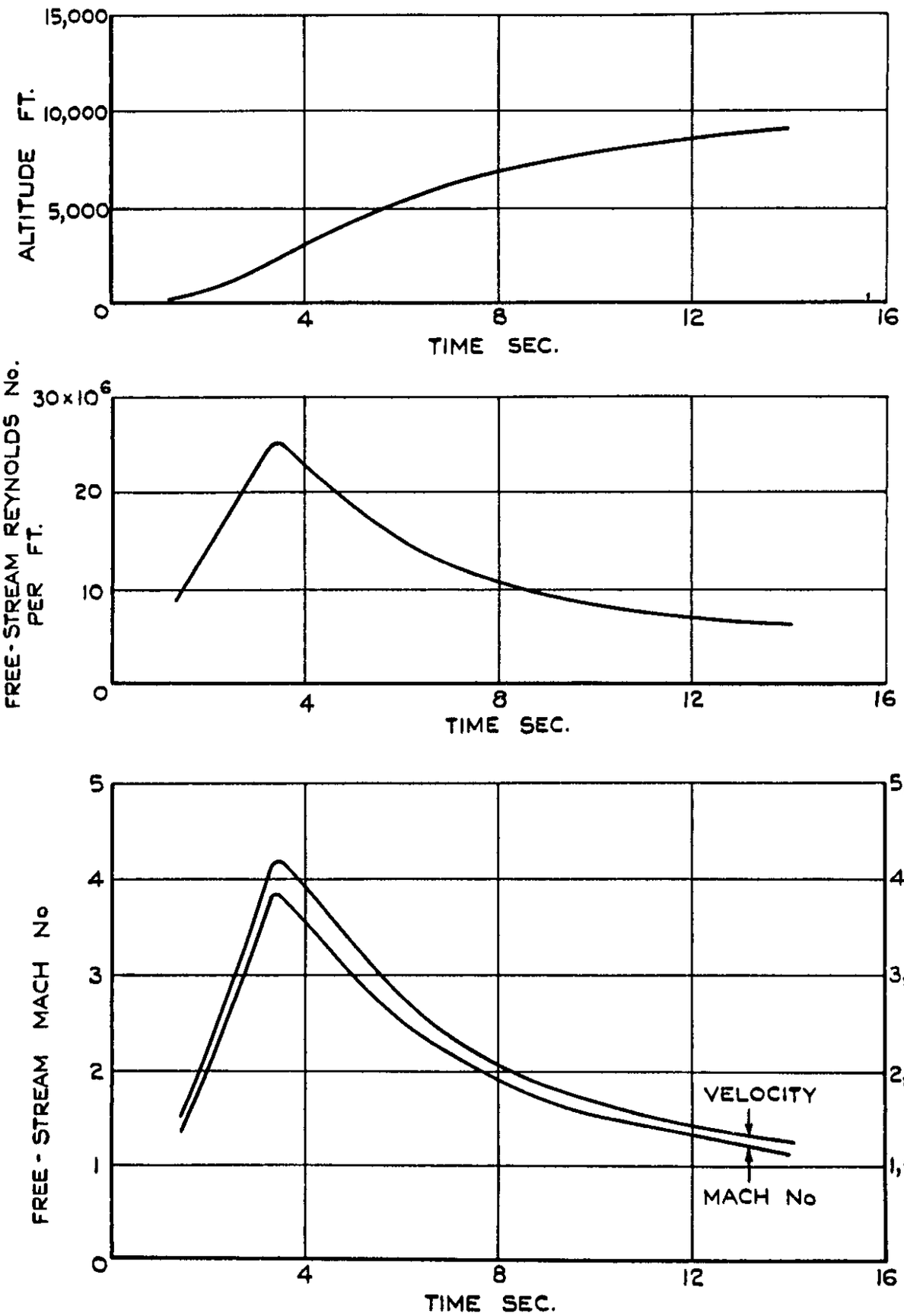

FIG. 5(a) TYPICAL TRAJECTORY DATA (HEAD H.2)

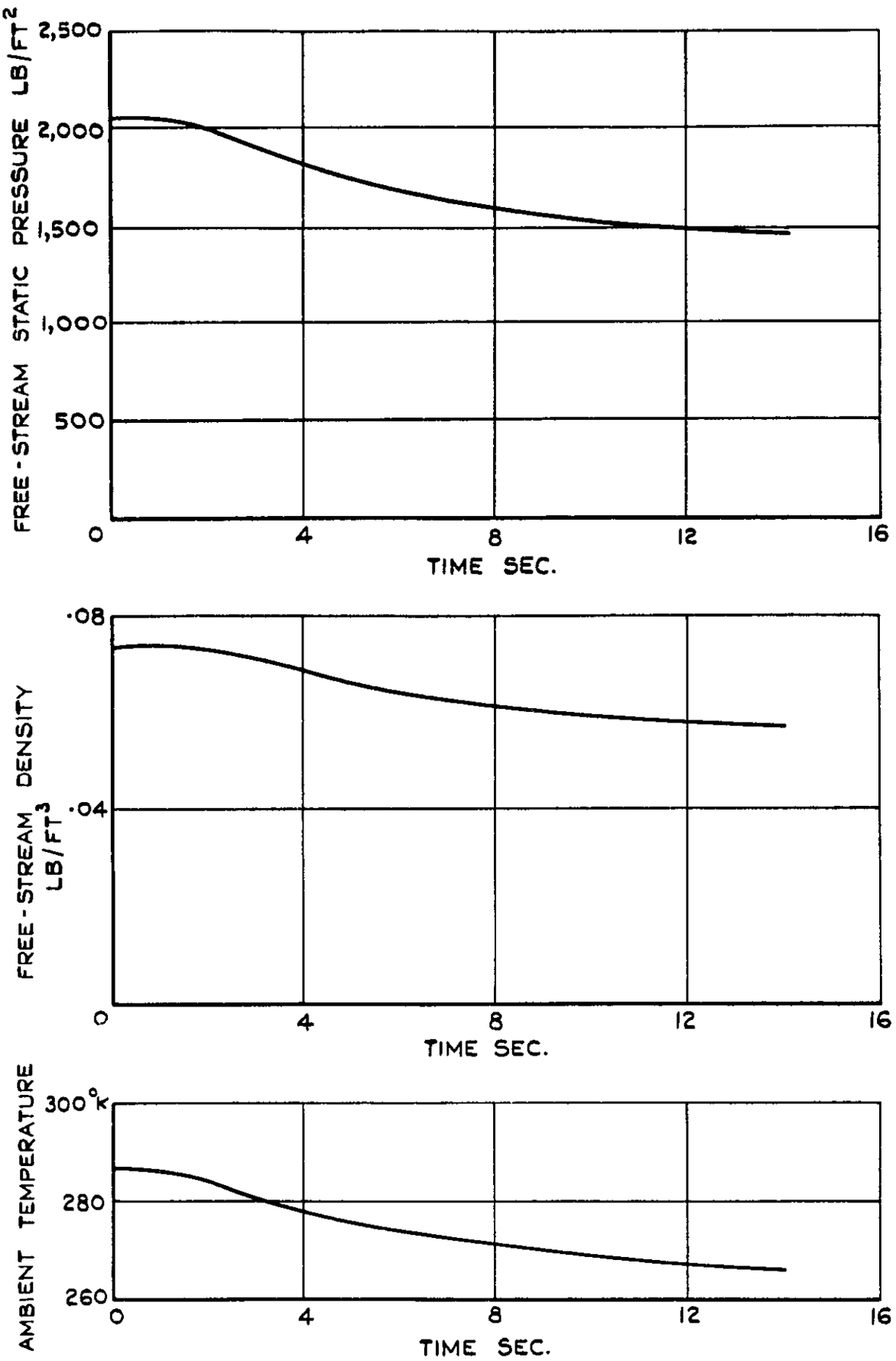

FIG. 5 (b) TYPICAL TRAJECTORY DATA (HEAD H.2)

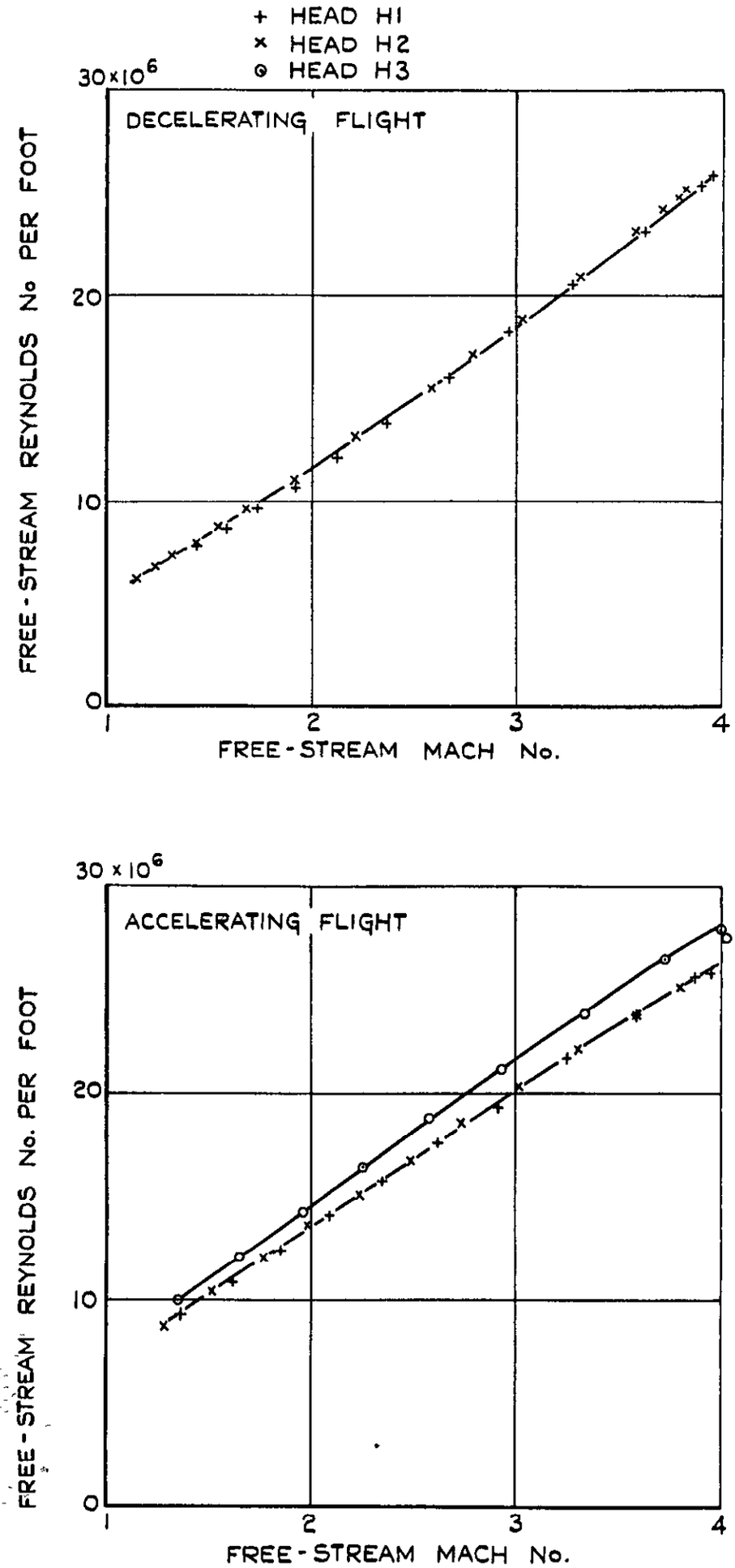

FIG.6. VARIATION OF REYNOLDS No. PER FOOT WITH MACH No. FOR HEADS H1, H2 AND H3.

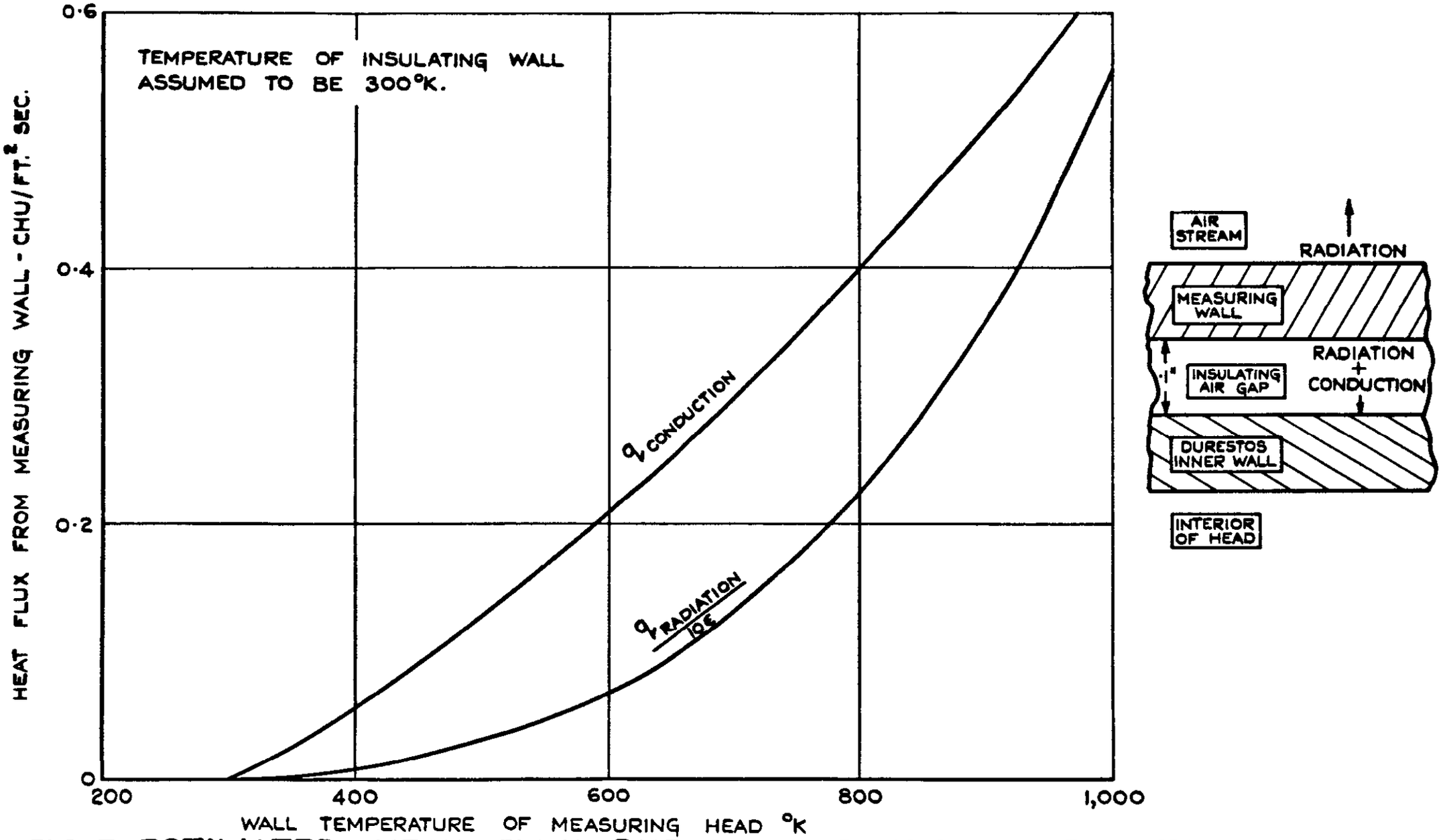

FIG. 7. ESTIMATED HEAT FLUX DUE TO RADIATION AND INTERNAL CONDUCTION FROM THE MEASURING WALL.

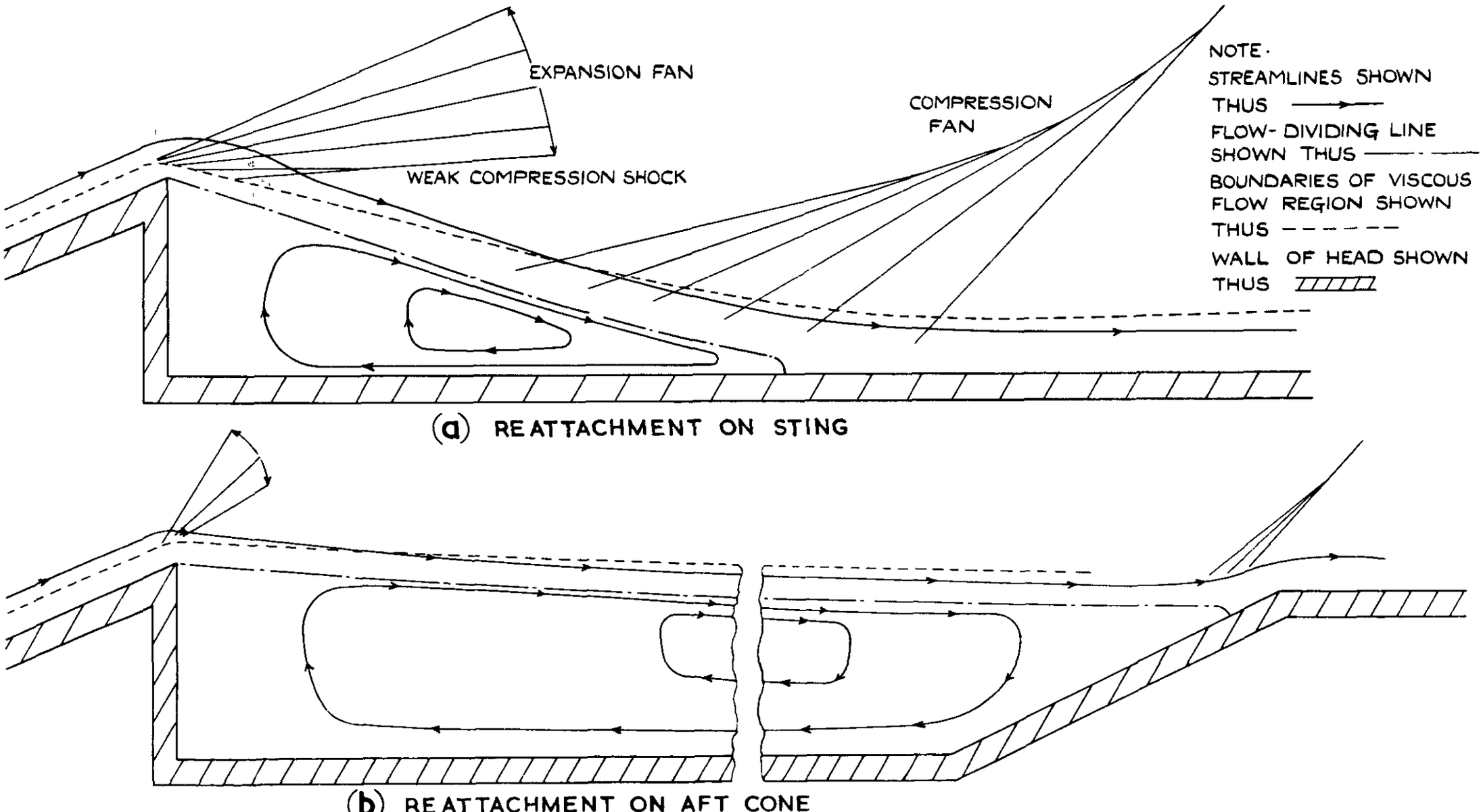

FIG. 8. SCHEMATIC DIAGRAM SHOWING TWO MODES OF REATTACHMENT.
(AFTER REF. 18)

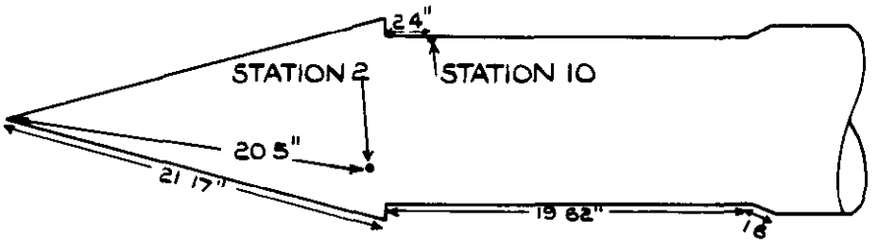

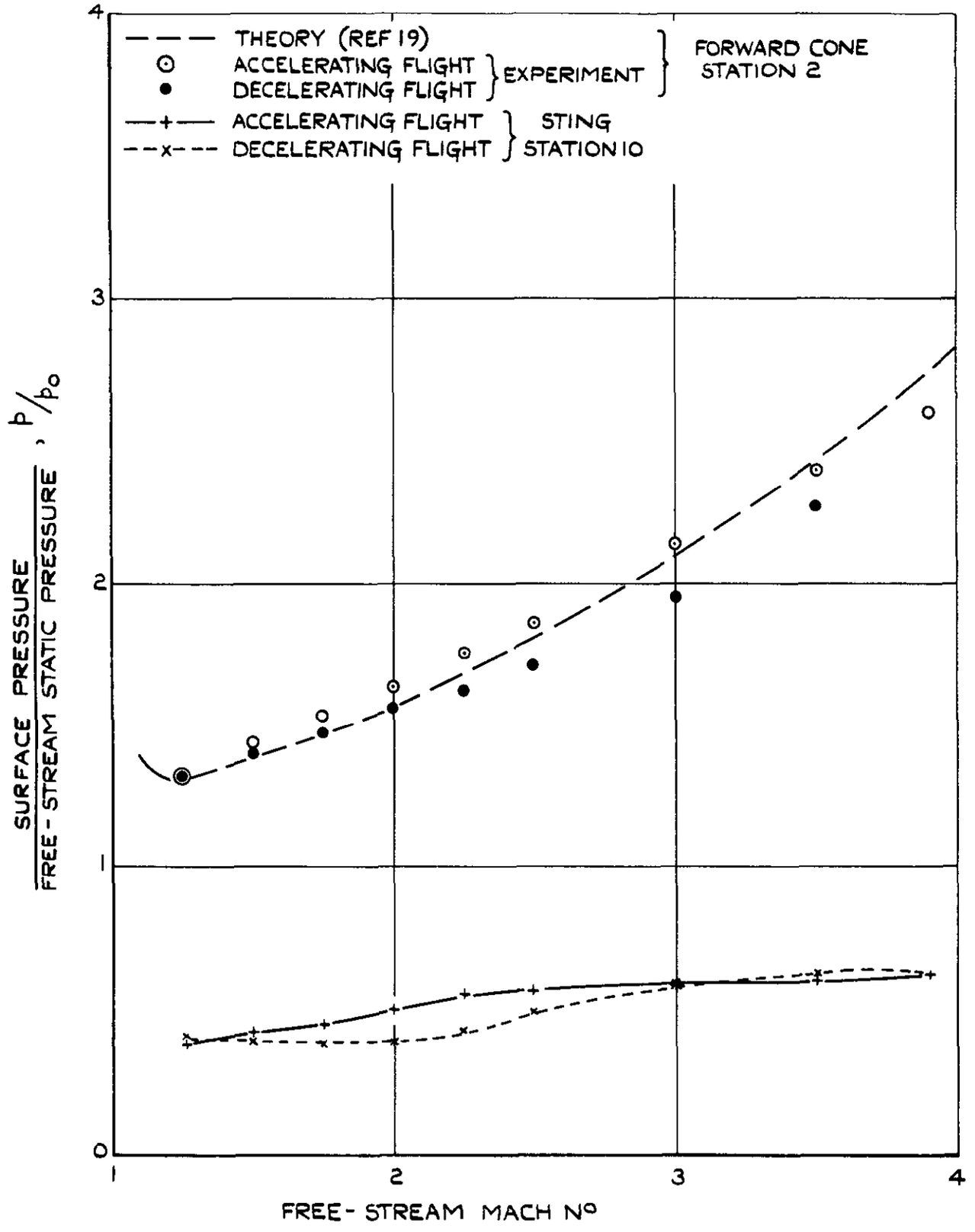

FIG. 9 (a) TYPICAL VARIATIONS OF SURFACE PRESSURE RATIOS WITH MACH No.-HEAD P1 FORWARD CONE AND STING.

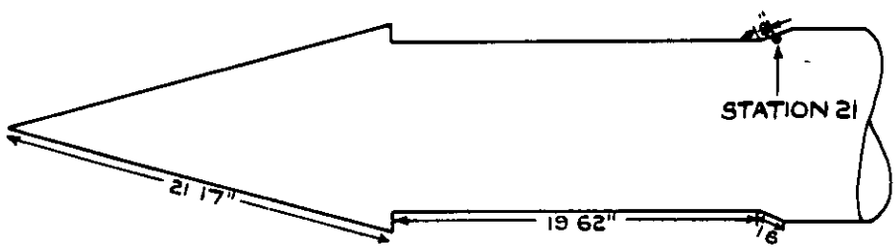

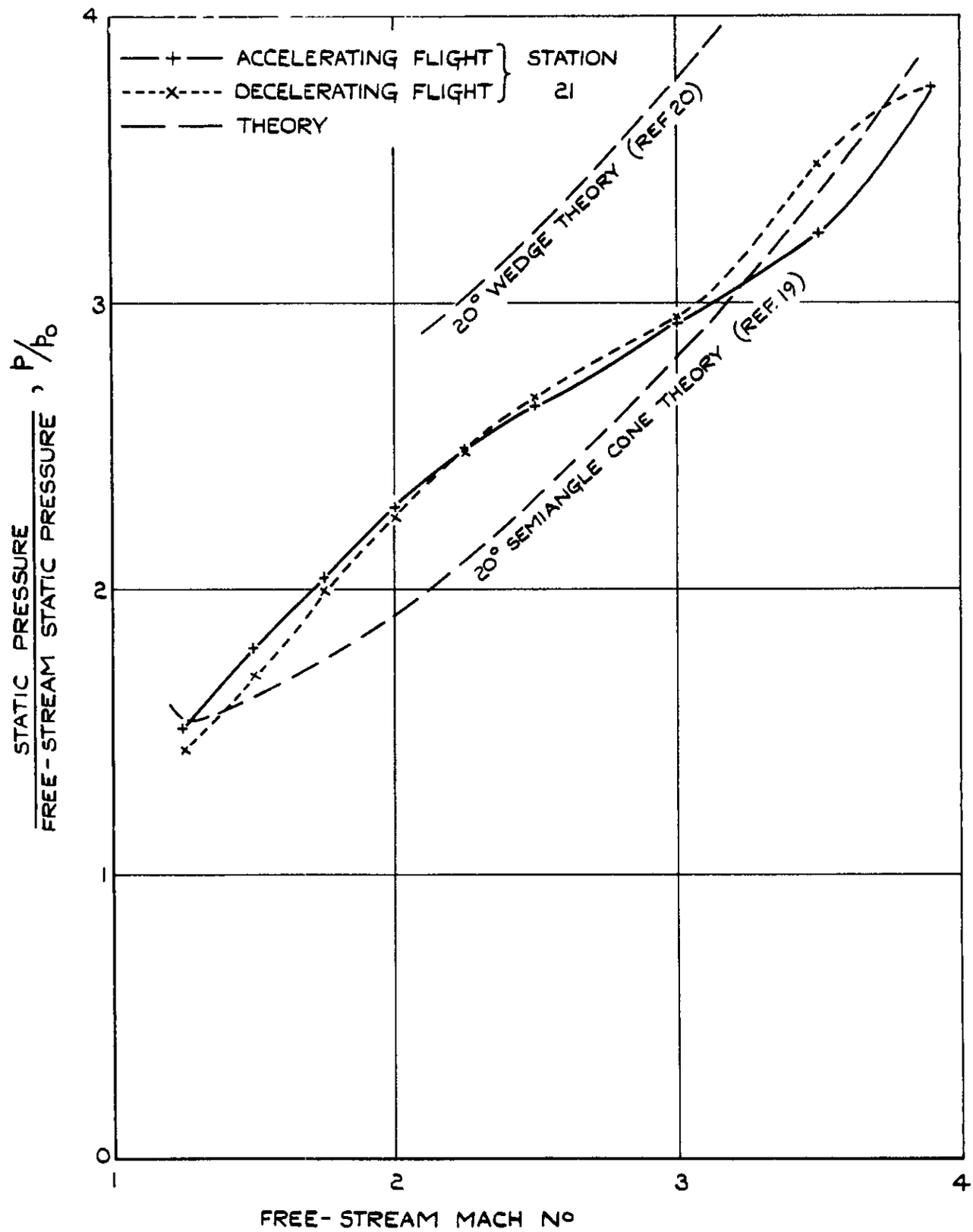

FIG. 9(d) CONCLD. TYPICAL VARIATIONS OF SURFACE PRESSURE RATIOS WITH MACH No. – HEAD P1 AFT CONE.

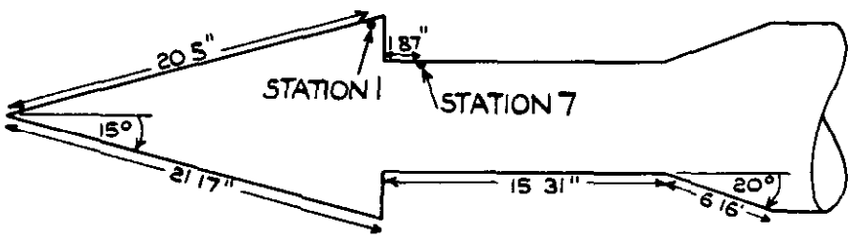

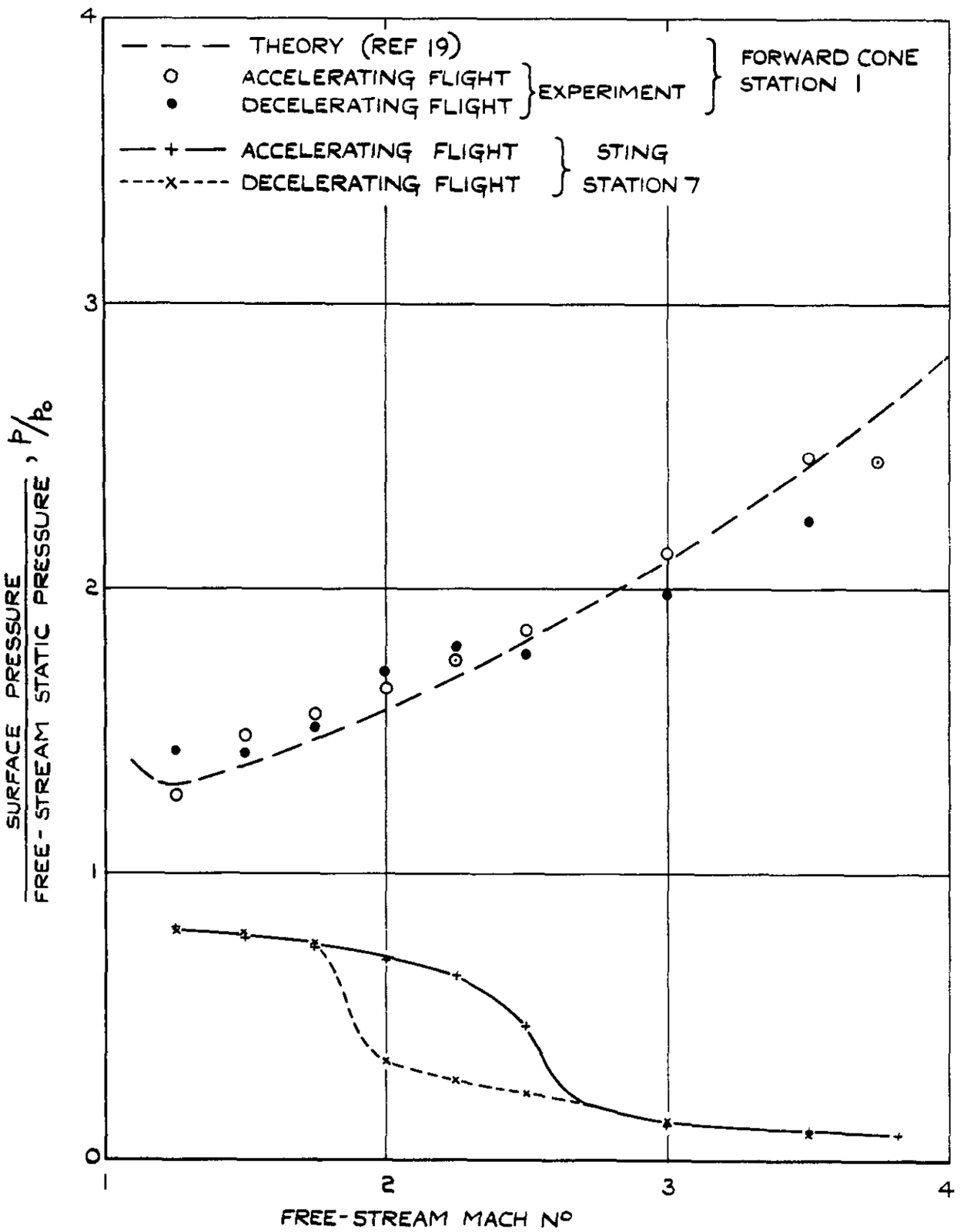

FIG. 9 (b) TYPICAL VARIATIONS OF SURFACE PRESSURE RATIOS WITH MACH No.- HEAD P2 FORWARD CONE AND STING.

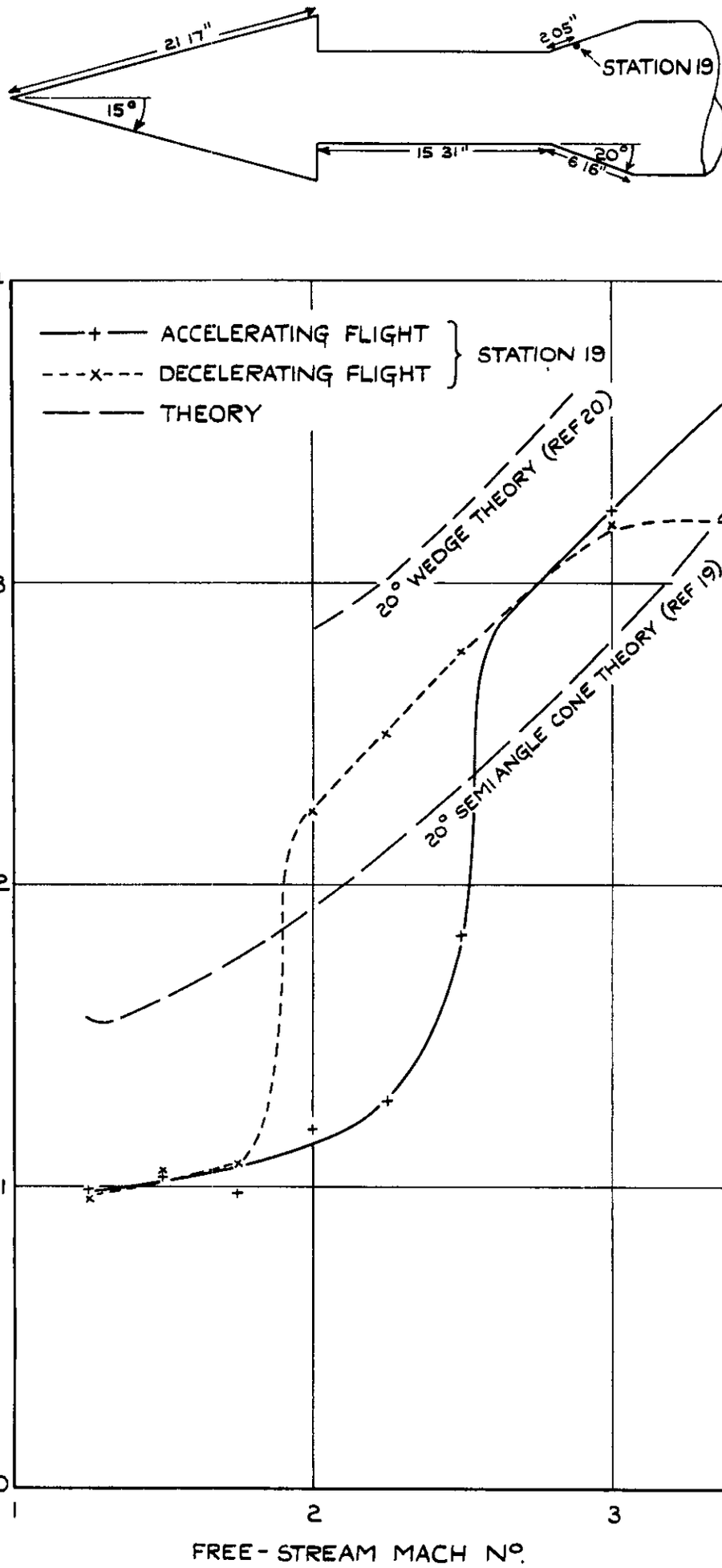

FIG.9(b) CONCLD. TYPICAL VARIATIONS OF SURFACE PRESSURE RATIOS WITH MACH No. - HEAD P2 AFT CONE.

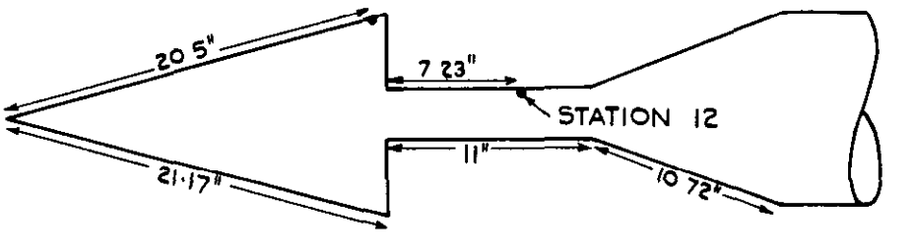

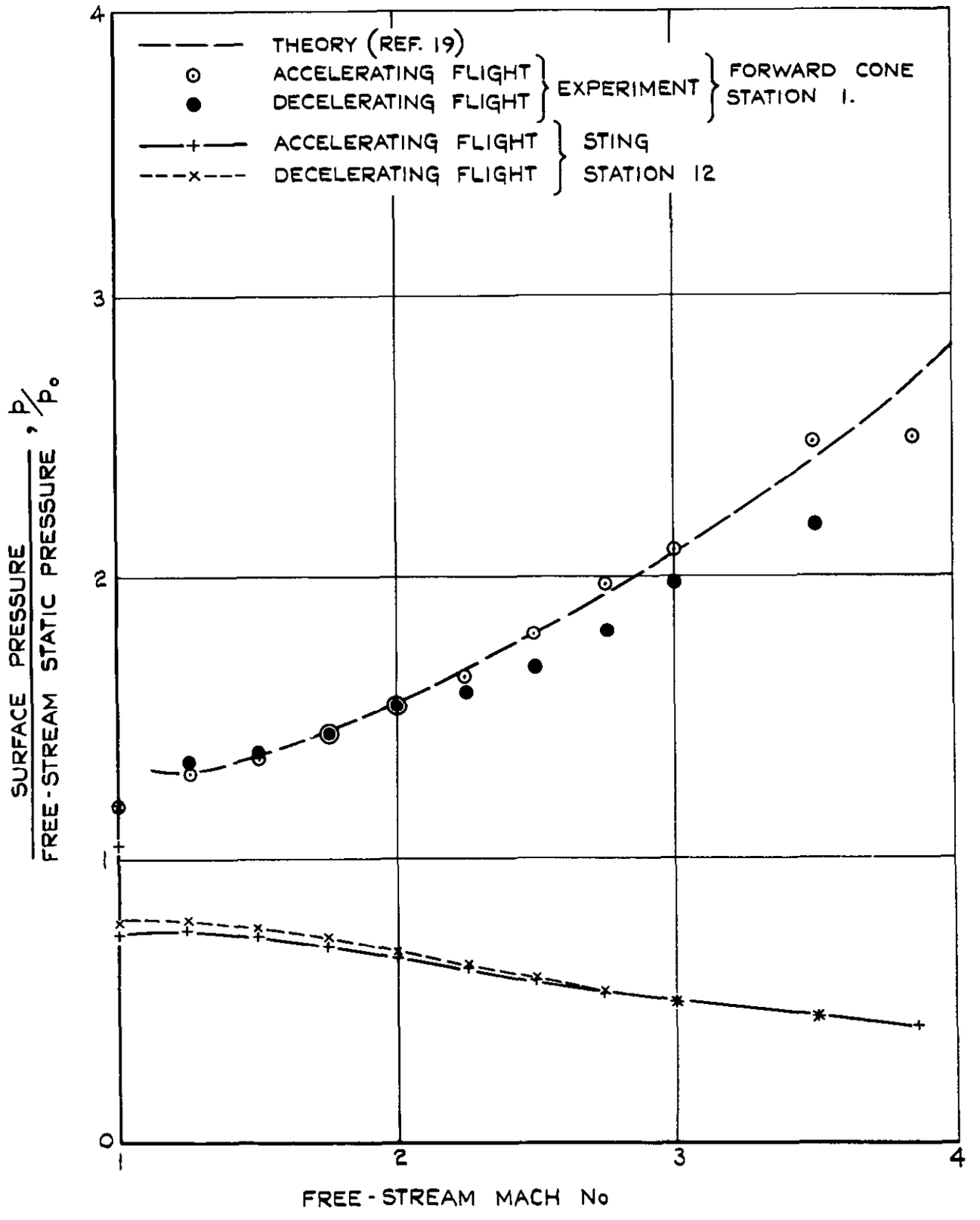

FIG. 9(c) TYPICAL VARIATIONS OF SURFACE PRESSURE RATIOS WITH MACH No.- HEAD P3 FORWARD CONE AND STING.

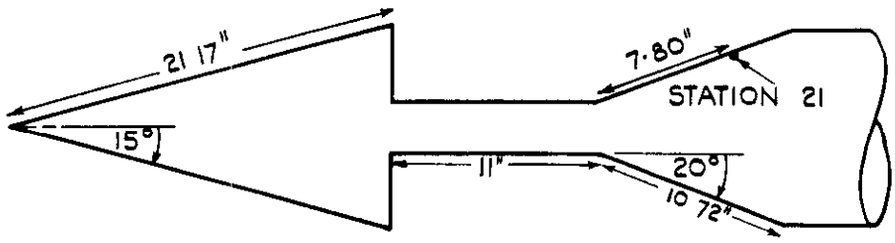

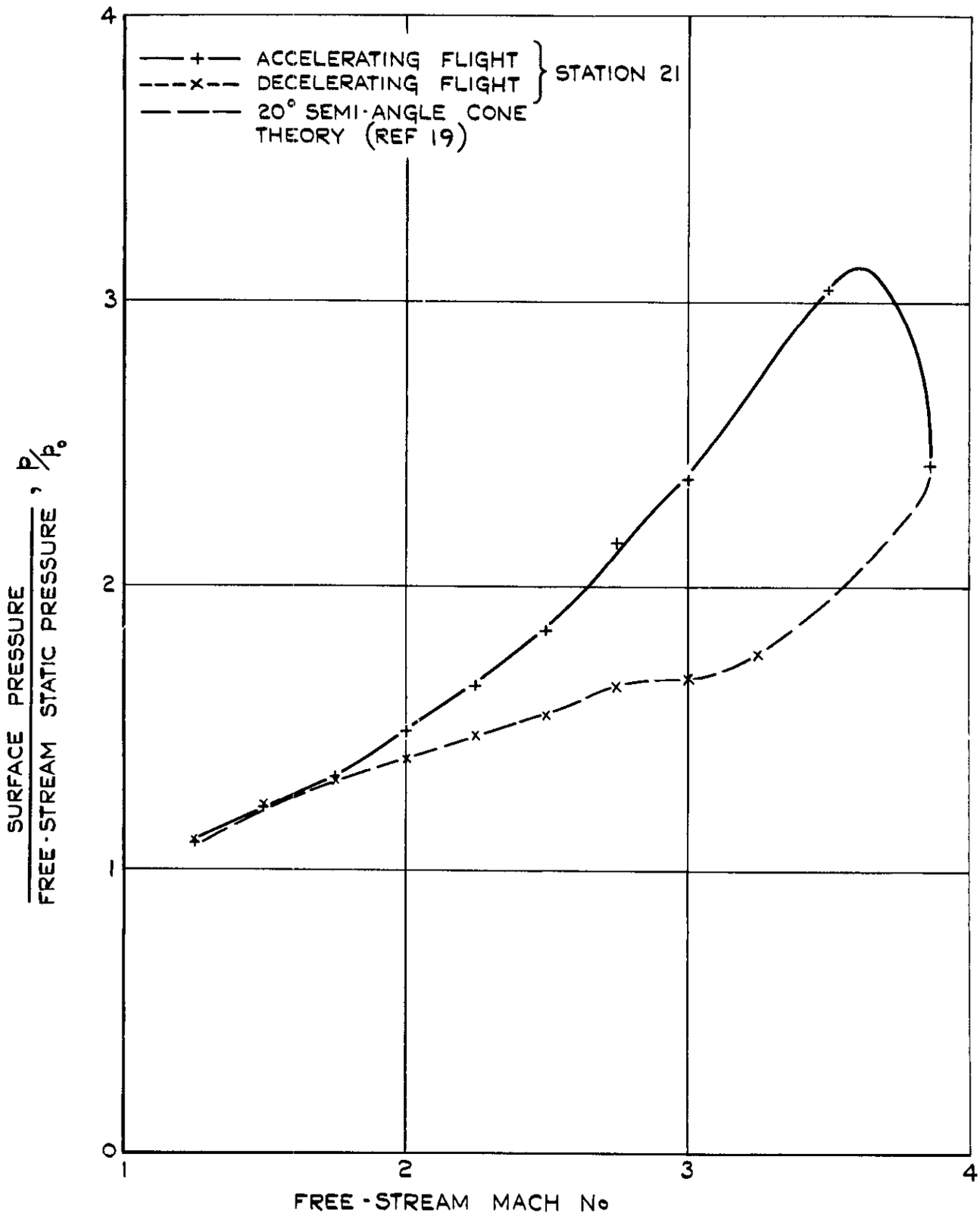

FIG. 9(c) CONCLD. TYPICAL VARIATIONS OF SURFACE PRESSURE RATIOS WITH MACH No. - HEAD P3 AFT CONE

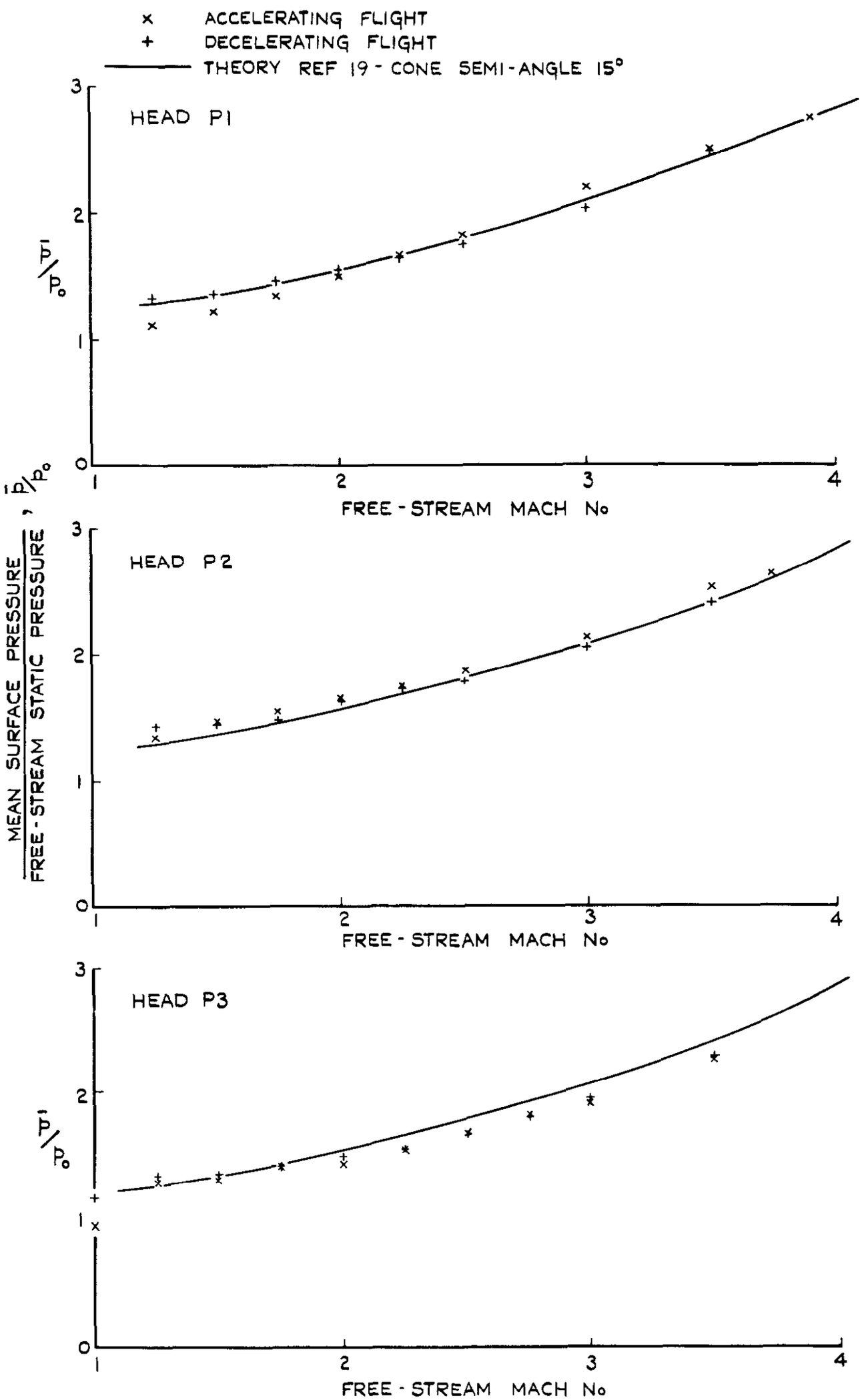

FIG. 10. VARIATION OF MEAN SURFACE PRESSURE RATIO WITH MACH No. ON FORWARD CONES.

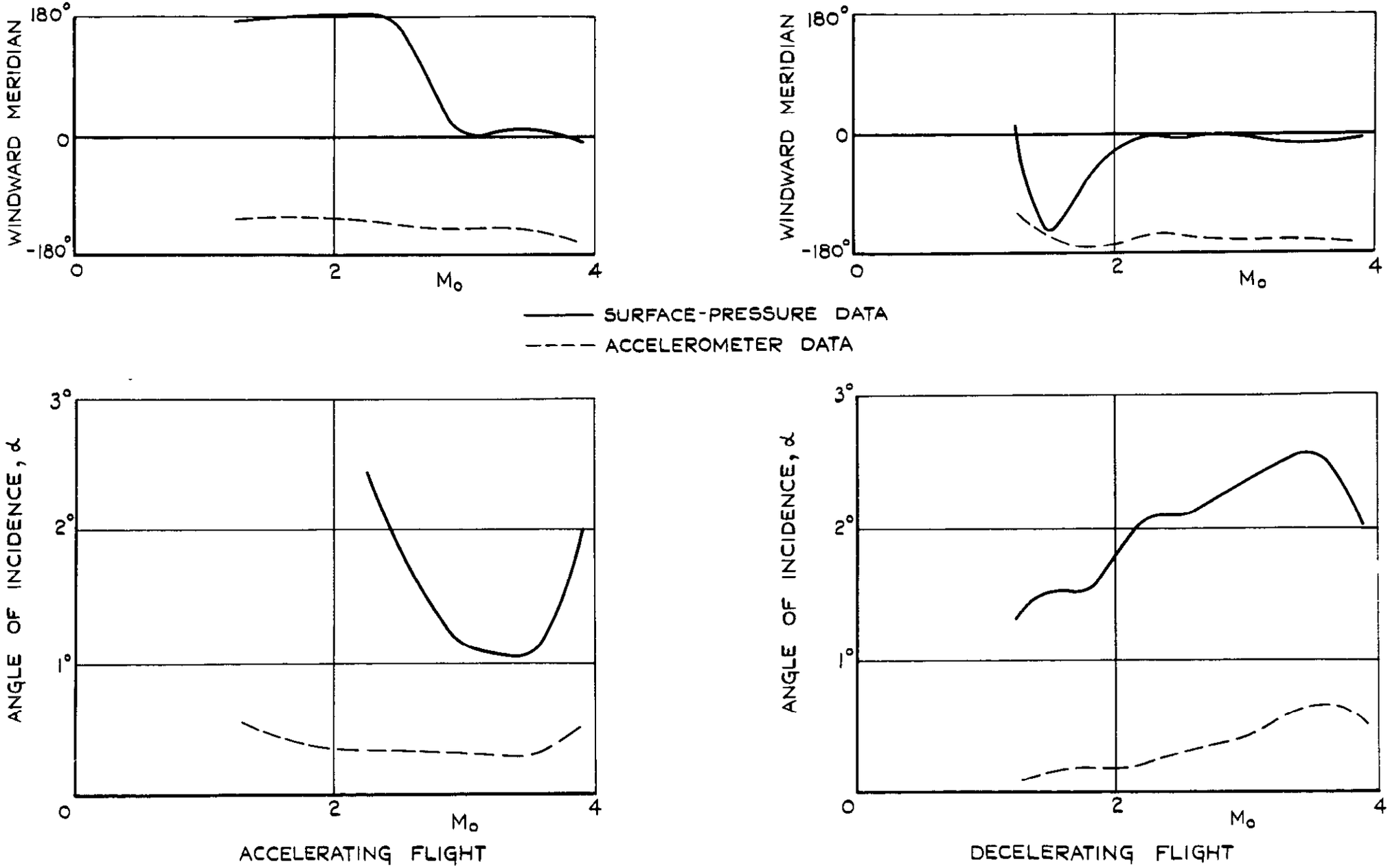

FIG. 11(a) VARIATION OF ANGLE OF INCIDENCE WITH MACH No. FOR HEAD PI.

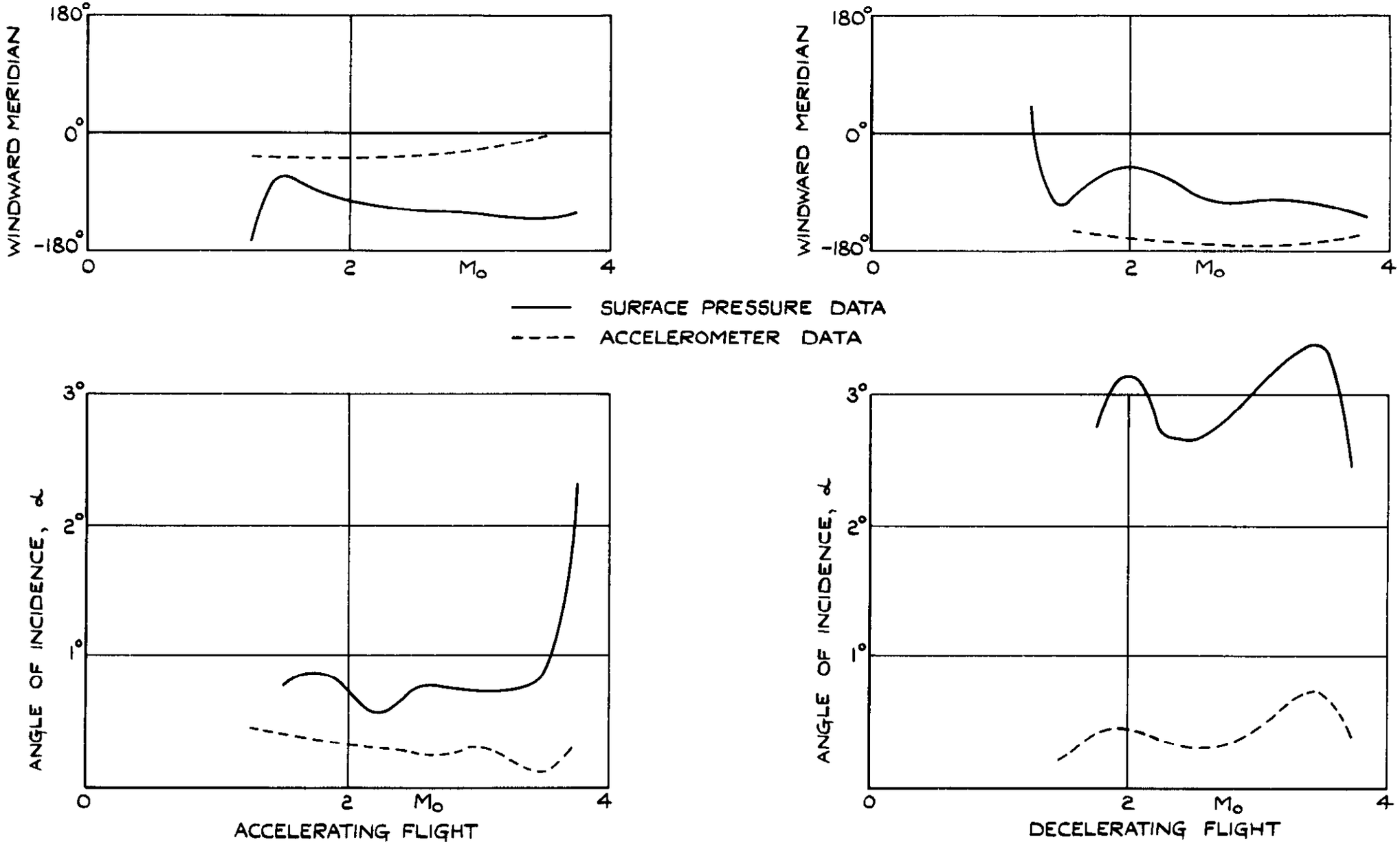

FIG.11 (b) VARIATION OF ANGLE OF INCIDENCE WITH MACH No. FOR HEAD P2.

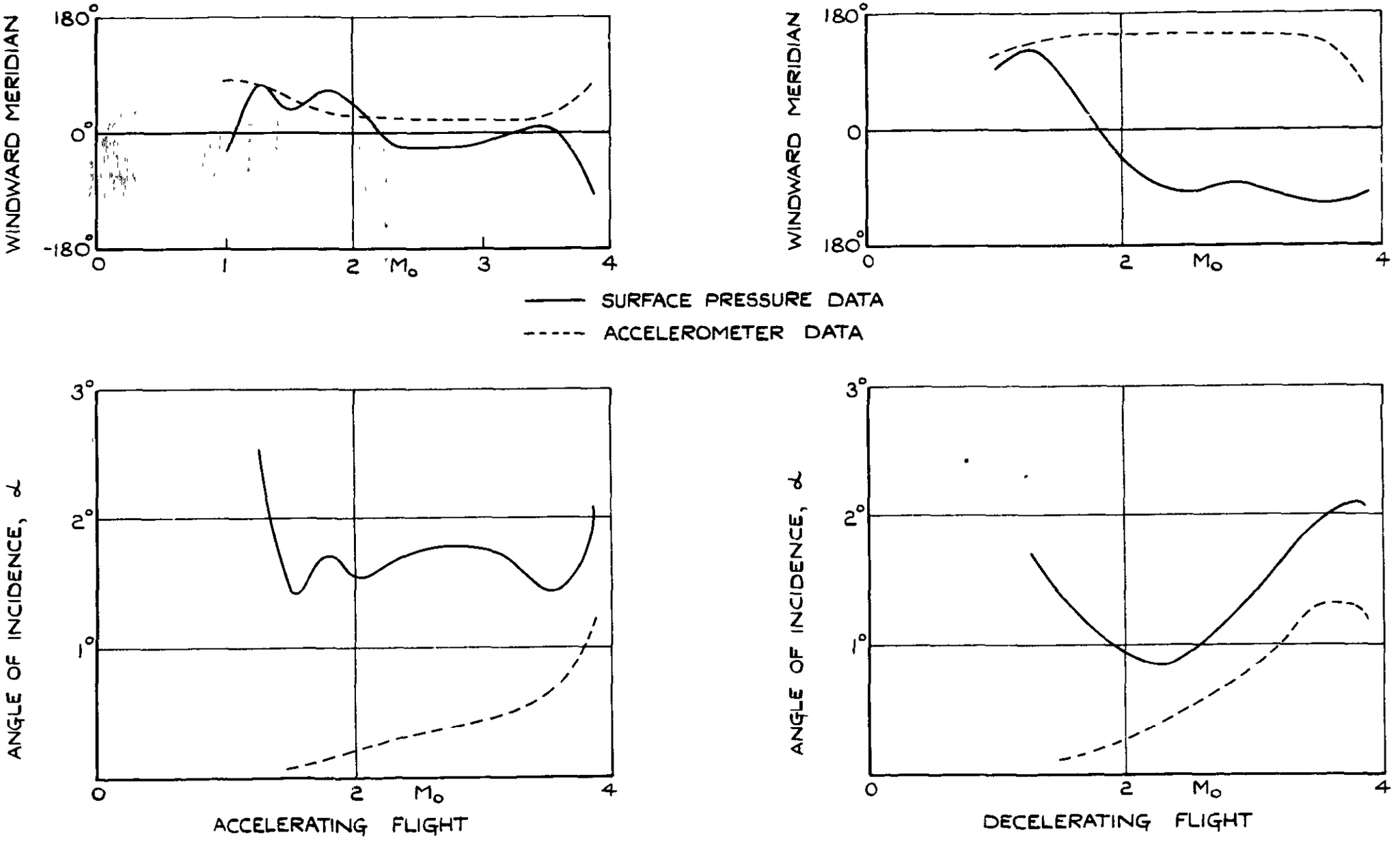

FIG.11(c) VARIATION OF ANGLE OF INCIDENCE WITH MACH No. FOR HEAD P3.

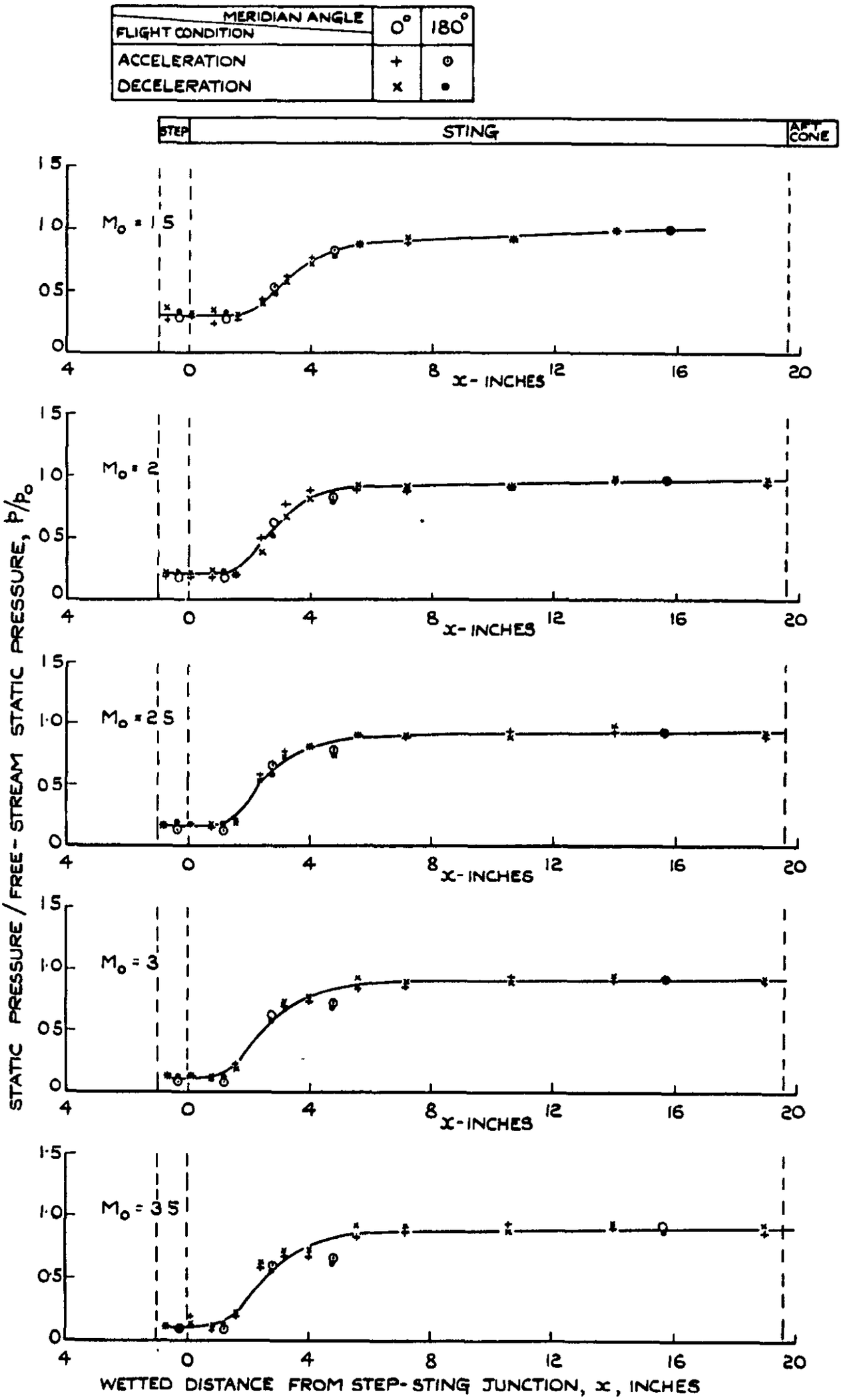

FIG. 12(a) PRESSURE DISTRIBUTION IN THE SEPARATED-FLOW REGION (HEAD P1).

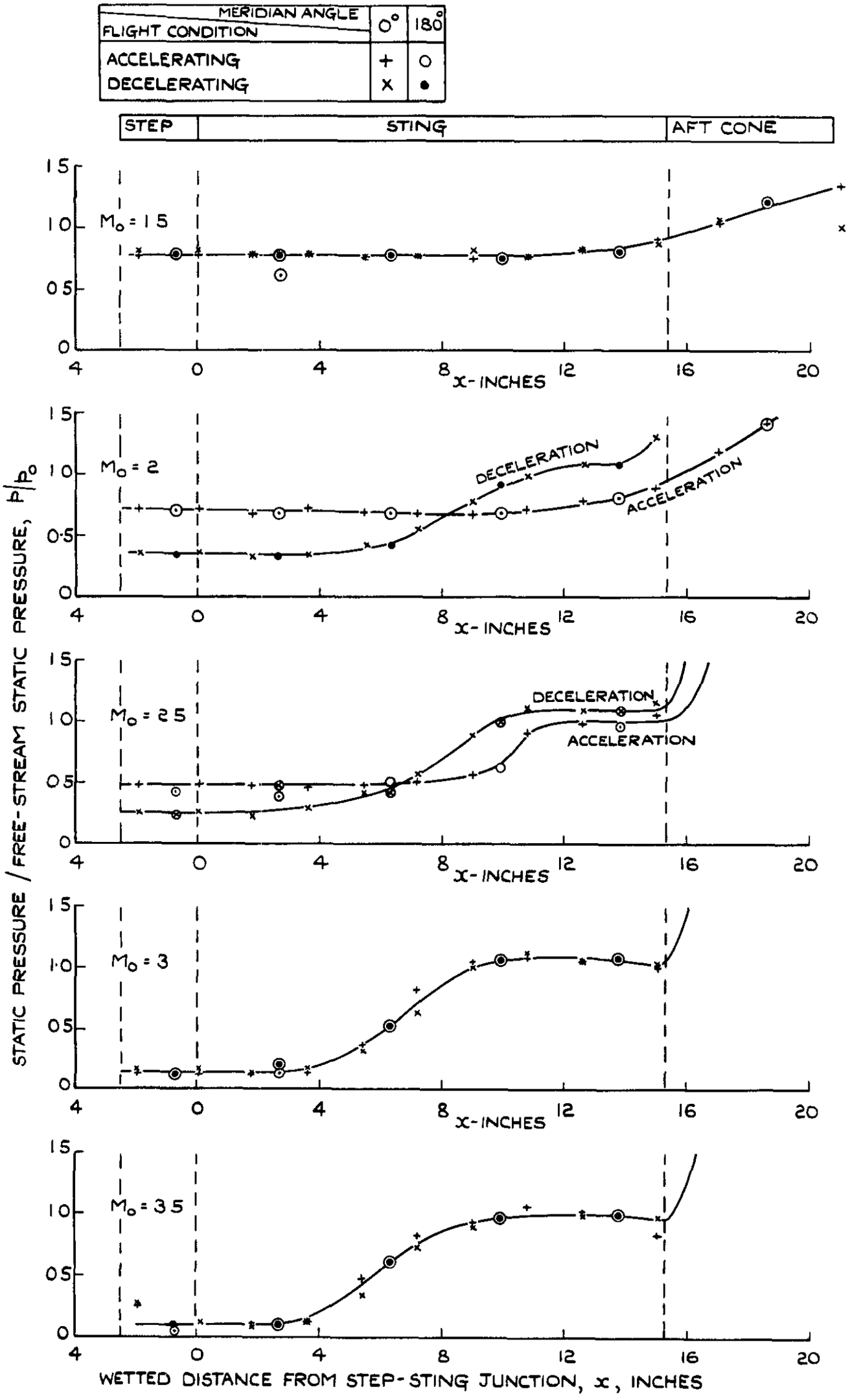

FIG.12(b) PRESSURE DISTRIBUTION IN THE SEPARATED-FLOW REGION (HEAD P2).

FLIGHT CONDITION \ MERIDIAN ANGLE	0°	180°
ACCELERATION	+	⊙
DECELERATION	×	●

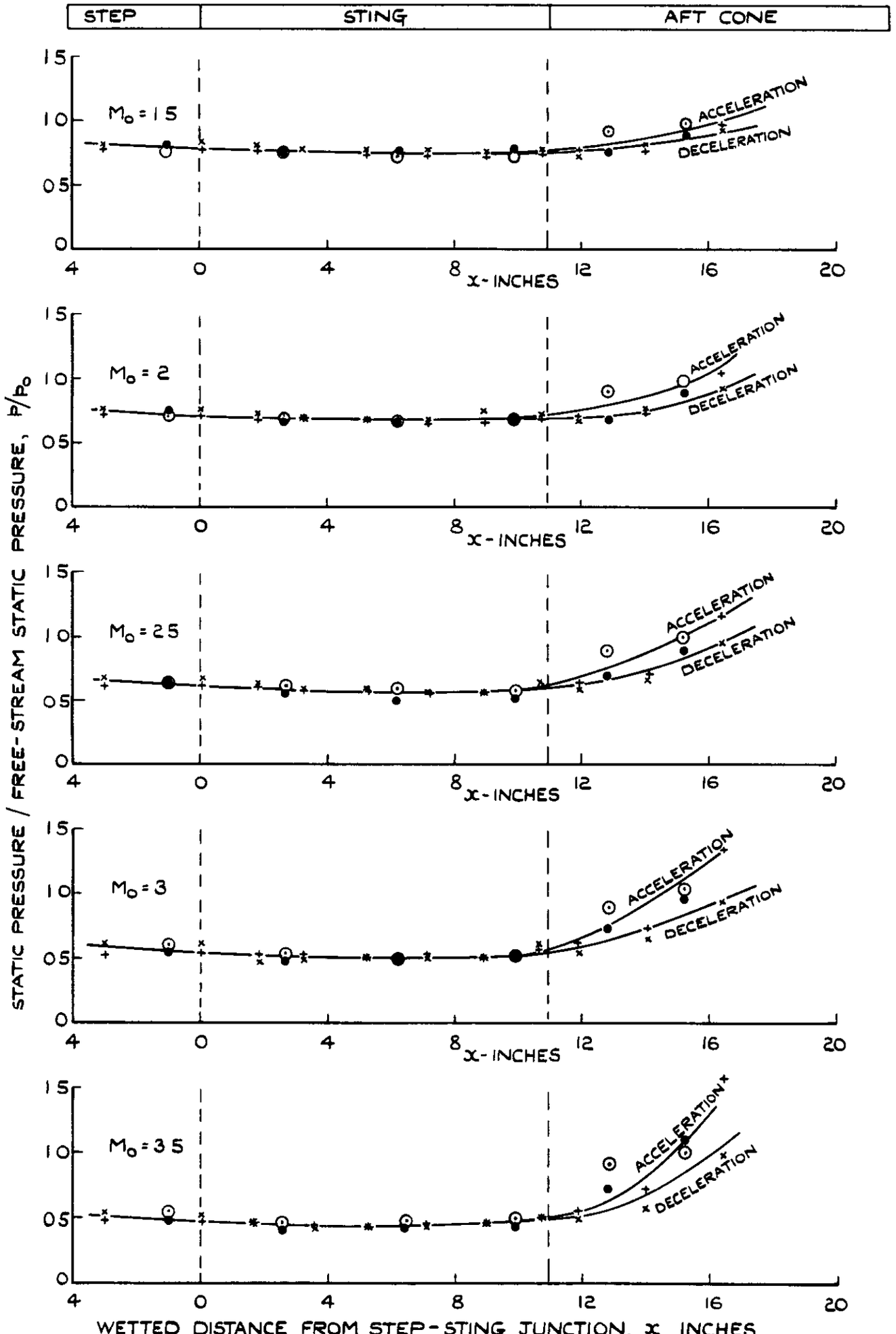

FIG. 12 (c) PRESSURE DISTRIBUTION IN THE SEPARATED-FLOW REGION (HEAD P 3).

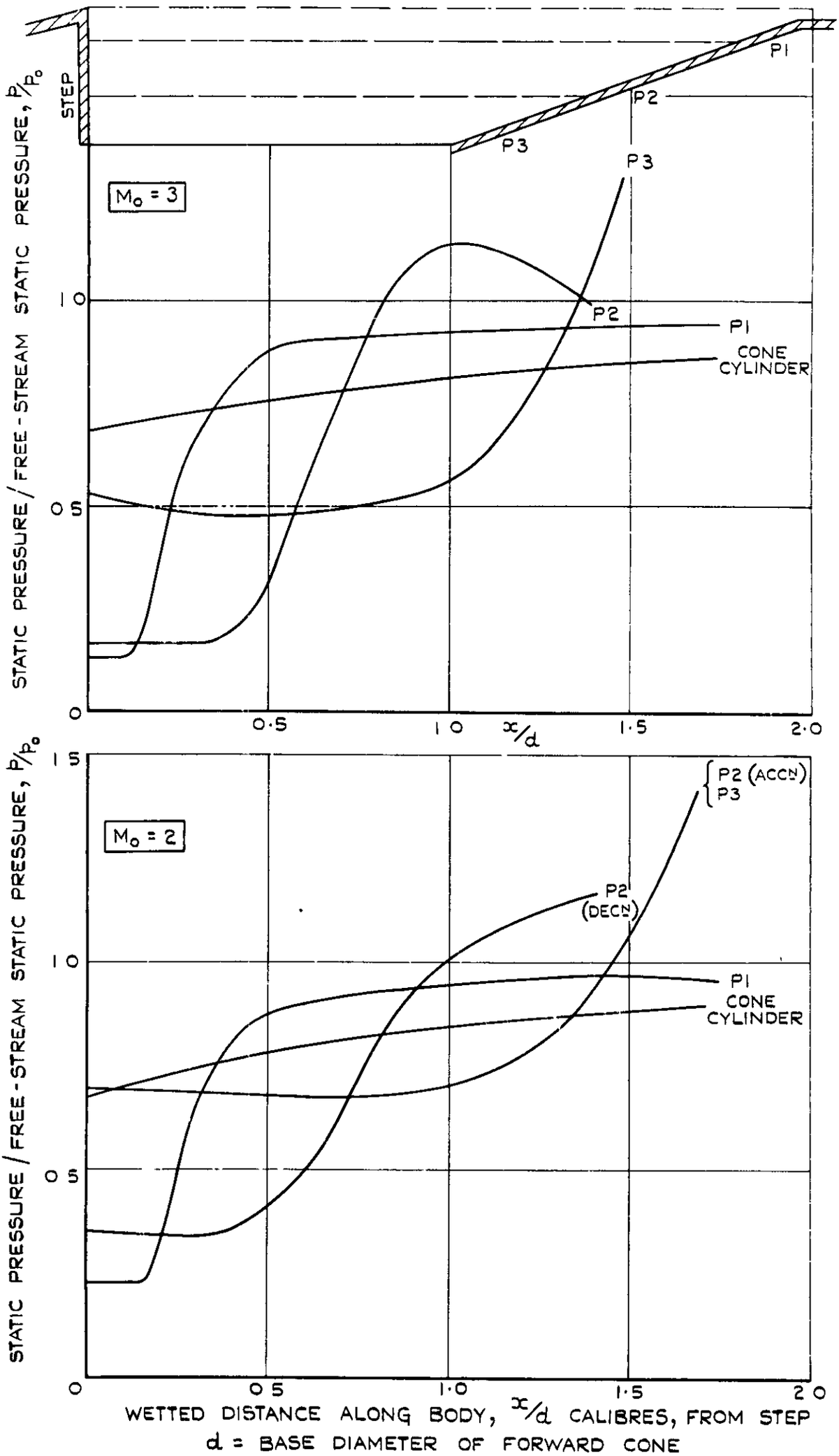

FIG. 13. COMPARISON OF PRESSURE DISTRIBUTIONS ALONG STING AND AFT CONE AT $M_o = 2$ AND 3.

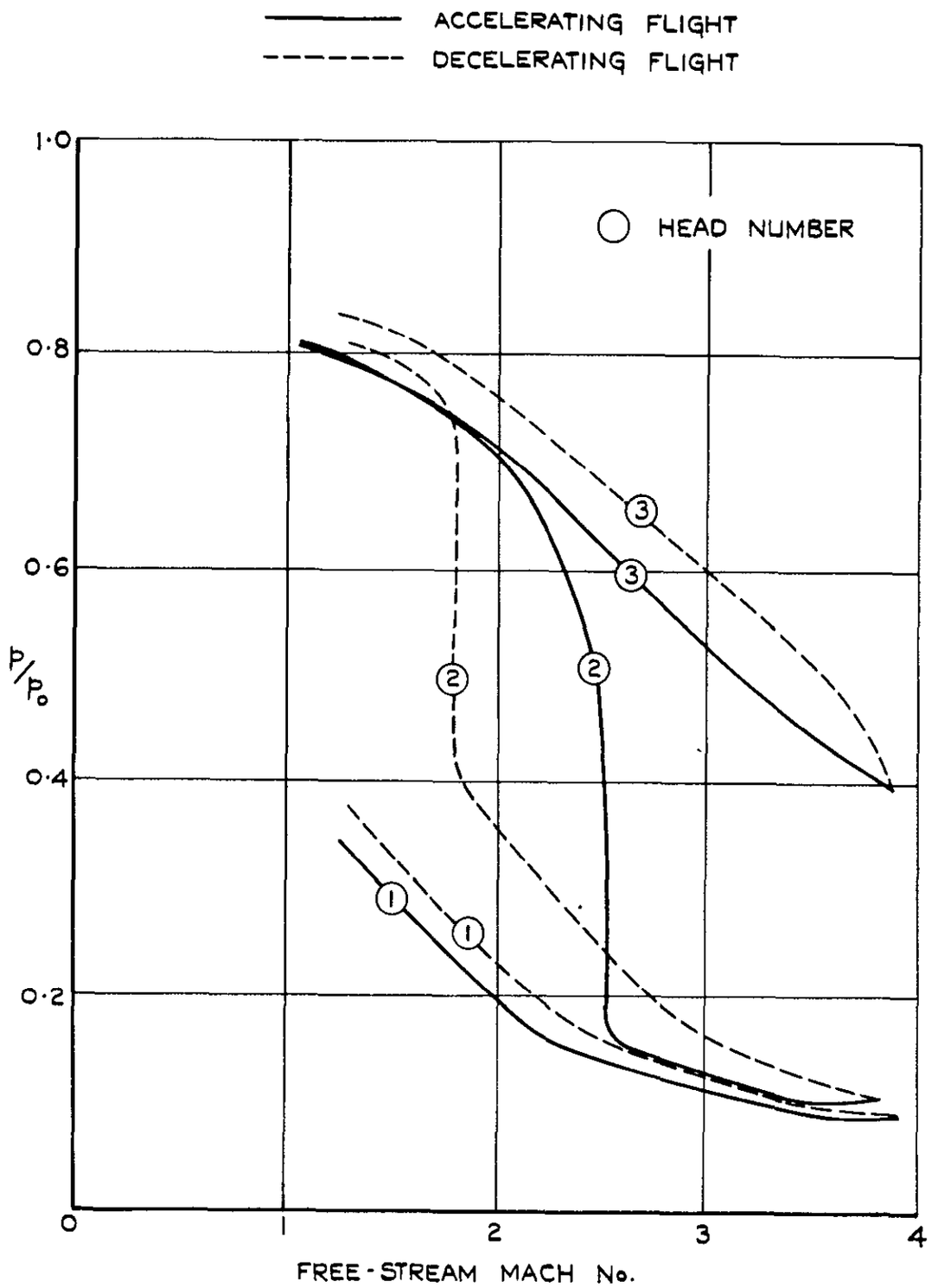

FIG. 14. VARIATION OF p/p_0 AT STEP / STING JUNCTION WITH MACH No.

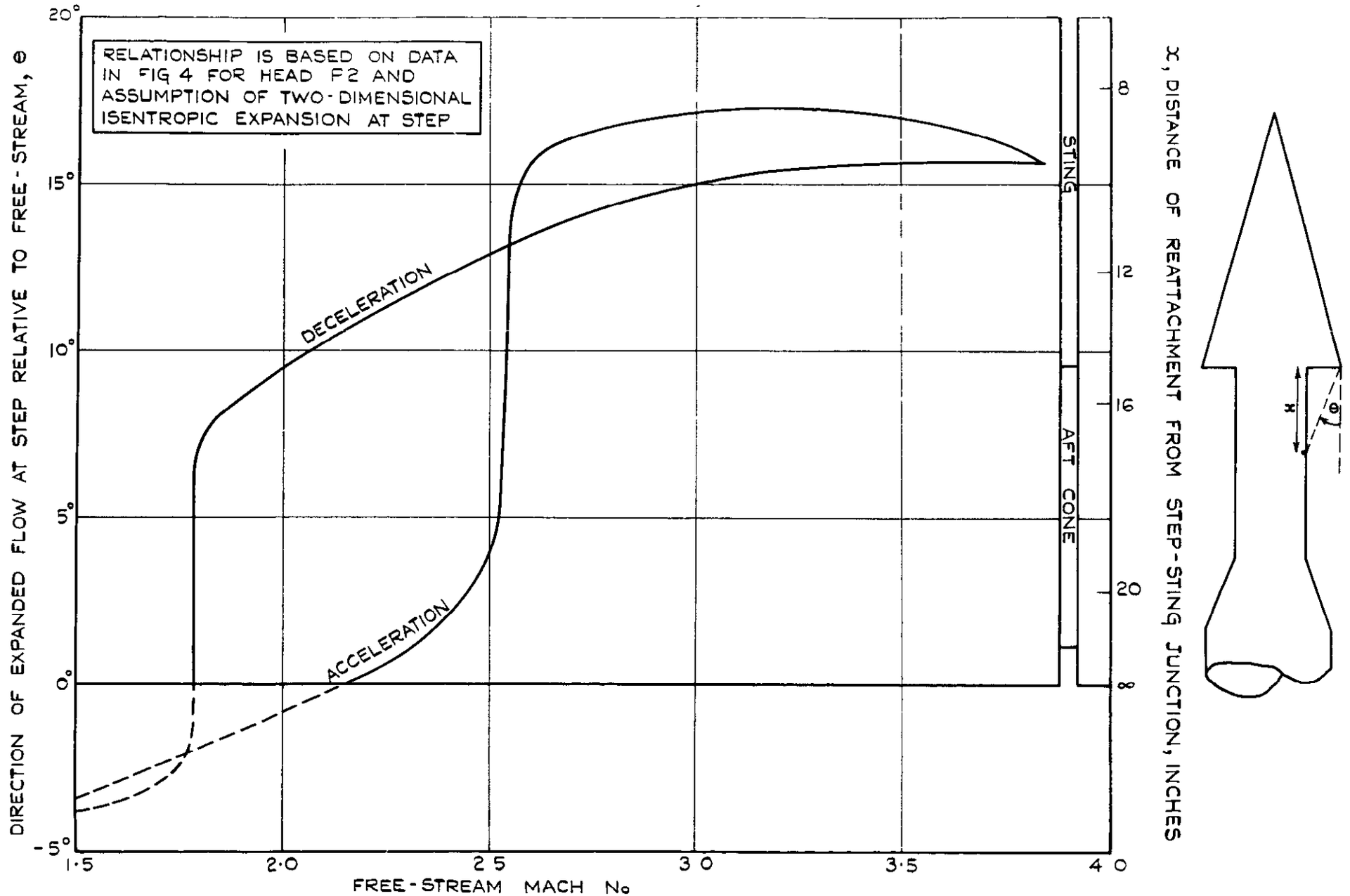

FIG. 15. VARIATION OF DIRECTION OF EXPANDED FLOW AT STEP WITH MACH No. FOR HEAD P2.

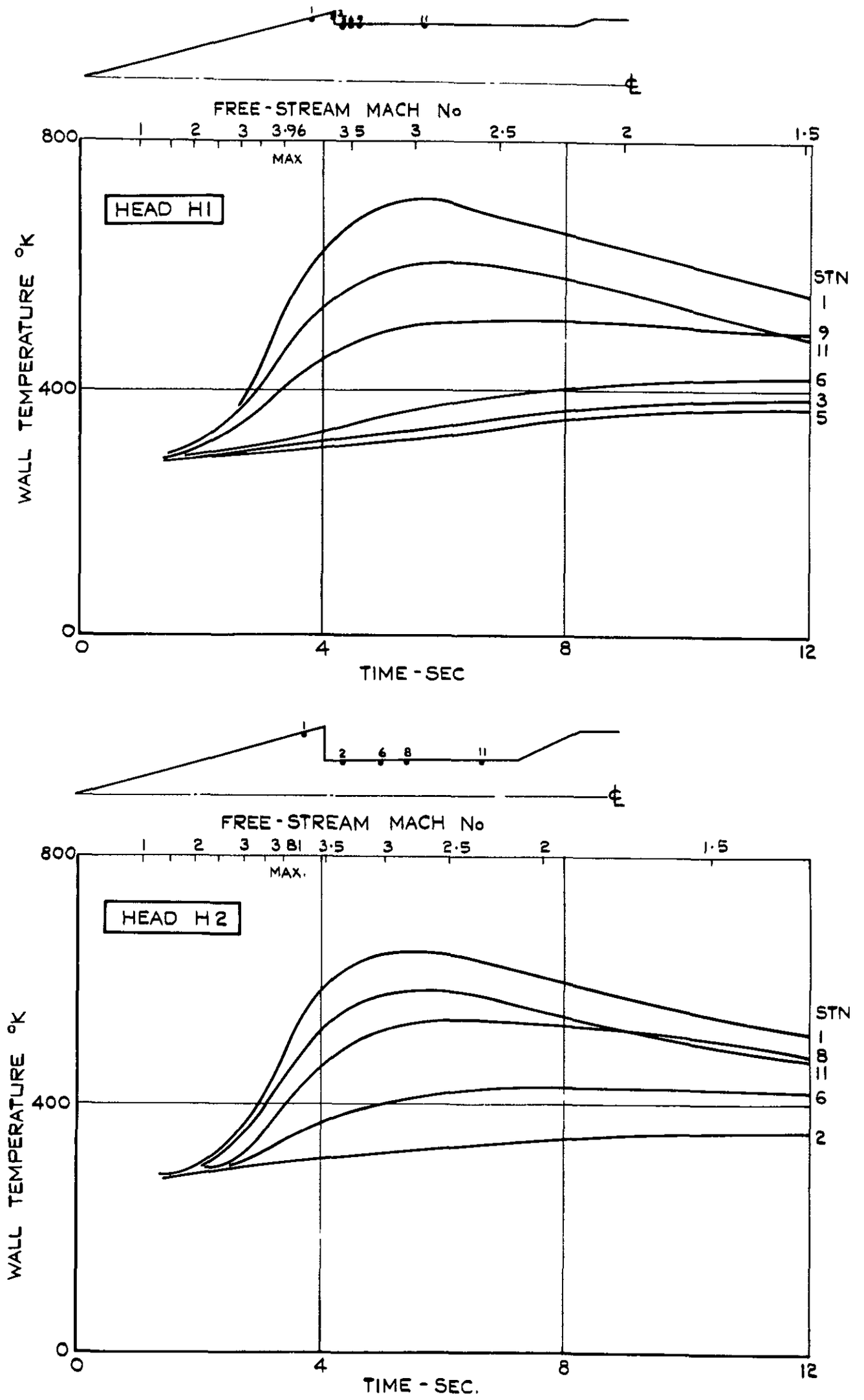

FIG. 16. TYPICAL WALL-TEMPERATURE HISTORIES.

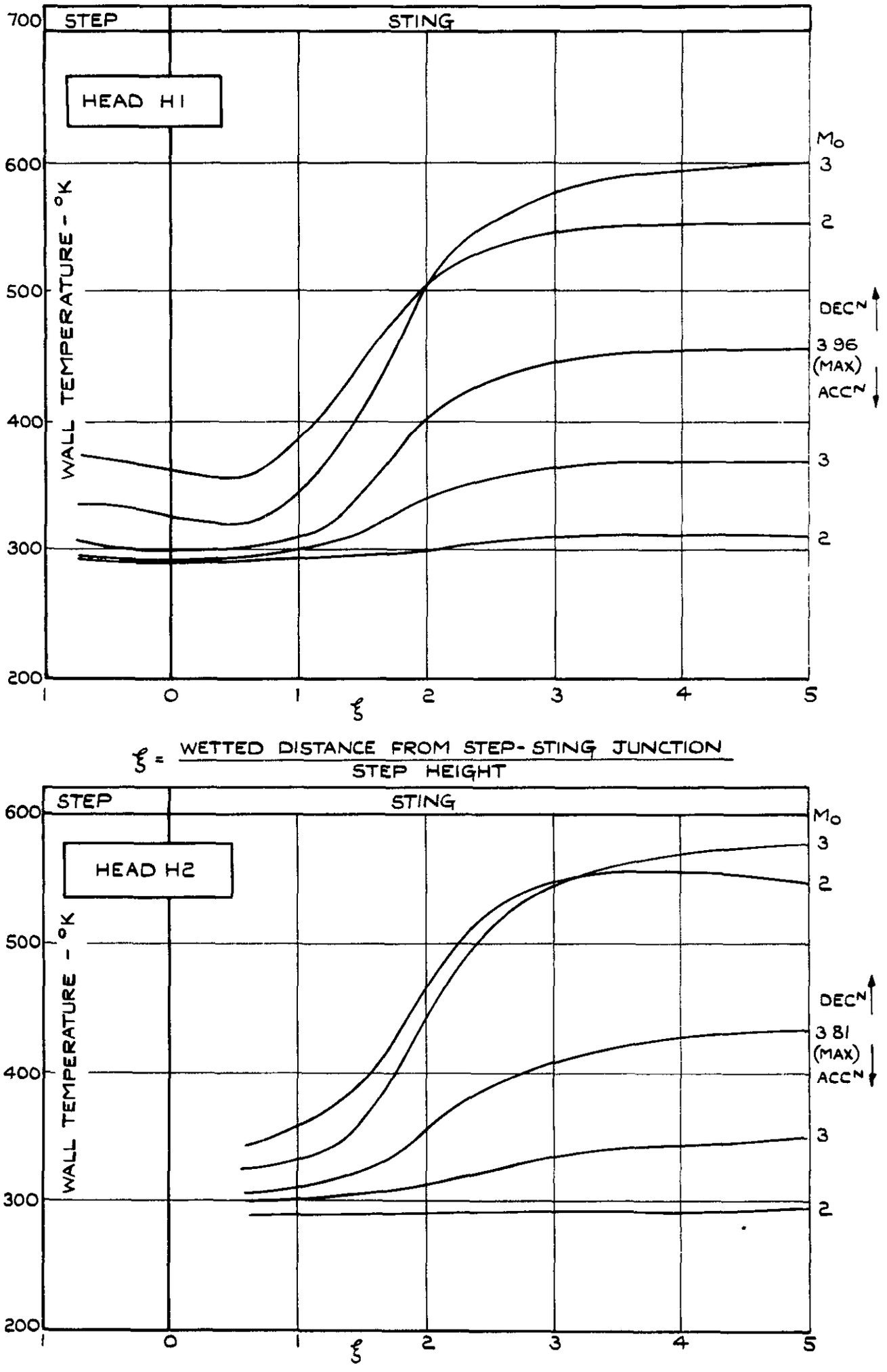

FIG.17. TEMPERATURE DISTRIBUTIONS AT VARIOUS MACH NOS.

NOTE

$$\xi = \frac{\text{WETTED DISTANCE FROM STEP-STING JUNCTION}}{\text{STEP HEIGHT}}$$

TEMPERATURES ARE RELEVANT TO ACCELERATING FLIGHT

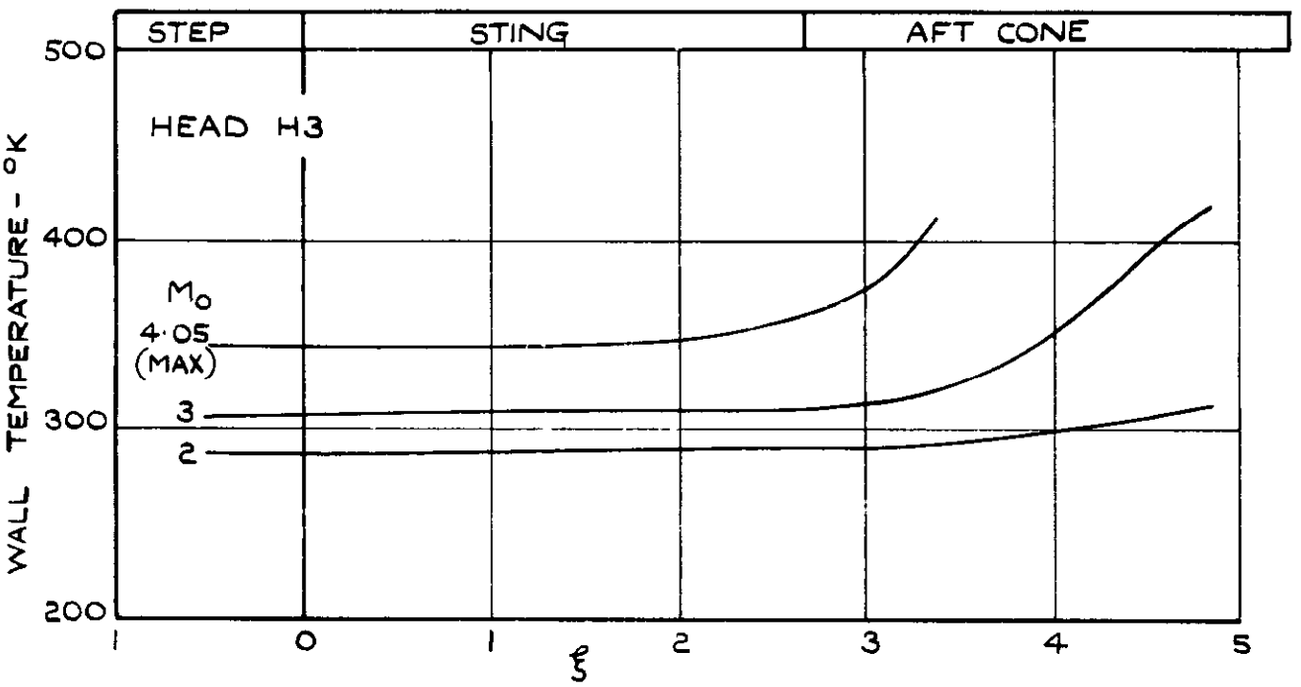

FIG.17 (CONCLD.). TEMPERATURE DISTRIBUTIONS AT VARIOUS MACH NOS.

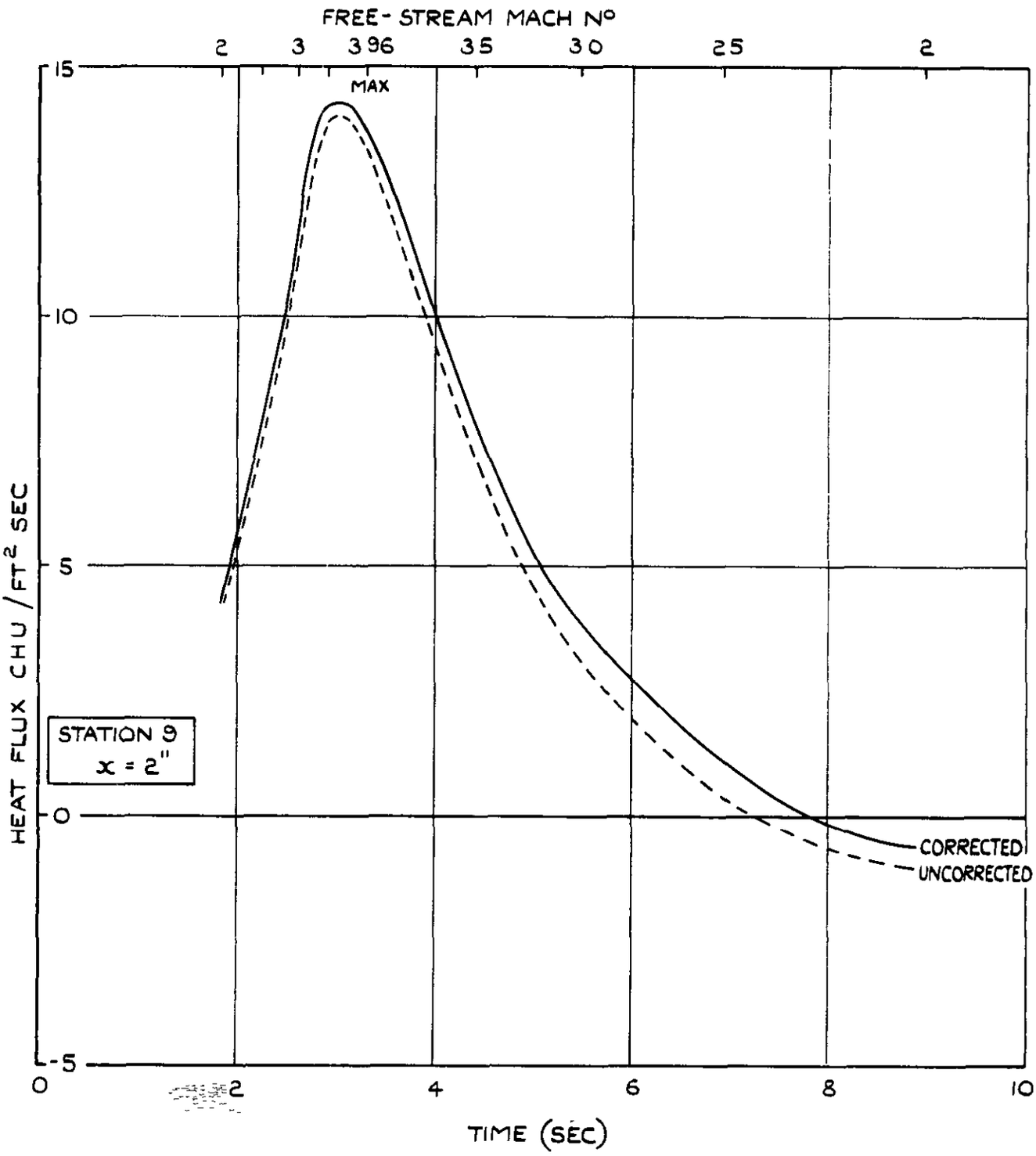

FIG. 18. TYPICAL LATERAL-HEAT-FLOW CORRECTION FOR HEAD HI.

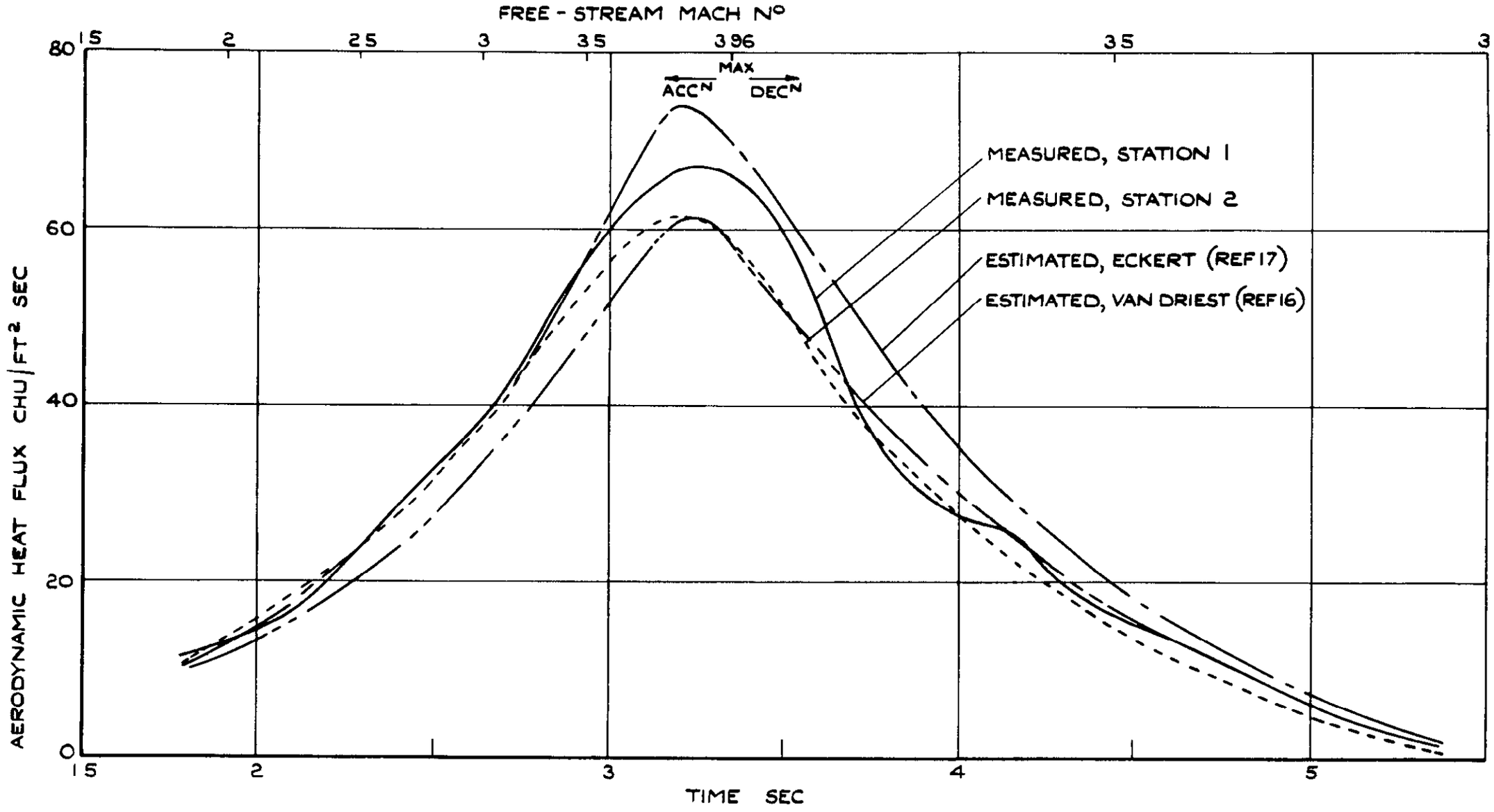

FIG.19 (a). COMPARISON OF HEAT FLUX TO FORWARD CONE OF HEAD HI WITH THEORETICAL ESTIMATES (HEATING).

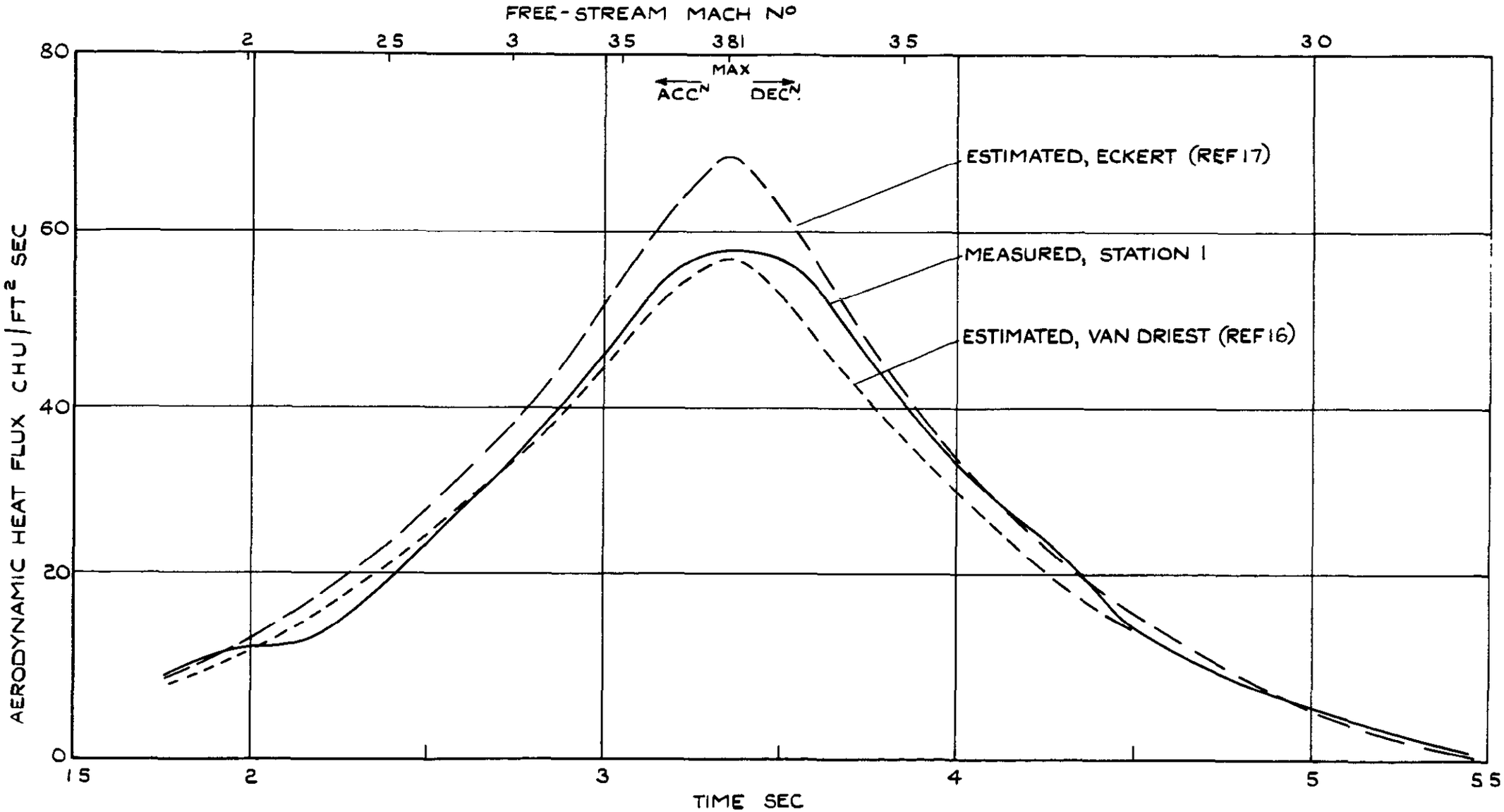

FIG 19 (b) COMPARISON OF HEAT FLUX TO FORWARD CONE OF HEAD H2 WITH THEORETICAL ESTIMATES (HEATING)

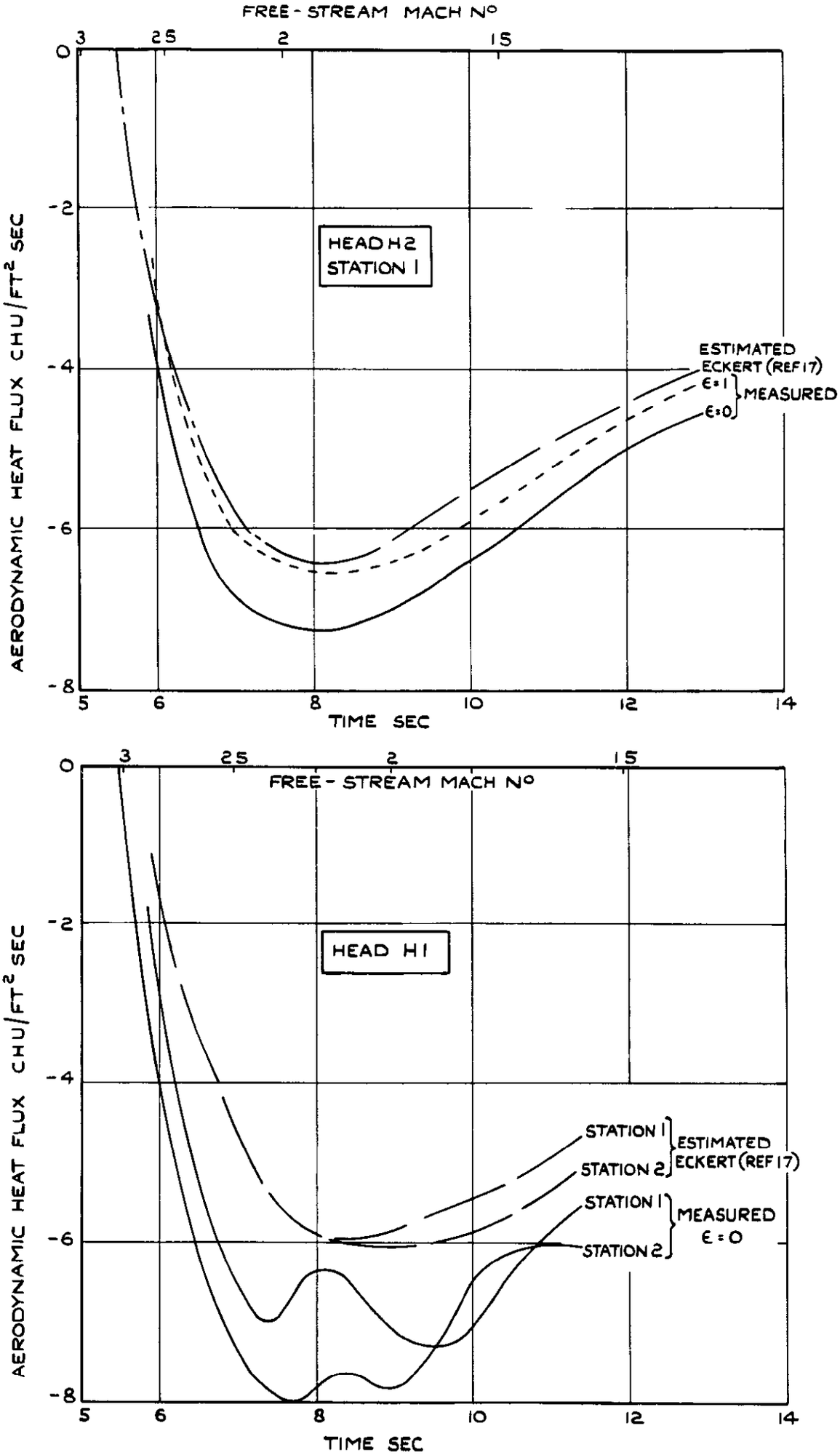

FIG. 19(c). COMPARISON OF HEAT FLUX TO FORWARD CONE WITH THEORETICAL ESTIMATES (COOLING).

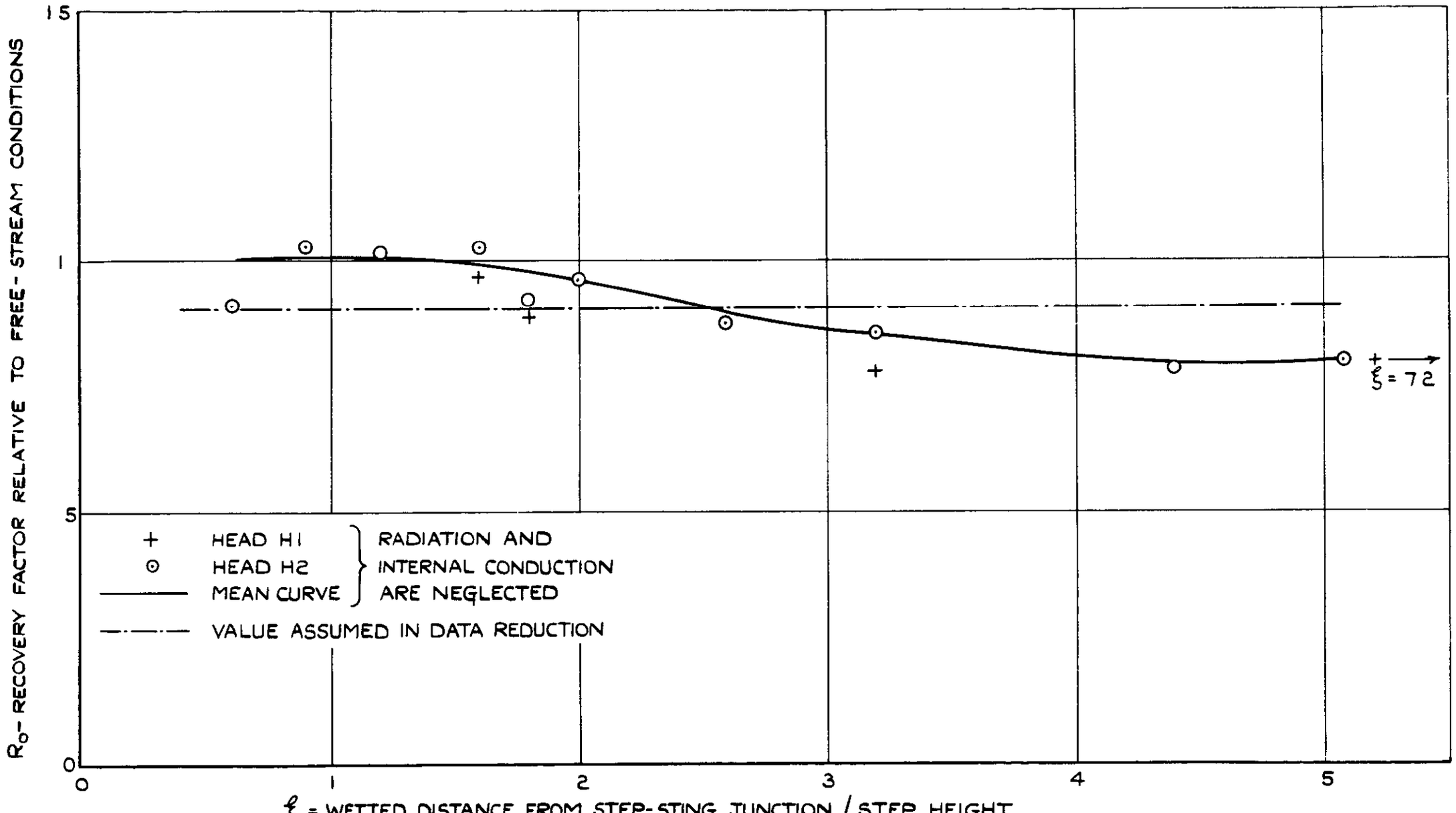

FIG. 20. VARIATION OF EXPERIMENTAL RECOVERY FACTOR WITH STATION POSITION.

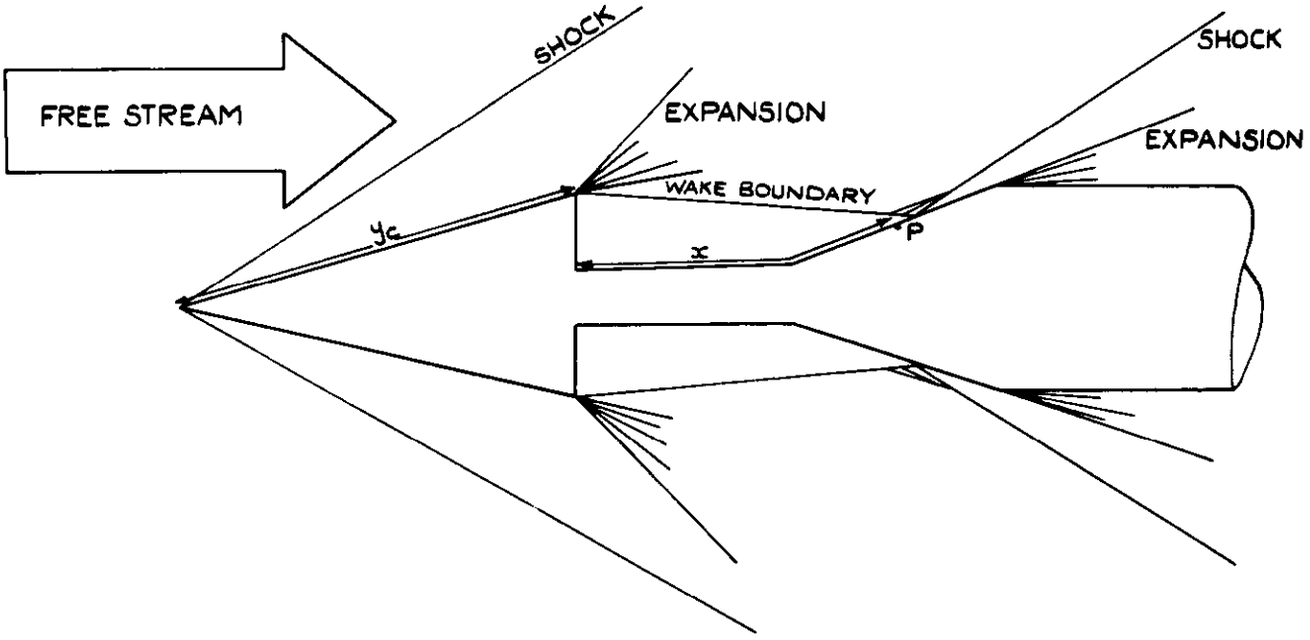

SALIENT FEATURES OF FLOW FIELD

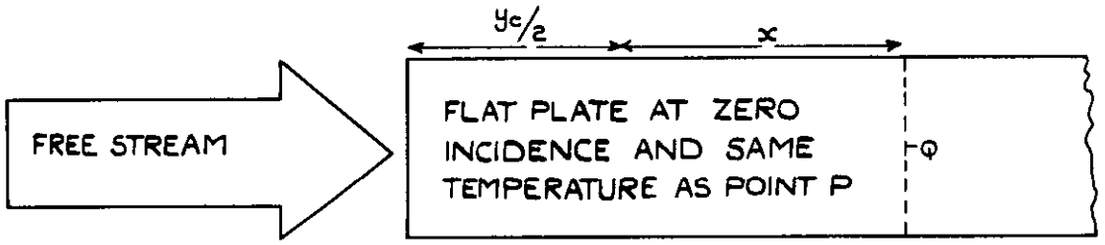

THE THEORETICAL HEAT TRANSFER COEFFICIENT (SECTION 4.2) AT POINT Q IS VALUE OF h_{fp} RELEVANT TO POINT P ON HEAD

BASIS OF h_{fp}

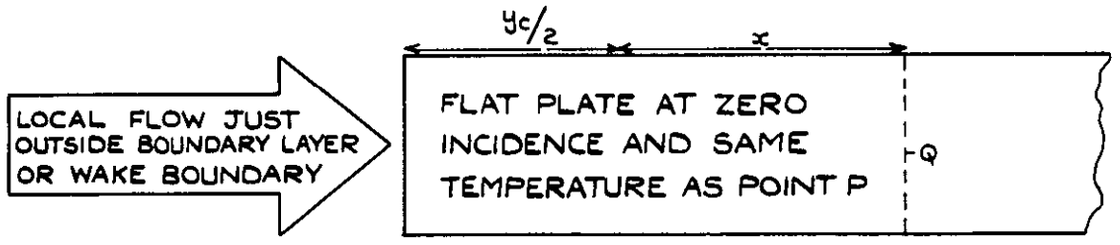

THE THEORETICAL HEAT TRANSFER COEFFICIENT (SECTION 4 2) AT Q IS VALUE OF h_A RELEVANT TO POINT P ON HEAD

BASIS OF h_A

FIG. 21. BASIS OF THEORETICAL HEAT-TRANSFER COEFFICIENTS h_{fp} AND h_A

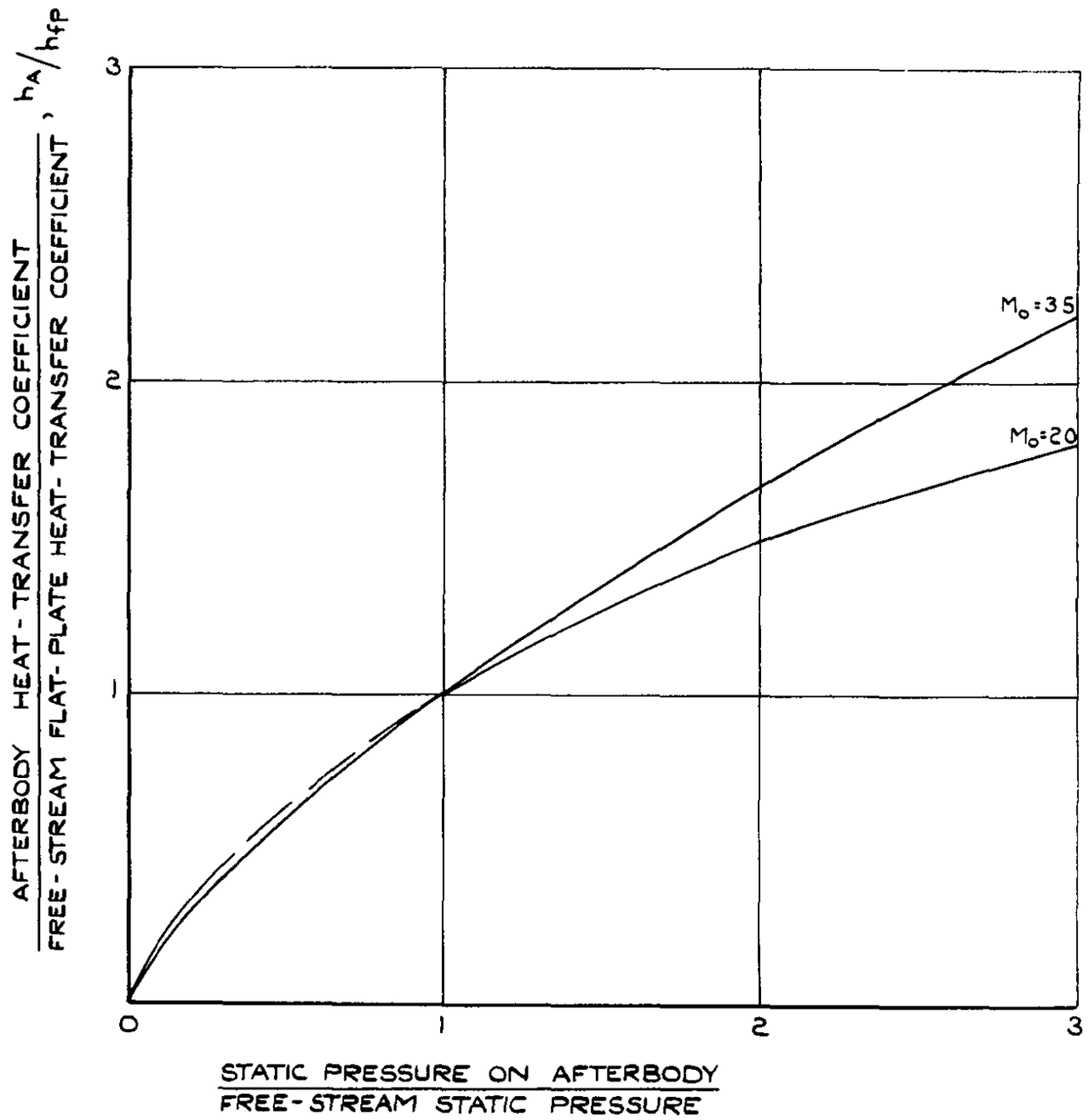

FIG. 22. ESTIMATED HEAT TRANSFER TO AFTERBODY WITH SOLID SURFACE IN PLACE OF WAKE BOUNDARY.

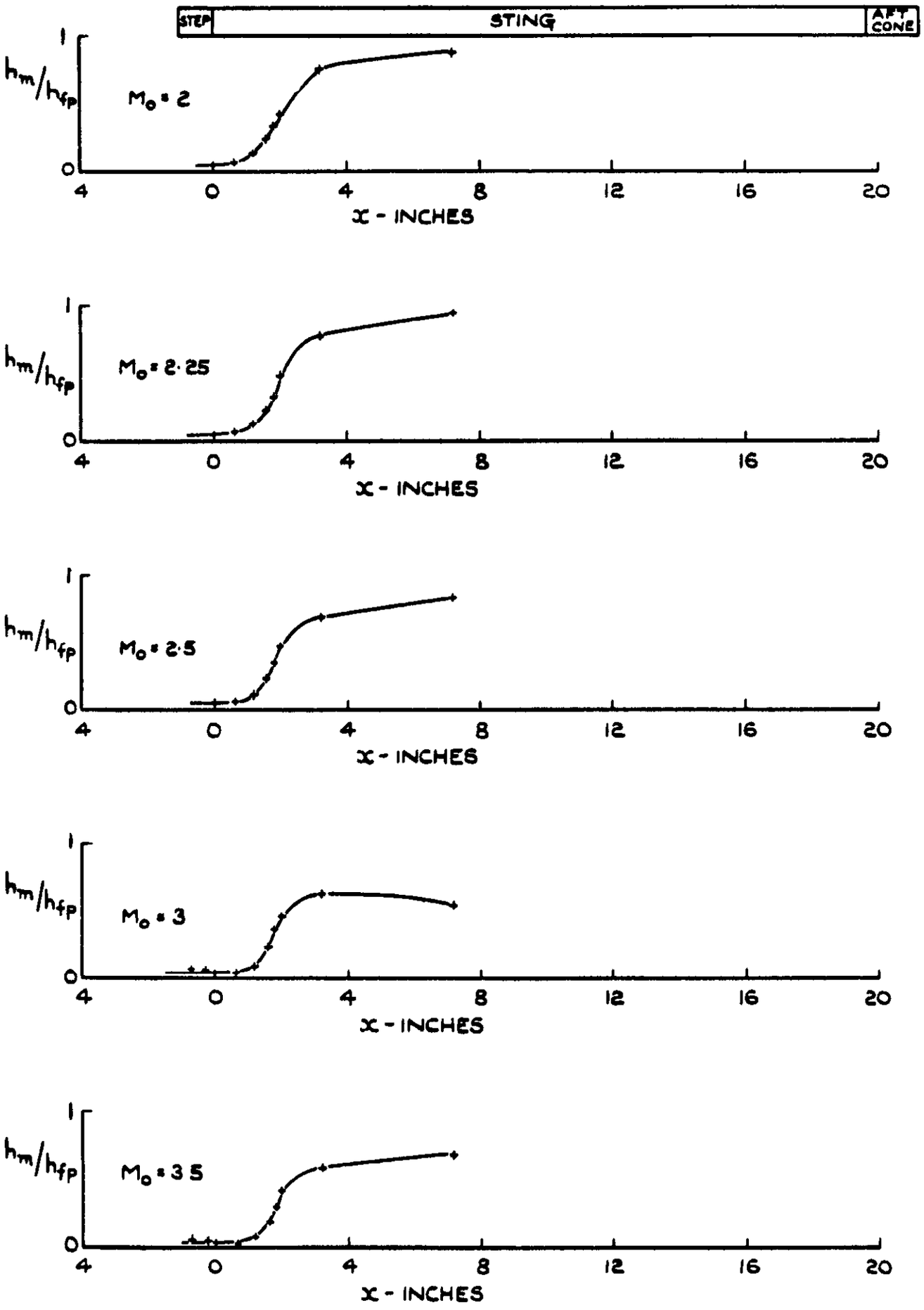

FIG. 23 (a) VARIATION OF HEAT TRANSFER OVER SEPARATED-FLOW AND REATTACHMENT REGIONS FOR HEAD HI-ACCELERATING FLIGHT.

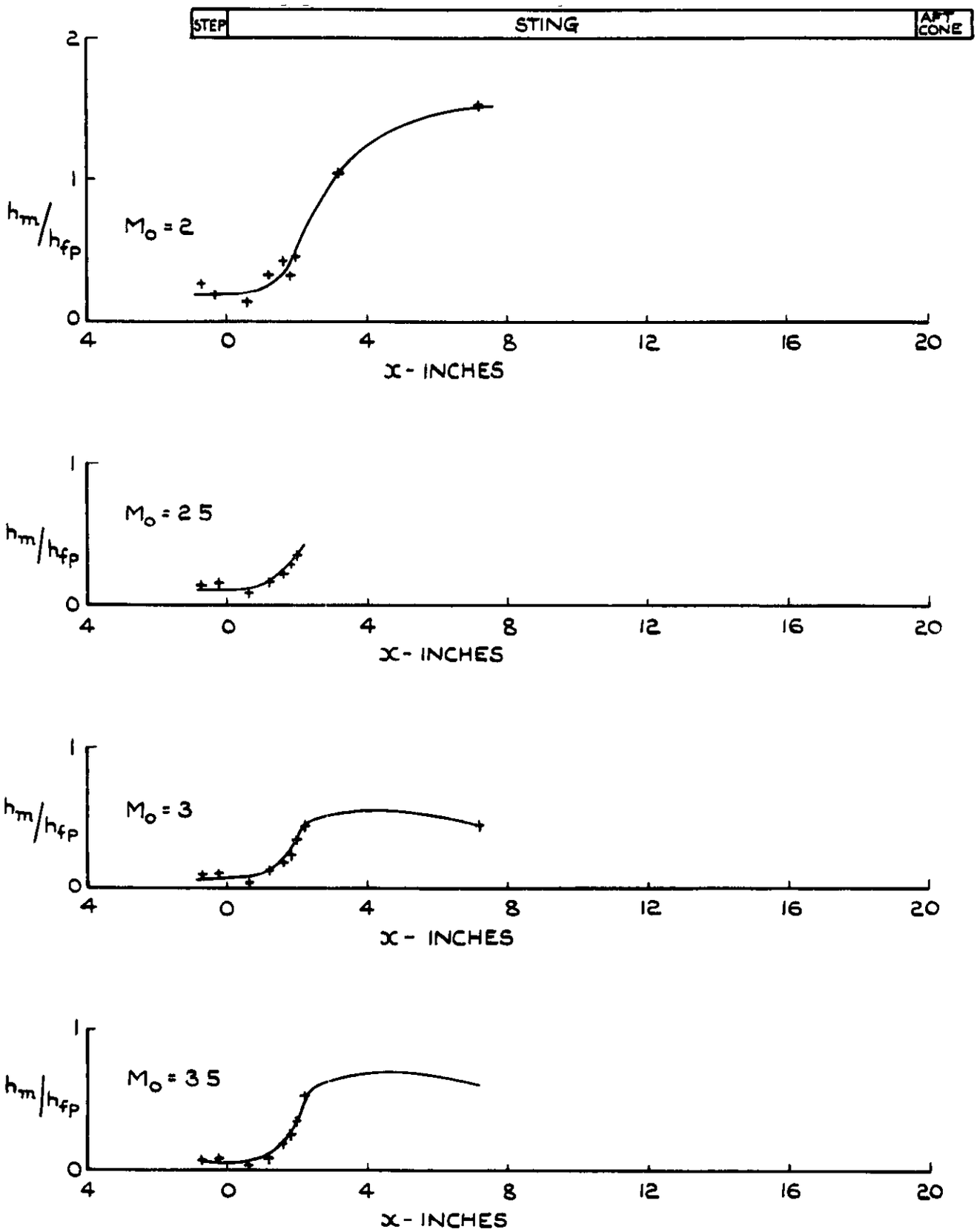

FIG. 23 (a) CONCLD. VARIATION OF HEAT TRANSFER OVER SEPARATED-FLOW AND REATTACHMENT REGIONS FOR HEAD HI-DECELERATING FLIGHT.

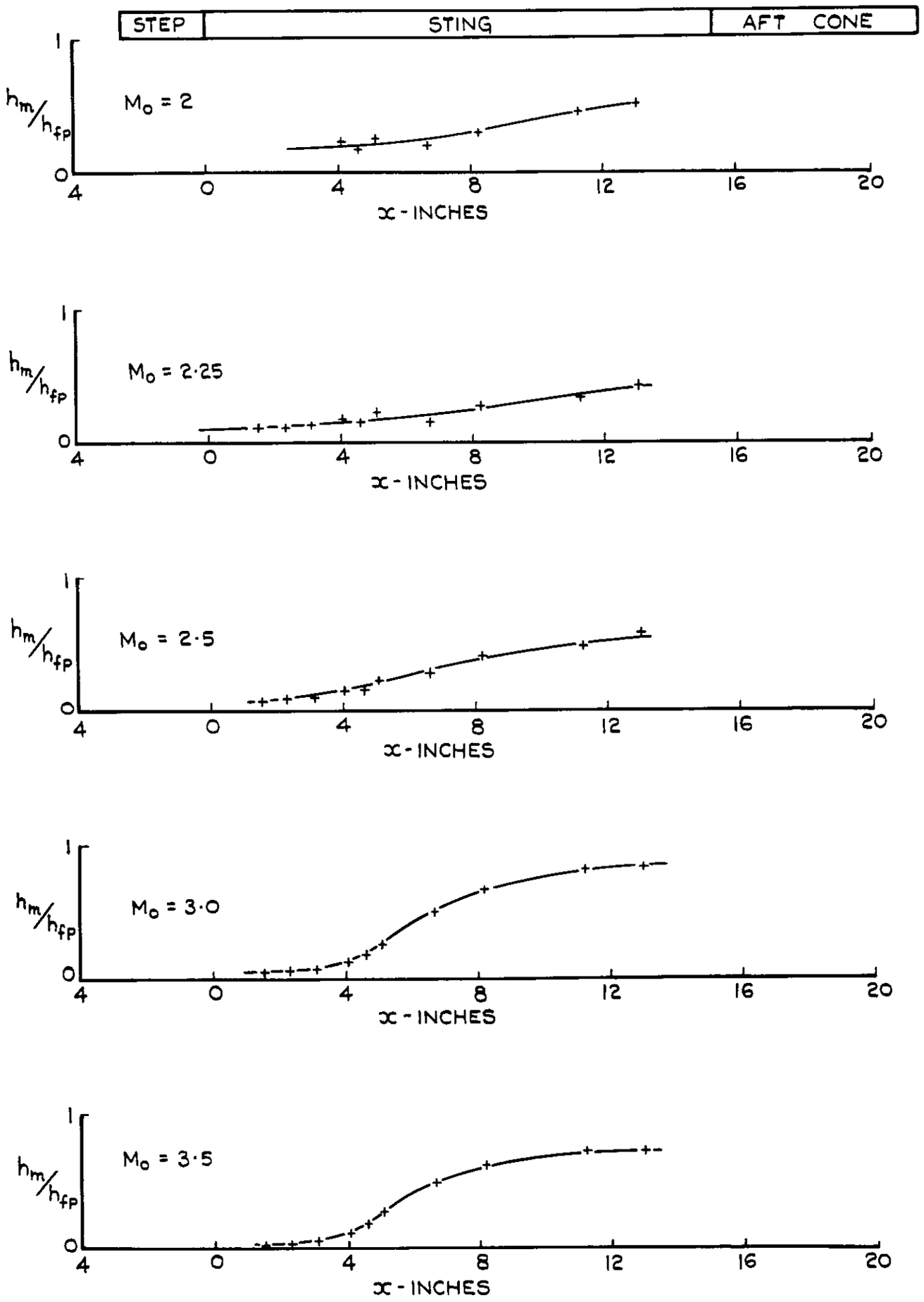

FIG. 23 (b) VARIATION OF HEAT TRANSFER OVER SEPARATED-FLOW AND REATTACHMENT REGIONS FOR HEAD H2 - ACCELERATING FLIGHT.

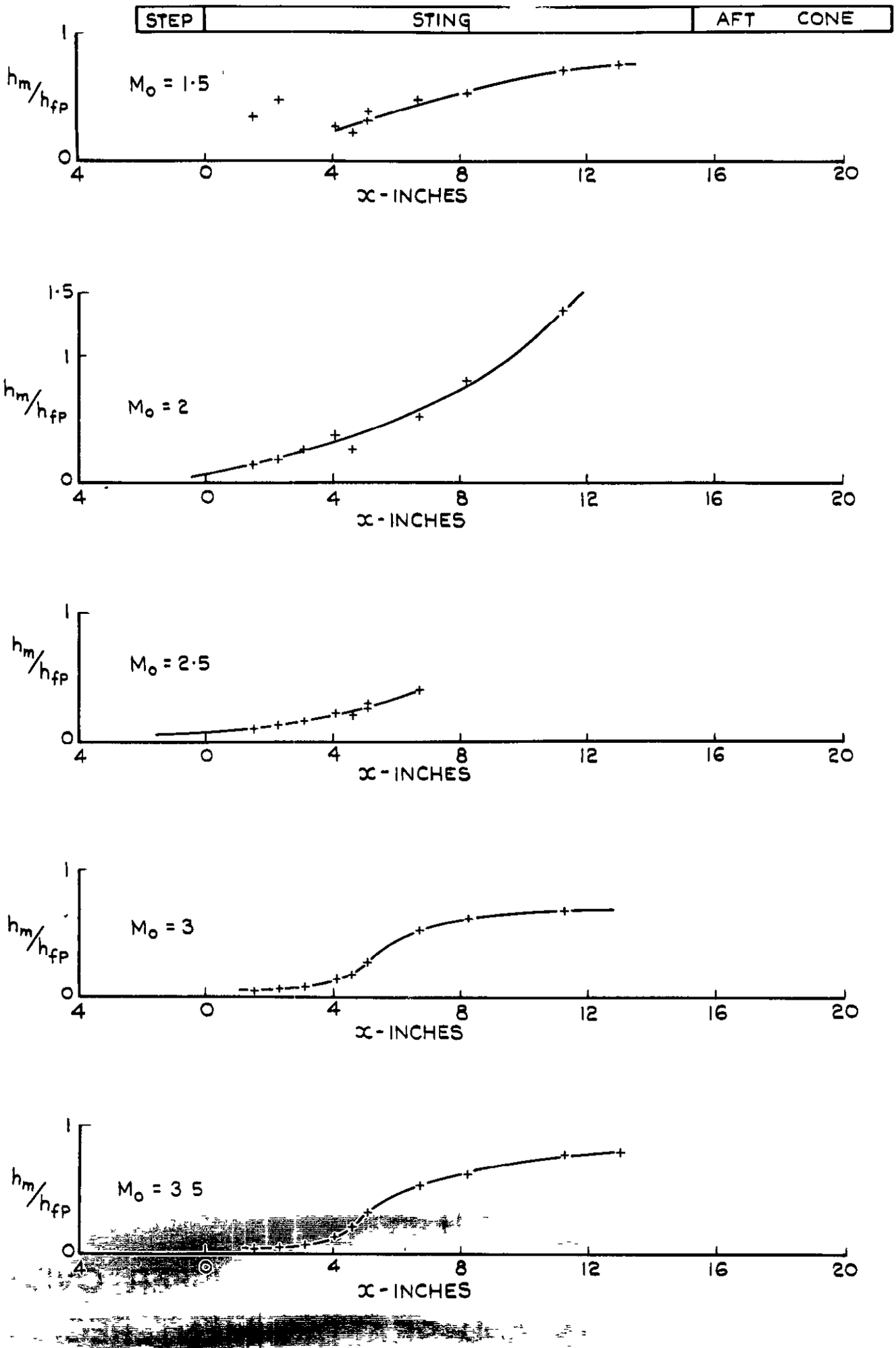

FIG. 23(b) CONCLD. VARIATION OF HEAT TRANSFER OVER SEPARATED-FLOW AND REATTACHMENT REGIONS FOR HEAD H2 - DECELERATING FLIGHT.

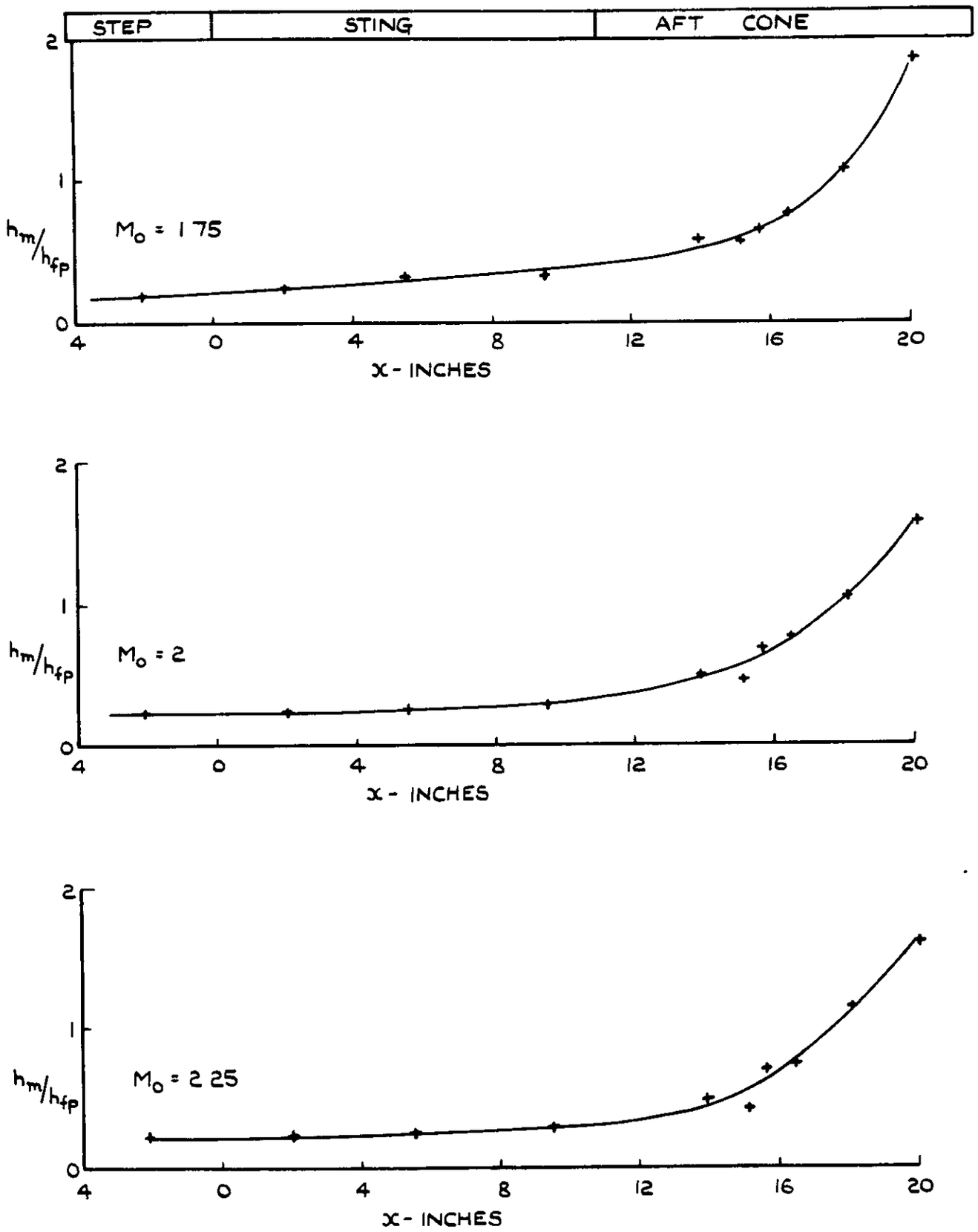

FIG.23 (c). VARIATION OF HEAT TRANSFER OVER SEPARATED-FLOW AND REATTACHMENT REGIONS FOR HEAD H3-ACCELERATING FLIGHT.

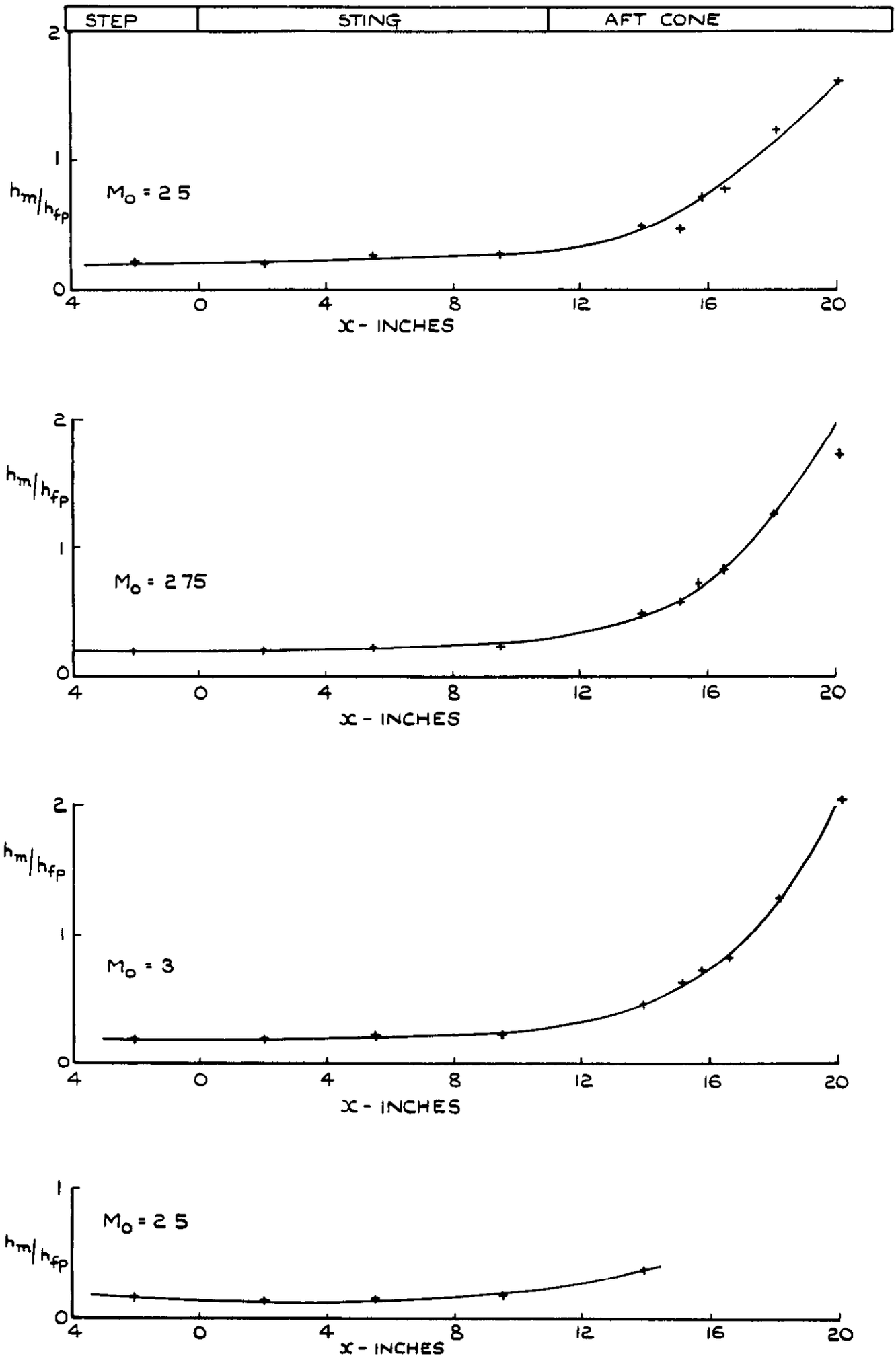

FIG. 23 (c) CONCLD. VARIATION OF HEAT TRANSFER OVER SEPARATED - FLOW AND REATTACHMENT REGIONS FOR HEAD H3 - ACCELERATING FLIGHT.

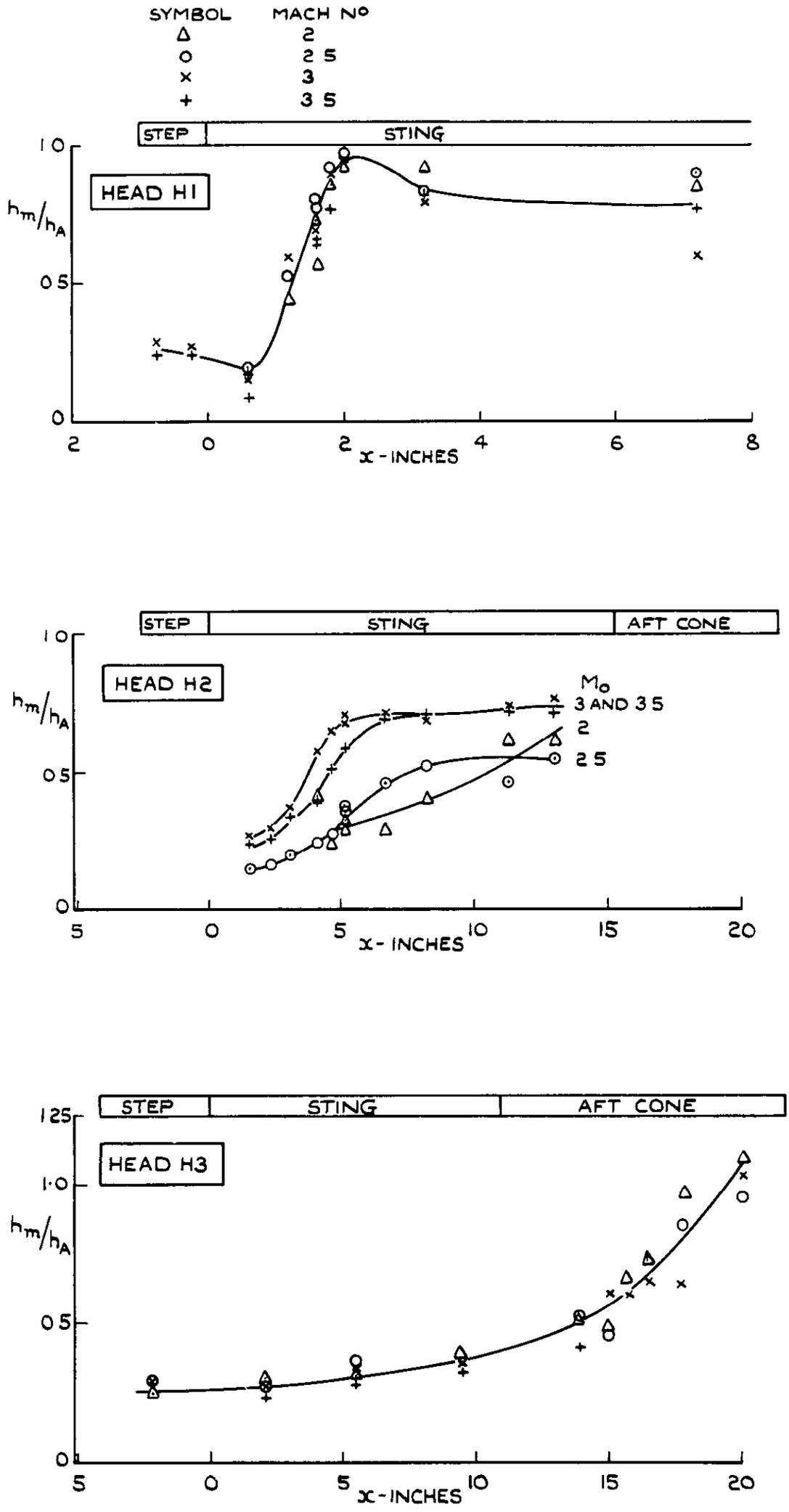

FIG. 24. DISTRIBUTION OF h_m/h_A FOR THREE HEADS - ACCELERATING FLIGHT.

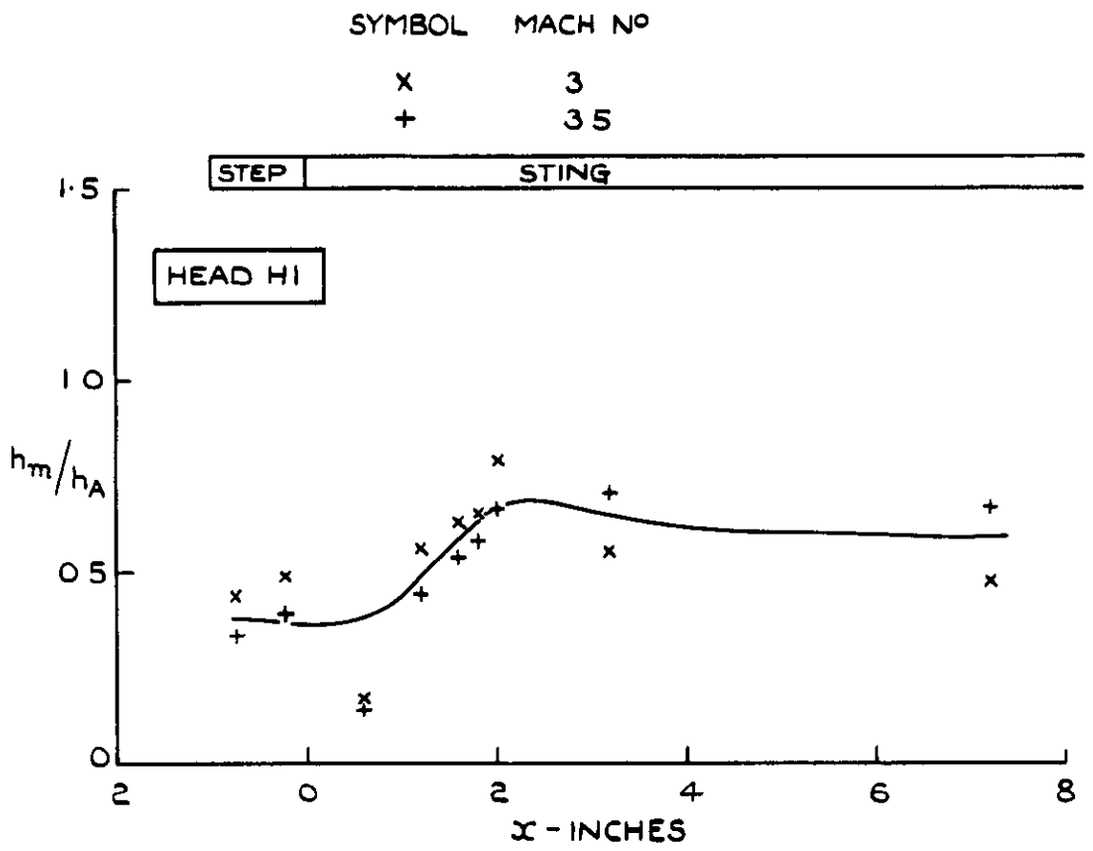

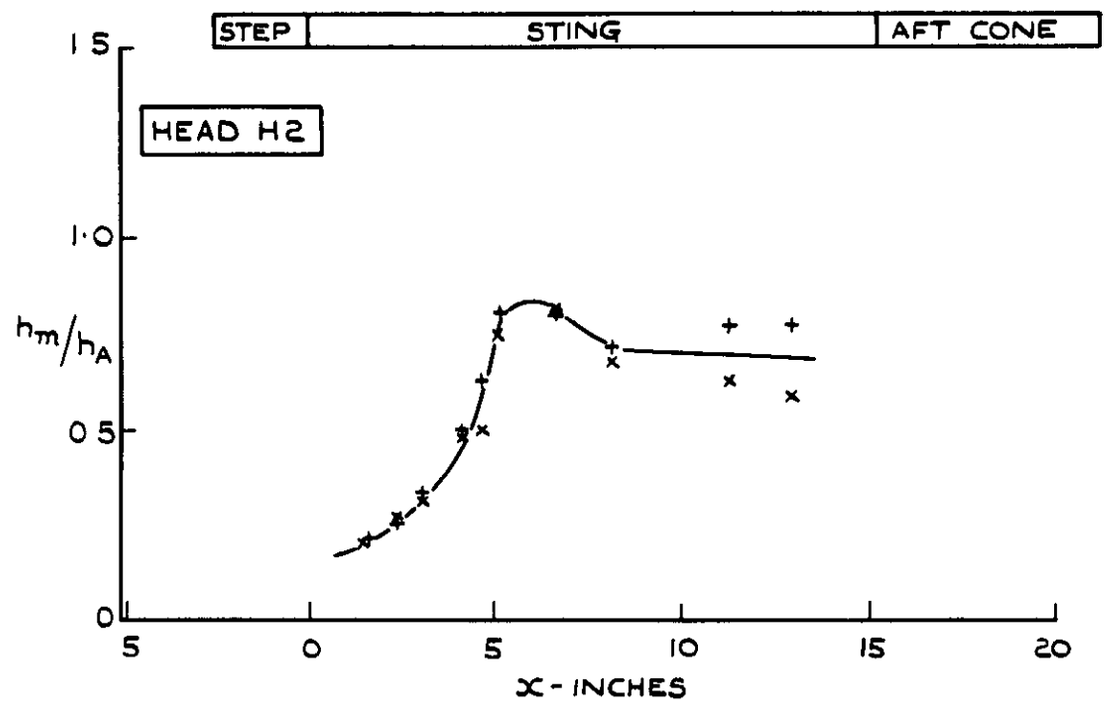

FIG. 24 CONCLD. DISTRIBUTION OF h_m/h_A FOR HEADS H1 AND H2 – DECELERATING FLIGHT.

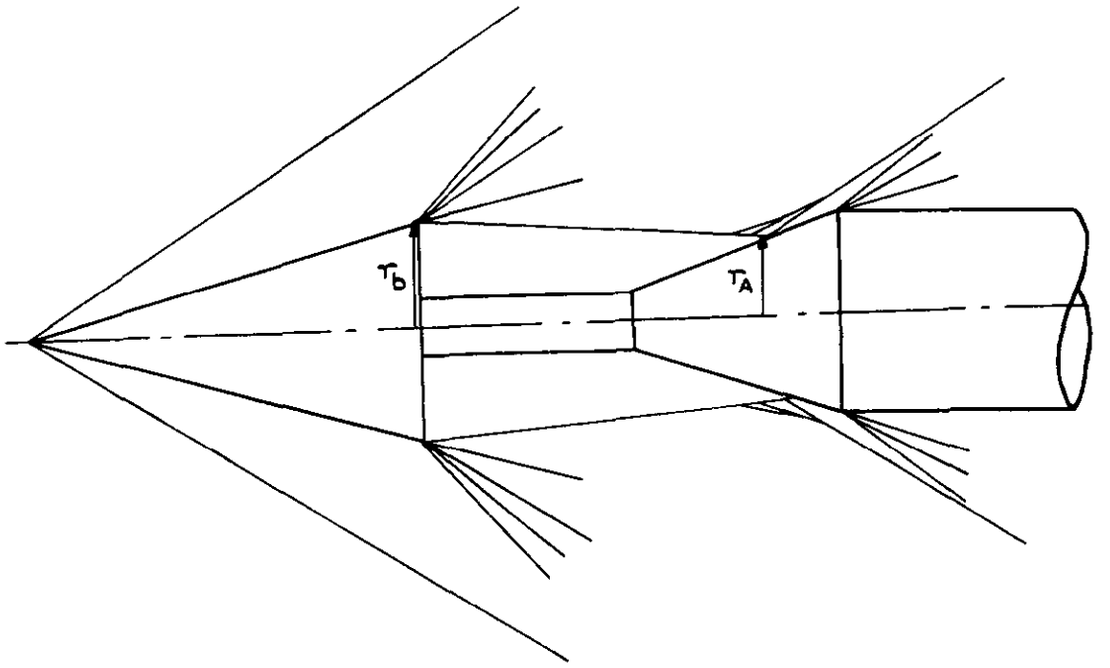

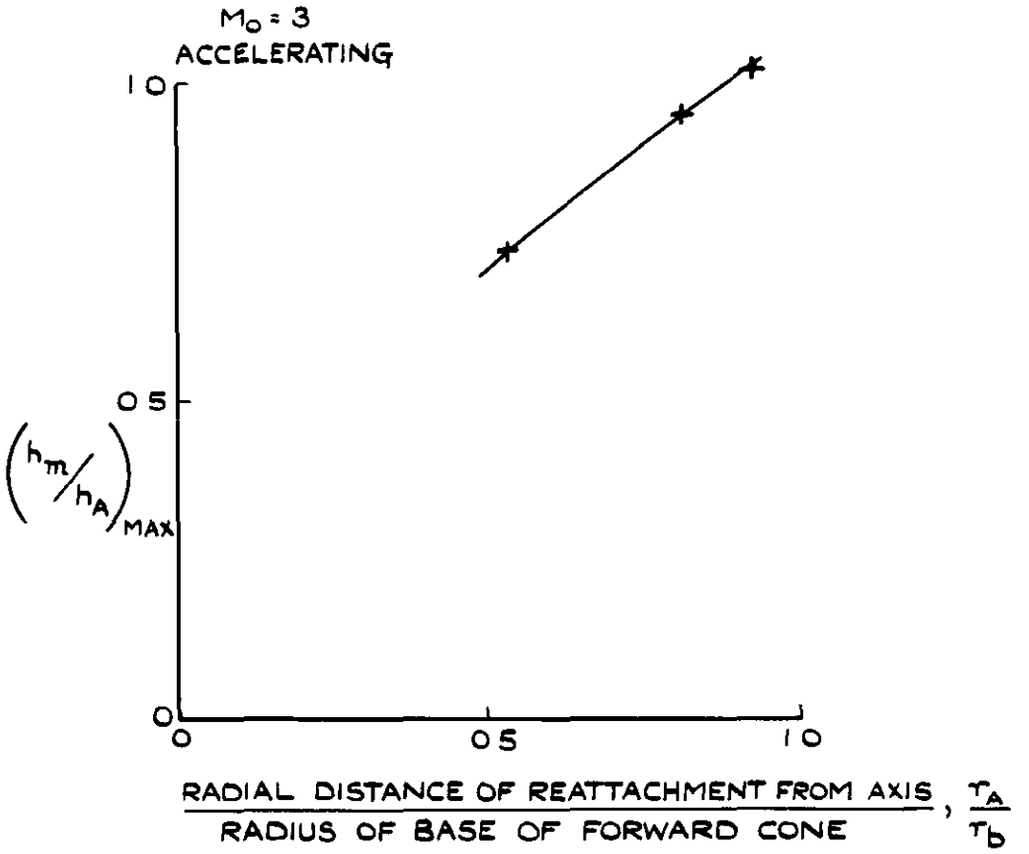

FIG. 25. VARIATION OF $\left(h_m/h_A\right)_{MAX.}$ WITH CONVERGENCE OF WAKE.

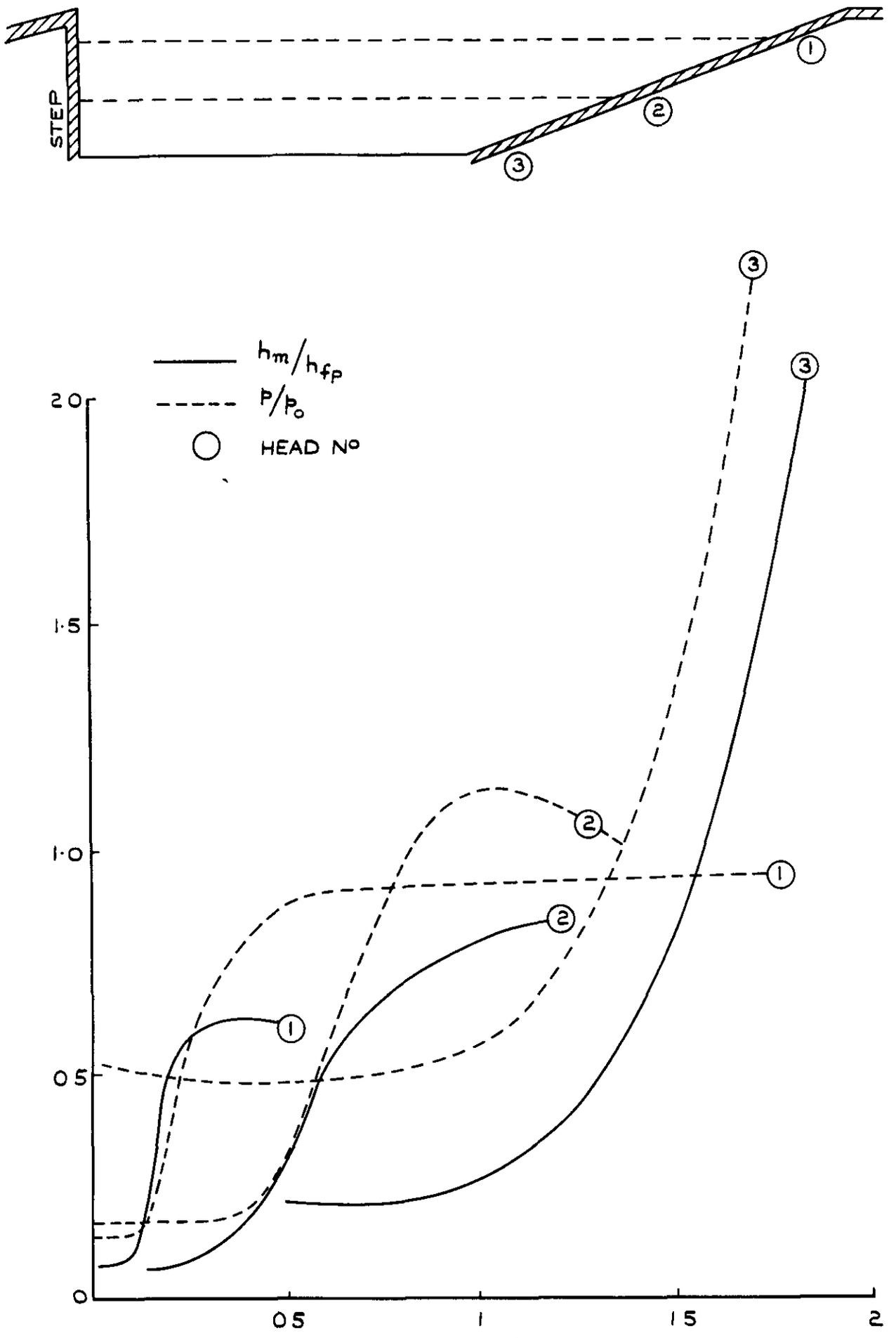

FIG.26. COMPARISON OF TRENDS IN HEAT TRANSFER AND PRESSURE VARIATIONS AFT OF STEP AT $M_o=3$.

A.R.C. C.P. No. 706

533.696.4:
533.6.011.6:
532.526.5

FREE-FLIGHT MEASUREMENTS OF PRESSURE AND HEAT TRANSFER IN REGIONS OF SEPARATED AND REATTACHED FLOW AT MACH NUMBERS UP TO 4. Picken, J. September 1960.

Local heat transfer and surface pressure have been measured over regions of separated flow associated with a turbulent boundary layer. The separated flow was appropriate to aft facing steps of various heights behind a sting mounted cone of 15^{0} semi-angle. The maximum Mach number achieved was about 4 and the maximum Reynolds number about 50×10^{6} based on cone length.

Two different forms of wake were detected: one associated with reattachment on the sting, i.e. a relatively great convergence of the wake boundary, and one associated with reattachment on a conical surface aft of the sting, i.e. a small wake convergence. Differing patterns of heat transfer and pressure distributions were obtained depending on which type of flow occurred.

(Over)

A.R.C. C.P. 706

533.696.4:
533.6.011.6:
532.526.5

FREE-FLIGHT MEASUREMENTS OF PRESSURE AND HEAT TRANSFER IN REGIONS OF SEPARATED AND REATTACHED FLOW AT MACH NUMBERS UP TO 4. Picken, J. September 1960.

Local heat transfer and surface pressure have been measured over regions of separated flow associated with a turbulent boundary layer. The separated flow was appropriate to aft facing steps of various heights behind a sting mounted cone of 15^{0} semi-angle. The maximum Mach number achieved was about 4 and the maximum Reynolds number about 50×10^{6} based on cone length.

Two different forms of wake were detected: one associated with reattachment on the sting, i.e. a relatively great convergence of the wake boundary, and one associated with reattachment on a conical surface aft of the sting, i.e. a small wake convergence. Differing patterns of heat transfer and pressure distributions were obtained depending on which type of flow occurred.

(Over)

A.R.C. C.P. No. 706

533.696.4:
533.6.011.6:
532.526.5

FREE-FLIGHT MEASUREMENTS OF PRESSURE AND HEAT TRANSFER IN REGIONS OF SEPARATED AND REATTACHED FLOW AT MACH NUMBERS UP TO 4. Picken, J. September 1960.

Local heat transfer and surface pressure have been measured over regions of separated flow associated with a turbulent boundary layer. The separated flow was appropriate to aft facing steps of various heights behind a sting mounted cone of 15^{0} semi-angle. The maximum Mach number achieved was about 4 and the maximum Reynolds number about 50×10^{6} based on cone length.

Two different forms of wake were detected: one associated with reattachment on the sting, i.e. a relatively great convergence of the wake boundary, and one associated with reattachment on a conical surface aft of the sting, i.e. a small wake convergence. Differing patterns of heat transfer and pressure distributions were obtained depending on which type of flow occurred.

(Over)

Some collapse of the separated flow heat transfer data with respect to Mach number was obtained by comparing them with estimated values appropriate to local conditions outside the wake. Close to the step the heat flow in the separated region was about 25% of the estimated value for attached flow to a solid surface replacing the wake boundary. Towards and beyond reattachment the ratio of the two values rose to near unity. The measurements suggest that the amount of heat transfer rise at and beyond reattachment is dependent upon the wake convergence, becoming smaller as the convergence increases. This is qualitatively consistent with the known effect that increasing convergence implies increasing boundary layer thickness at reattachment.

There was no evidence of a marked maximum in the heat flux in the reattachment region.

Some collapse of the separated flow heat transfer data with respect to Mach number was obtained by comparing them with estimated values appropriate to local conditions outside the wake. Close to the step the heat flow in the separated region was about 25% of the estimated value for attached flow to a solid surface replacing the wake boundary. Towards and beyond reattachment the ratio of the two values rose to near unity. The measurements suggest that the amount of heat transfer rise at and beyond reattachment is dependent upon the wake convergence, becoming smaller as the convergence increases. This is qualitatively consistent with the known effect that increasing convergence implies increasing boundary layer thickness at reattachment.

There was no evidence of a marked maximum in the heat flux in the reattachment region.

Published by
HER MAJESTY'S STATIONERY OFFICE

To be purchased from
York House, Kingsway, London W.C 2
423 Oxford Street, London W.1
13A Castle Street, Edinburgh 2
109 St. Mary Street, Cardiff
39 King Street, Manchester 2
50 Fairfax Street, Bristol 1
35 Smallbrook, Ringway, Birmingham 5
80 Chichester Street, Belfast 1
or through any bookseller

C.P. No. 706

S.O. CODE No. 23-9015-06